Report No. K-TRAN: KSU-06-7
FINAL REPORT

INTELLIGENT COMPACTION CONTROL OF HIGHWAY EMBANKMENT SOIL IN KANSAS

Farhana Rahman
Mustaque Hossain, Ph.D., P.E.
Stefan Romanoschi, Ph.D., P.E.*
Kansas State University
*currently affiliated with The University of Texas at Arlington

March 2008

A COOPERATIVE TRANSPORTATION RESEARCH PROGRAM BETWEEN:

KANSAS DEPARTMENT OF TRANSPORTATION
KANSAS STATE UNIVERSITY
THE UNIVERSITY OF KANSAS

KANSAS
DEPARTMENT OF TRANSPORTATION

<table>
<tr><td>1 Report No.
K-TRAN: KSU-06-7</td><td>2 Government Accession No.</td><td>3 Recipient Catalog No.</td></tr>
<tr><td colspan="2" rowspan="2">4 Title and Subtitle
Intelligent Compaction Control of Highway Embankment Soil in Kansas</td><td>5 Report Date
March 2008</td></tr>
<tr><td>6 Performing Organization Code</td></tr>
<tr><td colspan="2">7 Author(s)
Farhana Rahman, Mustaque Hossain, Ph.D., P.E., Stefan Romanoschi, Ph.D., P.E.*
*currently affiliated with The University of Texas at Arlington</td><td>8 Performing Organization Report No.</td></tr>
<tr><td colspan="2" rowspan="2">9 Performing Organization Name and Address
Department of Civil Engineering
Kansas State University
2118 Fiedler Hall
Manhattan, Kansas 66506</td><td>10 Work Unit No. (TRAIS)</td></tr>
<tr><td>11 Contract or Grant No.
C1571</td></tr>
<tr><td colspan="2" rowspan="2">12 Sponsoring Agency Name and Address
Kansas Department of Transportation
Bureau of Materials and Research
700 SW Harrison Street
Topeka, Kansas 66603-3745</td><td>13 Type of Report and Period Covered
Final Report
August 2005-Fall 2007</td></tr>
<tr><td>14 Sponsoring Agency Code
RE-0408-01</td></tr>
<tr><td colspan="3">15 Supplementary Notes
For more information write to address in block 9.</td></tr>
<tr><td colspan="3">16 Abstract
Mechanistic pavement design procedures based on elastic layer theory require characterization of pavement layer materials including subgrade soil. This paper discusses the subgrade stiffness measurements obtained from a new compaction roller for compaction control on highway embankment projects in Kansas. Three test sections were compacted using a single, smooth steel drum intelligent compaction (IC) roller that compacts and simultaneously measures stiffness values of the compacted soil. Traditional compaction control measurements such as, density, in-situ moisture content, soil stiffness measurements using soil stiffness gage, surface deflection tests using the Light Falling Weight Deflectometer (LFWD) and Falling Weight Deflectometer (FWD), and penetration tests using a Dynamic Cone Penetrometer (DCP), were also done. The results show that the IC roller was able to identify the locations of lower soil stiffness in the spatial direction. Thus the IC roller can be used in proof rolling. IC roller stiffness showed sensitivity to the field moisture content indicating that moisture control during compaction is critical. No universal correlation was observed among the IC roller stiffness, soil gage stiffness, backcalculated subgrade moduli from the LFWD and FWD deflection data, and the California Bearing Ratio (CBR) obtained from DCP tests. The discrepancy seems to arise from the fact that different equipment were capturing response from different volumes of soil on the same test section. Analysis using the newly released Mechanistic-Empirical Pavement Design Guide (M-EPDG) shows that pavement rutting, roughness and asphalt base thickness are significantly influenced by the subgrade strength. “Target” modulus for compaction quality control can also be obtained by this analysis.</td></tr>
<tr><td colspan="2">17 Key Words
Intelligent compaction, falling weight deflectometer (FWD), light falling weight deflectometer (LFWD), stiffness gage, nuclear gage, dynamic cone penetrometer (DCP), moisture content, soil stiffness</td><td>18 Distribution Statement
No restrictions. This document is available to the public through the National Technical Information Service, Springfield, Virginia 22161</td></tr>
<tr><td>19 Security Classification (of this report)
Unclassified</td><td>20 Security Classification (of this page)
Unclassified</td><td>21 No. of pages
122

22 Price</td></tr>
</table>

Form DOT F 1700.7 (8-72)

INTELLIGENT COMPACTION CONTROL OF HIGHWAY EMBANKMENT SOIL IN KANSAS

Final Report

Prepared by

Farhana Rahman
Mustaque Hossain, Ph.D., P.E.
Stefan Romanoschi, Ph.D., P.E.*

Kansas State University
2118 Fiedler Hall
Manhattan, Kansas 66506

*currently affiliated with The University of Texas at Arlington

A Report on Research Sponsored By

THE KANSAS DEPARTMENT OF TRANSPORTATION
TOPEKA, KANSAS

March 2008

© Copyright 2008, **Kansas Department of Transportation**

PREFACE

The Kansas Department of Transportation's (KDOT) Kansas Transportation Research and New-Developments (K-TRAN) Research Program funded this research project. It is an ongoing, cooperative and comprehensive research program addressing transportation needs of the state of Kansas utilizing academic and research resources from KDOT, Kansas State University and The University of Kansas. Transportation professionals in KDOT and the universities jointly develop the projects included in the research program.

NOTICE

The authors and the state of Kansas do not endorse products or manufacturers. Trade and manufacturers' names appear herein solely because they are considered essential to the object of this report.

This information is available in alternative accessible formats. To obtain an alternative format, contact the Office of Transportation Information, Kansas Department of Transportation, 700 SW Harrison, Topeka, Kansas 66603-3745 or phone (785) 296-3585 (Voice) (TDD).

DISCLAIMER

The contents of this report reflect the views of the authors who are responsible for the facts and accuracy of the data presented herein. The contents do not necessarily reflect the views or the policies of the state of Kansas. This report does not constitute a standard, specification or regulation.

ABSTRACT

Mechanistic pavement design procedures based on elastic layer theory require characterization of pavement layer materials including subgrade soil. This report discusses the subgrade stiffness measurements obtained from a new compaction roller for compaction control on highway embankment projects in Kansas. Three test sections were compacted using a single, smooth steel drum intelligent compaction (IC) roller that compacts and simultaneously measures stiffness values of the compacted soil. Traditional compaction control measurements such as, density, in-situ moisture content, soil stiffness measurements using soil stiffness gage, surface deflection tests using the Light Falling Weight Deflectometer (LFWD) and Falling Weight Deflectometer (FWD), and penetration tests using a Dynamic Cone Penetrometer (DCP), were also done. The results show that the IC roller was able to identify the locations of lower soil stiffness in the spatial direction. Thus the IC roller can be used in proof rolling. IC roller stiffness showed sensitivity to the field moisture content indicating that moisture control during compaction is critical. No universal correlation was observed among the IC roller stiffness, soil gage stiffness, backcalculated subgrade moduli from the LFWD and FWD deflection data, and the California Bearing Ratio (CBR) obtained from DCP tests. The discrepancy seems to arise from the fact that different equipments were capturing response from different volumes of soil on the same test section. Analysis using the newly released Mechanistic-Empirical Pavement Design Guide (M-EPDG) shows that pavement rutting, roughness and base thickness are significantly influenced by the subgrade strength. “Target” modulus for compaction quality control can also be obtained by the analysis.

ACKNOWLEDGEMENTS

The authors wish to acknowledge the financial support provide by the Kansas Department of Transportation under its Kansas Transportation and New Developments (K-TRAN) program. Contribution of Ms. Mbaki Onyongo, Mr. Christian Dumitru, and Mr. James Mulandi of Kansas State University is gratefully acknowledged. Participation of Bomag Corp. in this study is also gratefully acknowledged. The help of KDOT area personnel and contractors is also acknowledged. Dr. James Neil of the Statistics Department at Kansas State University served as the statistical consultant to this project. His contribution is duly acknowledged.

TABLE OF CONTENTS

LIST OF FIGURES

LIST OF TABLES

CHAPTER 1 - INTRODUCTION

1.1 General

During past four decades, pavements have been designed mostly using empirical design procedures. However, design of pavements using new tools requires detailed inputs on material response and damage properties. Example of such a tool is the newly developed Mechanistic-Empirical Pavement Design Guide (M-EPDG) of National Cooperative Highway Research Program (NCHRP) *(1)*. Pavement performance is highly influenced by foundation layer modulus, strength, and permeability as well as by the ease and permanency of compaction. Subgrade compaction increases strength, decreases permeability, and reduces undesirable settlement. Current compaction quality control methods are fully based on the results of the laboratory compaction tests. The in-situ dry density of the soil is measured after compaction and compared with the laboratory maximum dry density. A number of methods such as, sand cone, rubber balloon and nuclear gage, etc. are used to measure the in-situ density. The in-situ moisture is also measured by the nuclear gage and other measurement methods and controlled.

During a scan tour in Europe, the Federal Highway Administration (FHWA) identified some road building technologies that are implementable in the United States. The technologies are two lift construction, design feature catalog, high quality foundation construction, greater attention to mix design components, geotextile layer, and exposed aggregate surface. A new compaction technique named intelligent compaction came under the high quality foundation construction technology. Intelligent compaction was first introduced in some European countries for road and embankment construction in early 1970s. The aim of this new method was to provide higher quality road and embankment construction through a high quality control and interactive assurance system from the very beginning of the roadway construction. This report will describe a field testing using an intelligent compaction roller on two highway embankment projects in Kansas as well as the associated research results.

In the United States, the soil and rock fill materials are compacted using conventional static or vibratory rollers. The highway embankment of cohesionless soil is mainly compacted with a vibratory roller with parallel strips passes from edge to edge or with some overlapping. Each strip is compacted by a fixed number of passes with a constant roller speed, vibration frequency and amplitude. However, constant speed, frequency and amplitude do not necessarily lead to a homogeneous compaction level due to variation in subgrade material properties, in-situ moisture content of the compacted layer, and the stiffness of the underlying layer soil. Instead this process often leads to a certain part of the area insufficiently compacted, some portion over-compacted, and the rest sufficiently compacted.

1.2 Convention In-Situ Quality Control (Spot Tests)

The conventional in-situ quality control of compaction involves some spot tests such as static plate load test, soil stiffness gage for stiffness measurement, falling weight deflectometer (FWD) for modulus testing (Figure 1.1), the nuclear gage for density and in-situ moisture testing, rubber balloon and the sand replacement tests for density measurement. These methods are standardized and some are widely used for in-situ compaction control. However, it should be noted that the zone of influence within the compacted subgrade layer for each test method is different. For example, the modulus value obtained from plate load test covers the depth that is 1.5 times the plate diameter (ranges from 0.3 to 0.6 m). The soil stiffness gage (Geogage) provides subgrade stiffness for a depth of 0.5 ft (0.15 m). Again, the measured modulus value may differ significantly with depth due to heterogeneity of the natural soil. In addition, the moisture content will affect the average density value of the compacted subgrade.

FIGURE 1.1: Dynatest Model 8000 FWD device used in spot testing on US-56, Hugoton, Kansas

1.3 Relative Compaction Testing Methods

In this method, index values are compared for two successive passes of the compaction roller. The method does not provide any absolute value for percent compaction, stiffness or density achieved. These systems are available as an attachment for any compaction roller and are called “Compactometer”. A Swedish company, Geodynamic manufactures and sells this type of equipment.

This approach is also used in the “Continuous Compaction Control, CCC.” The measurement methods are based on integrated compaction meter attached to a roller that continuously measures the acceleration of the roller drum and continuously calculates meter value from the acceleration signal. Examples of such measures are compaction meter value (CMV) from GEODYNAMIK, and the Omegameter and Terrameter (Figure 1.2) from BOMAG. The basic objective is to obtain a quality assurance documentation which can also be used to identify the spot test locations for calibration.

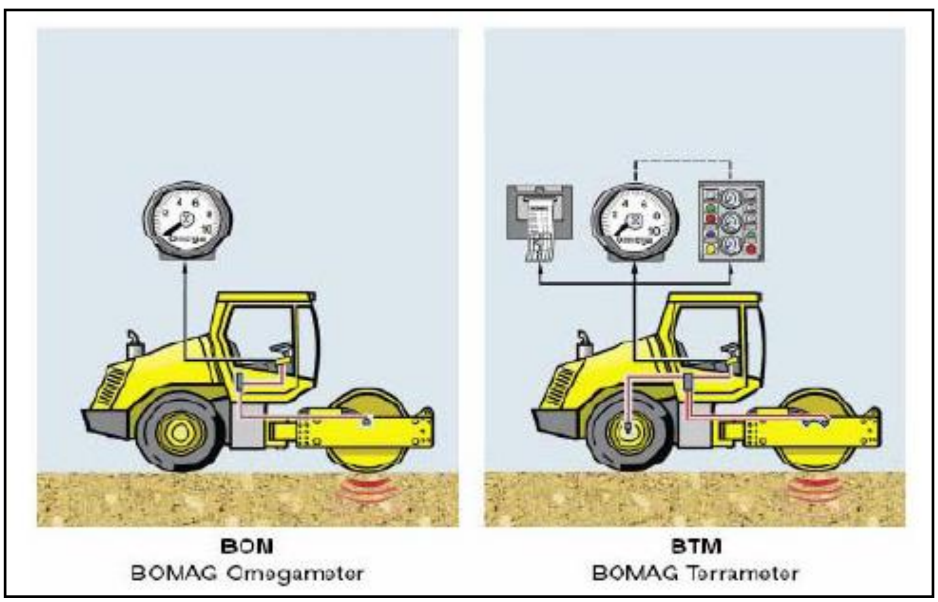

FIGURE 1.2: Omegameter and Terrameter (2)

1.4 Absolute Compaction Testing Method

This method provides the absolute values of compaction during operation. In the past, the absolute compaction results were provided by the individual or independent measuring units that were not attached to the compaction equipment. Currently, some manufacturers are providing an attachment that gives absolute instantaneous values of soil stiffness measures. These systems assure the operator that the proper compaction has been achieved. A Swiss company, AMMANN has such a system attached to their roller.

1.5 Intelligent Compaction Method

This method is a combination of the absolute measurement technology and an automatic control method. The system includes a vibratory roller that measures the material stiffness continuously and also has an automatic compaction control. The system controls different compaction parameters of the roller such as, amplitude, frequency and working speed. The stiffness measurements are made by the instrumented roller itself. The details of intelligent compaction process will be discussed in Chapter 2.

1.6 Problem Statements

Compaction of embankment, subgrade and base materials costs a significant portion of state highway agency construction budgets and is critical to the performance of highway pavements. Heterogeneity of the pavement materials, variability in the equipment and operators, difficulty in maintaining the uniform lift thickness and prescribed moisture content make the target compaction level difficult to achieve. Current quality control and quality assurance testing devices, such as, nuclear gage, the dynamic cone penetrometer, the geogage, the light falling weight deflectometer are typically used to asses less than one percent of the actual compacted area *(3)*. In addition, each of these testing devices measures parameters unique to the device. Other limitations of the conventional compaction and the compaction control process as identified by FHWA *(4)* are: (1) Density and density related material properties can not be measured before the compaction process is complete; (2) Density measurement from a small number of spots may not be representative of the density of the entire lot; (3) Conventional compaction methodology does not allow any or very little instantaneous feedback for the project personnel; and finally (4) Overcompaction can occur and hence reduce the density that has already been achieved in the previous passes.

Improper compaction control of subgrade soils may result in bridge approach settlement, rapid increase in pavement roughness, etc. The Kansas Department of Transportation (KDOT) has placed a major emphasis on the compaction control of soils on the "grade and pave" projects. Embankment compaction control is specified by the KDOT based on the maximum dry density and optimum moisture content results obtained from the standard proctor tests on typical embankment soil. Currently KDOT is in the process of implementing quality control/quality assurance (QC/QA) specifications for embankment compaction. A previous research project in Kansas showed that current compaction control procedures result in highly variable stiffness values of the finished subgrade *(5)*.

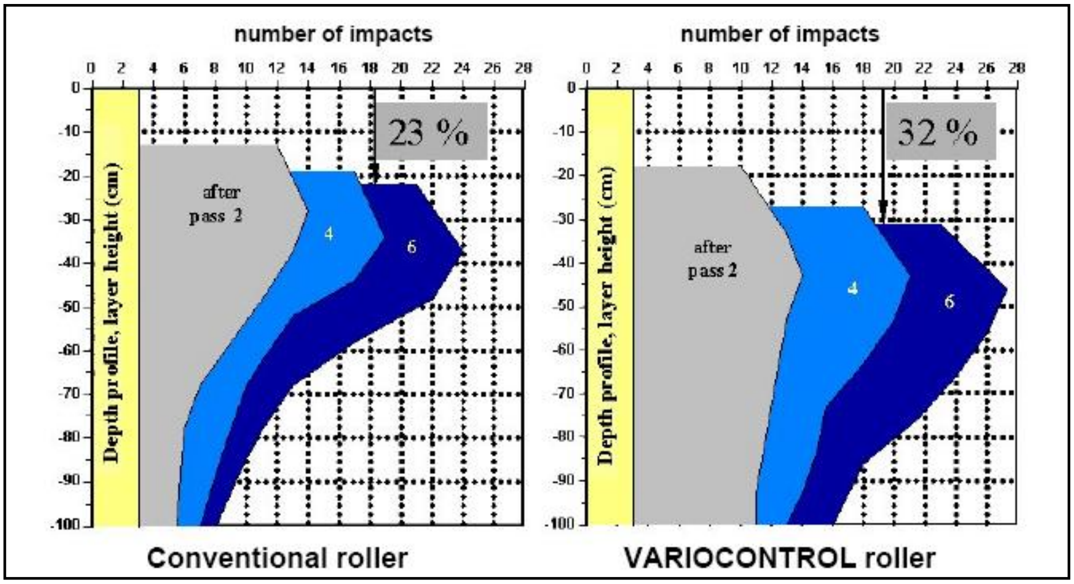

FIGURE 1.3: Comparison between Conventional roller and IC roller, (6)

The problem of variable stiffness of the pavement foundation layer has been addressed by the European countries using Intelligent Compaction Control (ICC). According to FHWA *(4)*, the primary reason to consider Intelligent Compaction (IC) technology is its stated capability to *optimize* and significantly *improve* the conventional compaction process as shown in Figure 1.3. This improvement is in several important areas: (1) Compaction efficiency (fewer passes); (2) Compaction quality (consistently higher and more uniform density); (3) Continuous material stiffness outputs that can be used in mechanistic-empirical pavement design; (4) Real time information to project personnel during compaction; (5) Identification of situations where adequate compaction cannot be accomplished. More details on ICC can be found elsewhere *(4, 7-11)*. But IC roller stiffness should be evaluated to achieve the target pavement performance for a given design. Again, recent research has shown that the M-EPDG overestimates pavement performance by assuming subgrade compaction to optimum moisture content

(12). In order to ensure a successful design, the distresses on the pavement must be predicted for in-situ subgrade modulus.

1.7 Objectives

The main objective of this study was to evaluate the soil stiffness measured by IC roller and its correlation with other stiffness and/or modulus values obtained from Geogage, Light Falling Weight Deflectometer (LFWD) and Falling Weight Deflectometer (FWD) deflections, and Dynamic Cone Penetrometer (DCP) data on compacted subgrade. Variation of IC roller measured stiffness with field moisture content and percent compaction was also analyzed. The final objective of this study was to evaluate the soil stiffness and/or modulus values measured by the IC roller and different non-destructive testing (NDT) devices using the Mechanistic-Empirical Pavement Design Guide software (version 1.0) so that a “target” modulus can be selected. Sensitivity analysis was also performed to examine the effect of subgrade modulus on the distresses of the whole pavement structure.

1.8 Report Organization

This report is divided into six chapters. The first chapter covers a brief introduction to the compaction technique and its quality control, problem statement, study objectives and the outline of the report. Chapter 2 is a review of the literature and a detailed background of intelligent compaction. Chapter 3 describes the test section and data collection procedure in the field. Chapter 4 presents the analysis of the test results. Results of M-EPDG analysis for the test sections are discussed in Chapter 5. Finally, Chapter 6 presents the conclusions and recommendations based on the present study.

CHAPTER 2 - LITERATURE REVIEW

2.1 Soil Compaction

In the construction of many engineering structures such as, highway embankment and earth dam, loose earth fills, etc. are required to be compacted to increase the soil density and hence the load bearing capacity. Soil compaction is a mechanical process to densify the soil by removing air mass from the void space within the soil structures. In time, loose material would settle or compact itself naturally. By applying various mechanical forces, the time required to get is significantly reduced. Pavement performance is basically influenced by the subgrade strength, drainage properties of the soil, ease of compaction and also the permanency of the compaction. Proper soil compaction increases the bearing capacity of the soil, reduces water seepage, swelling and shrinkage potential, protects the soil from uneven settlements and frost damage and also provides stability of the compacted soil mass.

The degree of compaction of soil is measured in terms of dry unit weight. In general, the dry unit weight will increase with increasing moisture content for similar compacting effort. However, beyond a certain point, additional moisture tends to reduce the dry unit weight as excess moisture try to displace soil particles from their compacted position. Figure 2.1 shows the general nature of dry unit weight to moisture content for a given soil and the compaction effort. The moisture content at which the maximum dry unit weight is obtained is called the *optimum moisture content*.

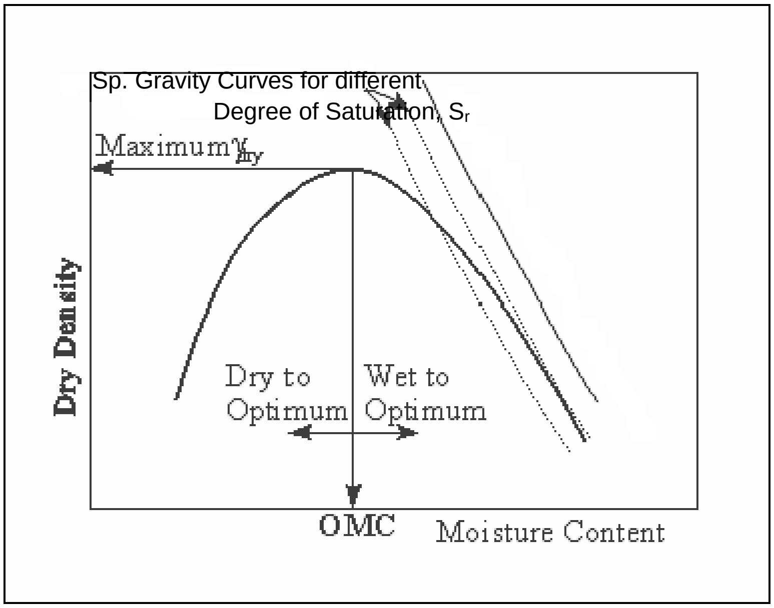

FIGURE 2.1: Relation of dry unit weight to the moisture content

2.1.1 Compaction Principles and Measurements

During compaction, the voids between the particles that are filled with air, water or a combination of both are expelled by a combination of force and movement. Four different types of forces may be present during compaction: (1) Static Pressure, (2) Manipulation, (3) Impact Force, and (4) Vibration.

STATIC PRESSURE: In static compaction, weighted loads, applied by rollers, produce shear stresses in the soil which cause the individual particles to slide across each other. These particles break their natural bonds to each other and move into a more stable position within the material. Static smooth-wheeled rollers, static sheepsfoot (or pad-foot) and tamping foot rollers work on this principle. Four factors influence compaction performance of static rollers. They are axle load, drum width, drum diameter and rolling speed.

MANIPULATION: Manipulation is a compactive force that rearranges particles into a more dense mass by a kneading process. The process is especially effective at the surface of the lift material. The longitudinal and transverse kneading action is essential during the compaction of heavily stratified soils such as, clay-type soils. Manipulation helps to close the small, hairline cracks through which moisture can penetrate and weaken the subgrade. Sheepsfoot rollers and staggered wheel, rubber tired rollers are specifically designed to deliver this type of compactive force.

IMPACT: Impact creates a greater compaction force on the surface than an equivalent static load. This is because a falling weight speed is converted to energy at the instant of impact. Impact creates a pressure wave, which goes into the soil from the surface. Impacts are usually a series of blows. Impact blows of 5 to 600 blows per minute are considered low frequency ranges and are used on impact hammers and hand tampers. Impact blows of high frequency (1400 to 3500 blows per minute) are used on vibratory compactors.

VIBRATION: Vibration is the final and most complex compactive force. Vibratory compactors produce a rapid succession of pressure waves, which spread in all directions. The vibratory pressure waves are useful in breaking the bonds between the particles of the material being compacted. When pressure is applied, the particles tend to reorient themselves in a more dense (fewer voids) state.

Vibratory compaction of soil is a complex process. More than 30 different factors influence the overall compaction effort. Vibratory compaction involves a drum which is moving up and down (amplitude) very rapidly (frequency) and moving forward (working speed) over a non-homogeneous material. All components influencing compaction should be considered as a whole, not as individual entities. It is the combined characteristics of the compactor and of the mass of soil it is attempting to compact that determines the degree of compactive effort. Vibratory rollers are used mostly for densification of the granular subgrade soil.

2.1.2 Factors Affecting Field Compaction

Field soil compaction basically depends on the soil structure and properties and the in-situ moisture content in the field. Besides these two factors, the thickness of the lift, the intensity of the pressure applied by the compaction equipment and the area over which the pressure is applied, greatly affect the degree of compaction. The pressure applied at the surface by the compaction equipment decreases with depth and hence will decrease the degree of compaction. During compaction, the dry unit weight of soil is also affected by the number of roller passes.

2.1.3 Field Tests for Compaction Control

Periodic field testing is done to measure two important parameters: (1) target density and (2) target moisture content. These tests can also indicate the effectiveness of the compaction equipment and construction method being used. The most common field testing methods are the Nuclear Method, the Sand-Cone Method and the Water Balloon Method.

NUCLEAR METHOD: Nuclear density meters emit radiation into the subgrade soil being tested and count the measures (both moisture content and density). The test is nondestructive and can be performed quickly. There are two basic methods of measuring density in this method: (1) The direct transmission method that gives the best accuracy, least composition error and least surface roughness error for testing over a range of depths from two to twelve inches; and (2) The backscatter method that eliminates the need to create an access hole in the compacted soil. However, accuracy is less and composition errors are likely. This method works best in shallow depths (2 to 3 inches).

SAND CONE METHOD: The sand-cone method is a multi-step procedure which is more time consuming than the nuclear density method, but has had proven accuracy. It is sometimes used in conjunction with the nuclear method to verify the calibration of the nuclear density meter.

WATER BALLON METHOD: The water balloon method is also called the Washing Densometer Test. The first three steps of this test are to excavate a sample, then weigh it, and dry it. These steps are same as performed in the sand-cone method. In this manner, moisture content is calculated. Limitations to the water balloon method are, again, the length of time needed to get results and also the accuracy depends on the ability of the balloon to conform to any irregularities along the sides of the hole

2.1.4 Compaction Quality Control in the Field

Current compaction quality control (QC/QA) in the field is fully based on laboratory compaction testing of soil (Standard Proctor Test). The procedures of the Proctor Test have been adopted and further standardized by the American Association of State Highway and Transportation Officials (AASHTO). The Standard AASHTO procedure (T-99) uses a 5.5 lb. (2.5 kg) hammer dropped freely from a height of 12 inches (3054 mm). Again, the soil is compacted in three layers by 25 hammer blows in a 4 inch (102 mm) diameter mold. This test imparts a total of 12,400 ft. lbs. of compactive effort to the soil sample.

Modified compaction test is also introduced by AASHTO in connection with structures require heavier bearing strength to support extremely heavy loads or to limit settlement. According to the Modified AASHTO procedure (T-180), a 10 lb. (4.5 kg) hammer is dropped from a height of 18 inches (457 mm). The soil sample is compacted in five layers with 25 blows per layer. The compaction energy is 4.5 times larger than the Standard AASHTO test that produces 56,200 ft-lbs. of effort.

Laboratory test determines the moisture content at which maximum density can be attained (figure 2.1). It is realized that this density cannot readily be achieved in the field by conventional compaction equipment. Therefore, field target densities are specified as a certain percent of the maximum laboratory dry density. Generally, a range of 90%-95% of maximum dry density of Standard AASHTO is considered during field compaction. Likewise, the moisture content must be within a range of the laboratory determined optimum moisture content.

2.2 Intelligent Compaction Control

FHWA (*4*) defined the intelligent Compaction (IC) technology as “Vibratory rollers that are equipped with a measurement/control system that can automatically control compaction parameters in response to materials stiffness measured during the compaction process. The roller is also equipped with a documentation system that allows continuous recordation, through an accurate positioning system, of roller location and corresponding density-related output, such as number of roller passes and roller-generated materials stiffness measurements.” The Intelligent Compaction (IC) is made possible because of the ability of a vibratory roller to first sense the material response of soil under loading. Then process this information and compare it to the input requirements. After that, it “decides” how to adjust compaction parameters to most efficiently compact the material *(4, 13)*. Since none of these features are available on conventional vibratory rollers, IC represents a major innovation in soil compaction technology (*4*).

2.2.1 Historical Background

Intelligent compaction is a concept during the last three decades. The concept is continued to be advanced by BOMAG in Germany, AMMANN in Switzerland and GEODYNAMIK in Sweden. In 1982, the first measurement system for soil compaction was introduced by BOMAG. In 1989, the first documentation system for soil compactors was presented. The German Ministry of Highways Construction gave its first recommendations on SCCC (Soil Continuous Compaction Control, a pioneer of Intelligent Compaction) in 1993. In 1994, the same highway agency introduced specification on SCCC. A volumetric roller was introduced for asphalt in 1996 and a variocontrol roller for soil in 1998. In the late 1990s, both AMMANN and BOMAG conducted studies to validate the relationship of the roller measured stiffness of soil and the material properties related to in-place density levels. The study was successful in identifying the proportional relationship between the plate load test data and roller-measured soil stiffness for granular soil when the compacted soil mass reached near to its optimum density level. Then finally, Ammann Compaction Expert (ACEE) introduced the modulus E_{vib} in 2000 and correlated its value with plate lad tests in 2001 (*4*).

Intelligent Compaction is more popular in Europe compared to US because different types of contracts are used for the construction projects (*4*). European methods of contract procurements and administration were very similar to those in the United States until the late 1980s. Public transportation agencies retained tight control over the design and construction of the highway systems. In the late 1980s, European agencies began to make significant changes to contract administration technique. During a European scan tour, FHWA identified certain technologies that could be implemented in US. High quality embankment contraction was one of them and hence intelligent compaction idea was introduced by FHWA for field testing in the US environment. As of now, the technology has been (or being) field tested in a number of states (Figure 2.2).

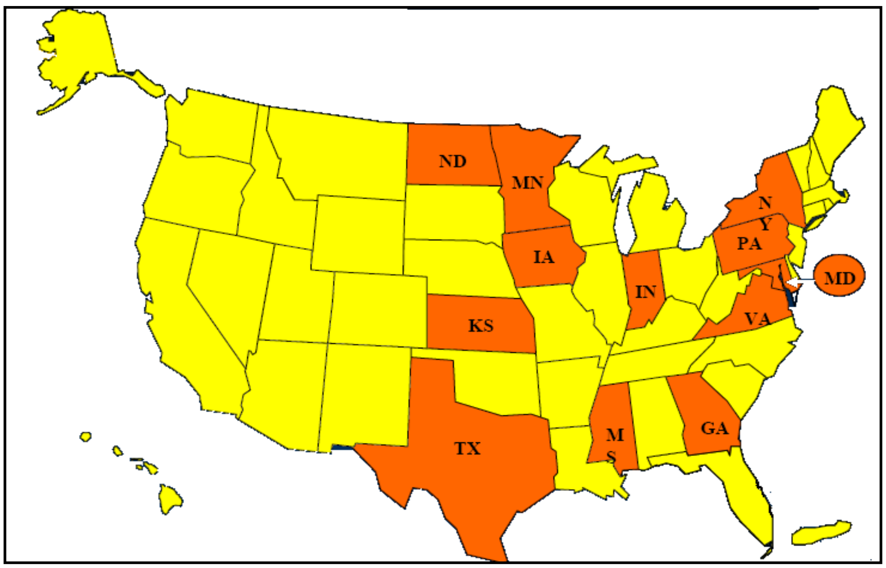

FIGURE 2.2: Application of Intelligent Compaction in US (7)

A survey of US roller manufacturers has concluded that Ammann-America, Bomag-America, Dynapac US and Caterpillar are the four major compaction equipment manufacturers. They are actively developing the technologies that have intelligent related capabilities at this time *(4)*. Some of these companies have already started to market their technologies in the United State.

2.2.2 Background Mechanics of Intelligent Compaction

It is important to understand the term “material stiffness” as it is the conceptual basis for intelligent compaction. The stiffness is calculated continuously, around 30 to 60 times per second, as a function of the acceleration or force of the roller drum and the displacement of the material that is being compacted. In general, stiffness is totally a function of internal friction or aggregate interlocking of the pavement materials. In this situation, the underlying material is considered as a rigid or semi-rigid solid foundation.

CONCEPT OF STIFFNESS AND MODULUS

The fundamental definition of stiffness is the ratio of the force applied to the material by a loaded area and the resulting displacement experienced by the loaded area. Stiffness (k) is expressed in units of force per unit length (kN/m). Soil modulus is defined as the applied force per unit area of the loaded plate since it is not the slope of the stress-strain curves of the material under pressure *(6)*. Its unit is expressed as (kN/m^2). The loaded plate area could be square, circular or in the shape of a ring. For the case of a circular plate having a diameter of D, the soil modulus can be expressed as:

$$E = f\left(k/D \right) \qquad \text{Equation 2.1}$$

This relation shows that modulus is a material property while stiffness is not a soil property and depends on the size of the loaded area. Therefore, for an elastic material, stiffness measurement of a particular material will vary from one test to another. But, modulus of an elastic material is more or less the same for all tests performed and is the best way to evaluate the material behavior.

OBTAINING THE STIFFNESS kB USING IC ROLLER

A dynamic soil compactor produces nonlinear oscillations during compaction. The characteristics properties of a nonlinear oscillation can be described by an analytical procedure (14). Figures 2.3 and 2.4 describe a theoretical, lumped parameter model of the interaction between a vibratory roller and the underneath material. The soil-drum-interaction force (FB) is defined as follows:

$$F_B \cong -m_d \ddot{x}_d + m_u r_u \Omega^2 \times \cos \ \Omega t \ + \ m_f + m_d \ \times g \qquad \text{Equation 2.2}$$

where,

m_d = mass of the drum (kg);

x_d = vertical displacement of the drum (m);

$\ddot{x}_d$ = acceleration of the drum (m/s^2);

m_f = mass of the frame (kg);

m_u = unbalanced mass (kg);

r_u = radial distance at which m_u is attached (m);

$m_u r_u$ = static moment of the rotating shaft (kg.m); and

$\Omega = 2 \cdot \pi \cdot f$;

f = frequency of the rotating shaft (Hz)

t = time elapsed, (sec)

g = acceleration due to gravity (m/sec^2)

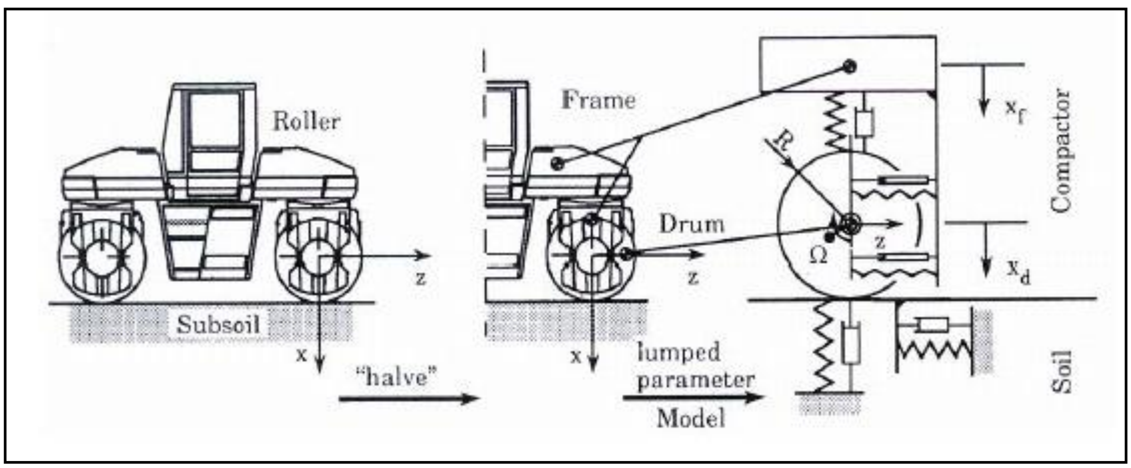

FIGURE 2.3: Theoretical, Lumped parameter model of interaction between a vibratory roller and underneath material, (15)

In equation 2.2, the downward force is always considered as positive and the inertia force, $m_d\ddot{x}_d$ is should be directed negatively. If the subsoil is considered as spring and dashpot system, the soil-drum interaction force can also be expressed as:

$$F_B \cong k_B x_d + d_B \times \dot{x}_d \qquad \text{Equation 2.3}$$

Where,

k_B= Stiffness of the soil, (kN/m);

d_B = Damping coefficient, (kN.s/m) (a damping ratio of 0.2 is assumed);

and

$\dot{x}_d$= Velocity of the drum, (m/s).

The acceleration of the roller drum and the phase angle between excitation and oscillation can also be measured. Measuring oscillation will help to calculate F_B by using equation (2.2). As all the quantities are known on the right hand side of the equation, the stiffness value can be obtained by combining equation (2.2) and (2.3).

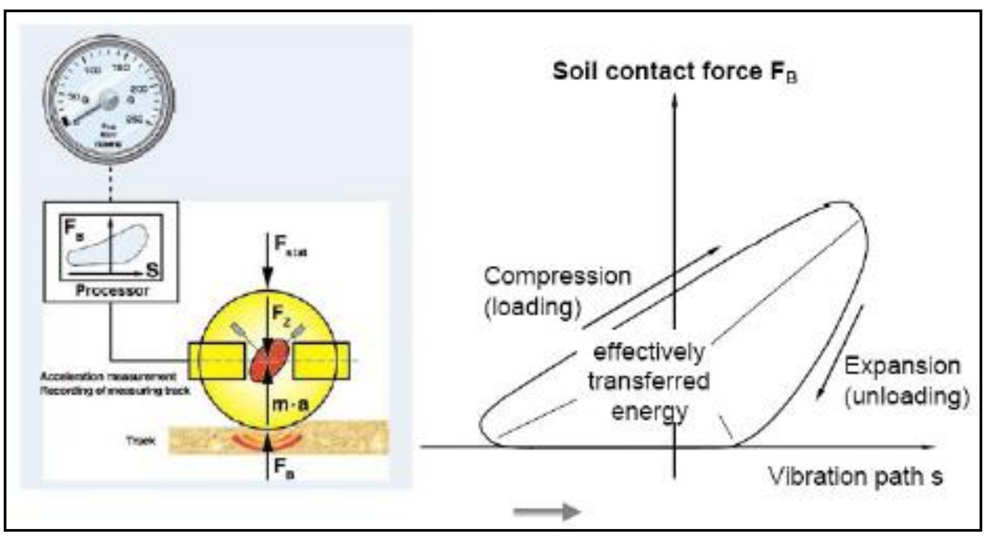

FIGURE 2.4: Loading loop due to applied force on the roller drum, (7)

Alternatively, the force settlement curve can be plotted, as shown in Figure 2.5, and the slope of the curve on the loading portion can be calculated as the dynamic stiffness of the material being compacted.

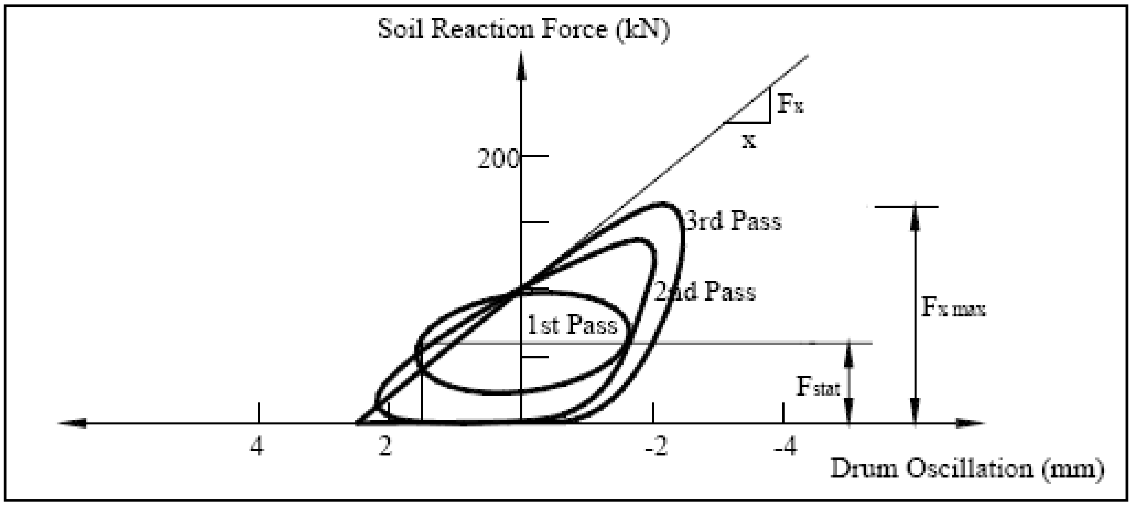

FIGURE 2.5: Soil reactions vs. roller amplitudes (after 7)

OBTAINING THE MODULUS, E

As mentioned earlier, the soil stiffness is a dependent parameter and modulus E is an independent parameter. Thus it is necessary to obtain soil modulus E from the soil stiffness value. This problem was solved by Hertz in 1895 and further developed by Lundberg in 1939. Hertz and Lundberg postulated the relationship between the load on the roller and the imprint area created by the roller on an elastic half space. Thus this solution was used to develop the relationship between the stiffness k_B and soil modulus, E.

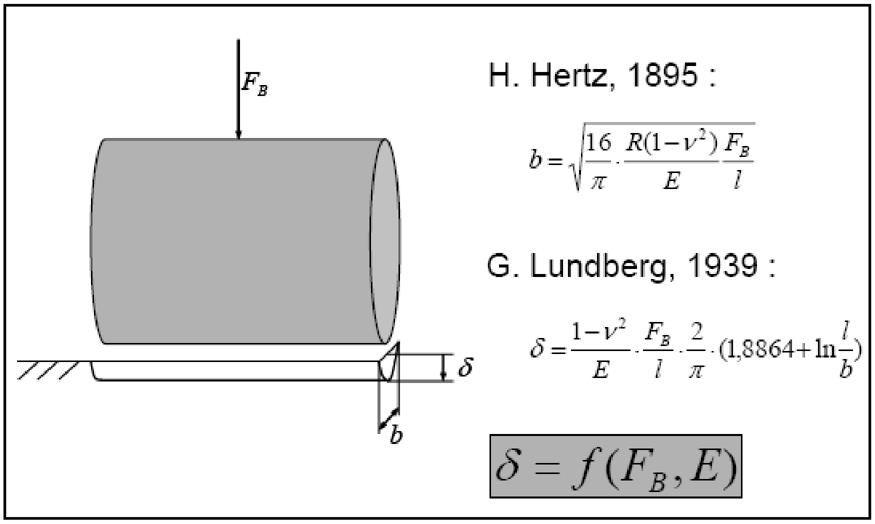

FIGURE 2.6: Hertz (1895), and Lundberg (1939) solution for modulus (7)

The relation between the stiffness and the modulus can be expressed as:

$$k_B = \frac{E_{VIB}\cdot L\cdot\pi}{2\cdot(1-\nu^2)\cdot\left(2.14+\frac{1}{2}\cdot\ln\left[\frac{\pi\cdot L^3\cdot E_{VIB}}{(1-\nu^2)\cdot 16\cdot(m_f+m_d)\cdot R\cdot g}\right]\right)} \qquad \text{Equation 2.4}$$

Where, L is the drum width, ν is Poisson's ratio, ln is natural logarithm, m_f and m_d are the masses contributed by the frame and the drum of the roller, R is the radius of the drum, and g is the acceleration due to gravity. Knowing k_B, Equation (2.4) gives E_{VIB}.

The relationship between the stiffness k_B and soil modulus, E was also established on an experimental basis. The experiments were performed by testing the IC roller and the plate load test in parallel. Figure 2.7 shows the relationship obtained between the roller stiffness k_B and soil moduli M_{E1} and M_{E2} form the first load and the reload of the plate load test.

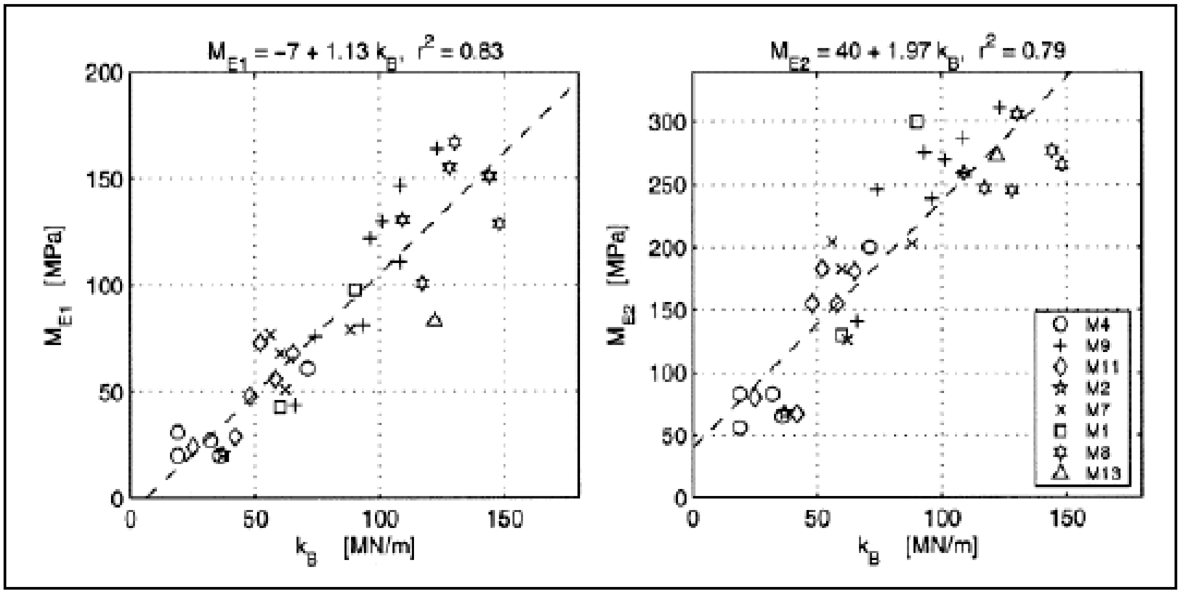

FIGURE 2.7: Relationship between stiffness and modulus (6)

2.2.3 Compaction Measurement and Documentation Systems of IC Roller

The intelligent compaction roller has a powerful range of compaction of all types of material used in the earth and rock works because of the adjustable amplitude. The instant and continuous adjustment of amplitude and compaction energy produces maximum compaction per pass and also avoids loosening of the surface especially on gravel, sand and anti-frost layers. Currently intelligent compaction rollers are marketed by BOMAG, AMMANN and Geodynamik. This section will briefly describe the working principles and compaction measurement and documentation system of the BOMAG IC roller used in this study.

2.2.3.1 Measurement System

The BOMAG measurement system E_{VIB} meter (BEM) and the Terrameter BTM plus/BTM prof are used as an integrated system for continuous assessment of compaction. BOMAG compaction measurement systems are used to support the roller operator to optimize the construction schedule as well as surface area dynamic compaction control. BOMAG measuring system consists of

- Two acceleration transducers
- Distance measuring unit
- Electronic unit
- E_{VIB} analogue display (for BEM) and BOMAG operation panel (BOP) as operation and control unit (for Terrameter BTM plus/BTM prof).
- Printer as standard for the Terrameter BTM plus/BTM prof.

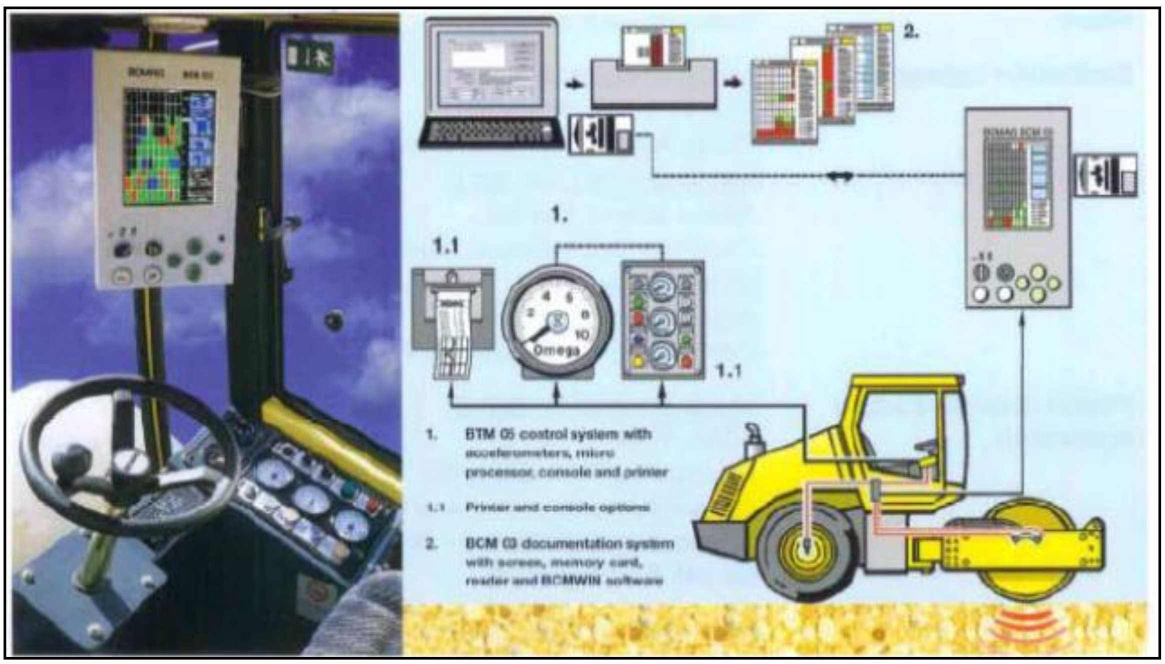

FIGURE 2.8: BOMAG measurement and documentation system, (2)

The BOMAG BCM 05 compaction management system is used as a supplement to the BOMAG compaction measurement systems on single drum rollers (BEM, and the Terrameter BTM plus/BTM prof). BCM 05 includes tablet PC with touch screen (Pentium *III*), USB memory stick, 128 MB suitable for measuring 100,000 m^2 and BCM 05 mobile and BCM 05 office software.

2.2.3.2 Measurement Principle

BVC (BOMAG VarioControl) single-drum roller is equipped with the BOMAG Vario Vibration system. This system generates the linear vibration of the roller drum. The direction of vibration is adjusted progressively between vertical and horizontal direction. Adjustment of the direction of vibration significantly influences the transmitted compaction energy. VARIOCONTROL has the capacity to use much larger amplitudes than the conventional vibratory roller. Figure 2.9 shows the automatic adjustment of the compaction energy in response to the soil conditions and the display of the compaction results and documentations.

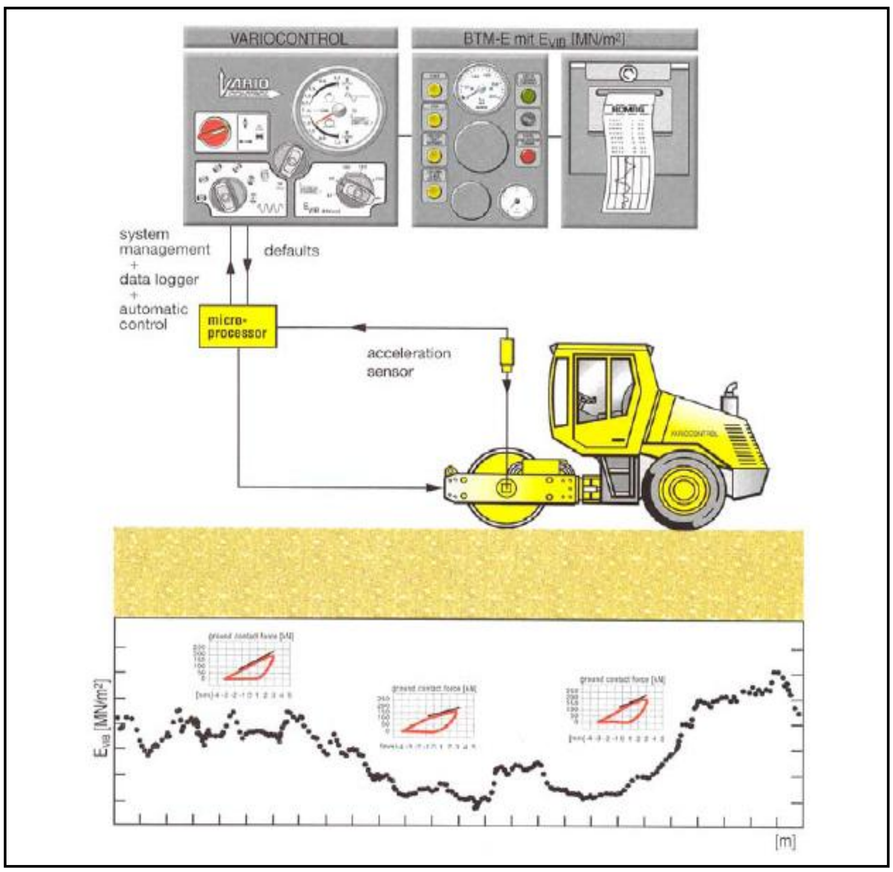

FIGURE 2.9: BOMAG Intelligent Compaction System, (2)

BOMAG compaction measurement systems use the reciprocal effect of the acceleration of the vibrating drum and the dynamic stiffness of the soil that generally increases with compaction. The energy required for the compaction of soil is defined by the soil itself, its layer thickness, the sub-base and the degree of compaction as well as the resulting soil stiffness *(2)*. With increasing stiffness of the soil, the contact force also increases. Two accelerator sensors record and evaluate the stiffness developed and continuously measure the dynamic behavior of the roller drum. This information is used for the automatic adjustment of the vibration direction of the roller drum.

The measuring systems record the acceleration and determine the contact force acting between the soil and the drum as well as the vibration amplitude of the roller body. During application of the contact force, a loading and unloading curve is developed for each revolution and the enveloped area of the loading-unloading curves represents the compaction energy released during compaction. The E_{VIB} value is calculated from the analysis of the loading curve.

The different position of the acceleration transducer is set to maintain the degree of compaction in the field. The vertical direction gives the maximum energy available for the roller and used in higher depth of compaction. The angled position results in moderate compaction output while the horizontal position of the transducer gives the minimum lever of compaction. The minimum energy available from the horizontal direction improves compaction close to the surface and reduces loosening (Figure 2.10).

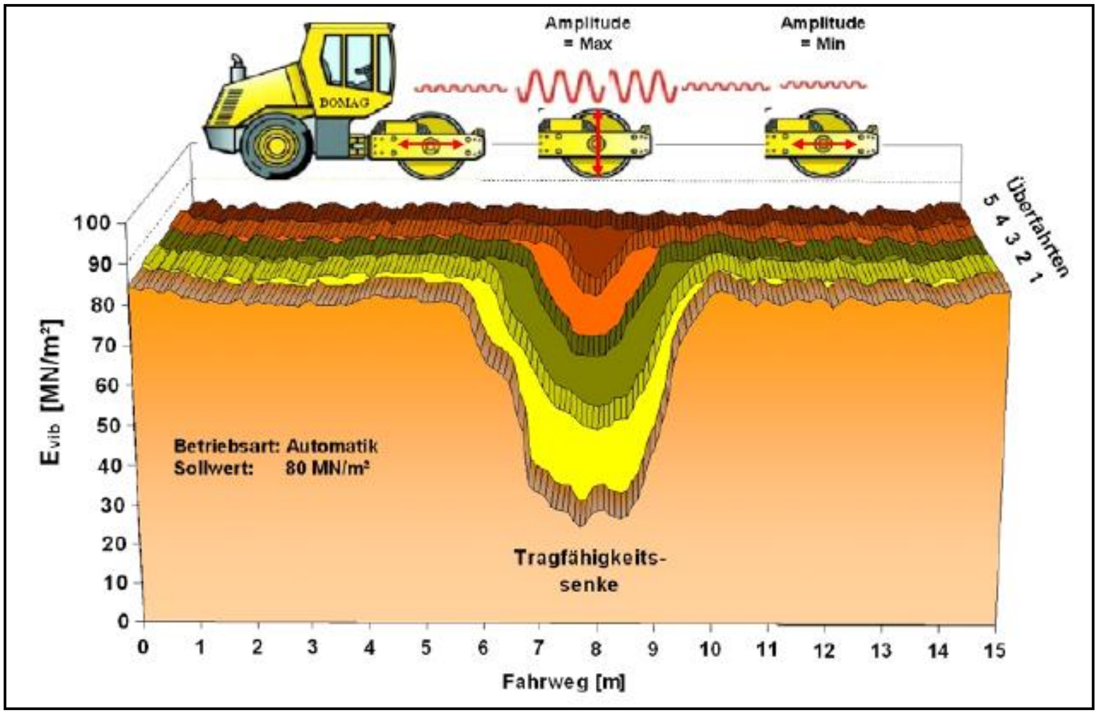

FIGURE 2.10: Direction of applied vibration to optimize compaction, (7)

CHAPTER 3 - FIELD TESTING AND DATA COLLECTION

3.1 General

FHWA acknowledged that compaction is an important factor for all pavement materials. Hence, emphasis should be placed on the proper densification of all pavement layers including subgrade soils, granular base and asphalt pavements. In addition, an understanding of the compaction model shows that the proper compaction of each layer depends on the proper densification of the underlying layer. If one or all of the pavement foundation layers lack sufficient stiffness, it will be more difficult or sometimes totally impossible to properly compact the layer on top of it.

In recent years, it has been proven that intelligent systems are comprehensive products where different technologies are integrated into a single product to work together. Intelligent products can make a conventional product perform its function more effectively and also can add capabilities to a product through sensing and mechanical and/or software improvements.

3.2 Description of Test Section

Two pavement reconstruction projects, one on US-56 and one on I-70, were selected for this study. The US-56 project had two 328 ft (100 m) sections. The first section was a “proof” section that had already been compacted by a conventional roller. IC roller stiffness measurements were made after one pass of the roller. The other section was a “growth” section that was compacted by the IC roller using multiple passes and densities were “built” up. The I-70 section had only one 328 ft (100 m) “growth” section. The stiffness on both “growth” sections were measured at each pass and compared with that obtained for the previous pass. A decrease in stiffness between two consecutive passes was meant to be the end of compaction. The target density and corresponding moisture content of the “growth” test sections were those required by the project special provisions. No proof rolling was performed on any of these test sections.

3.2.1 Laboratory Testing

Soil samples were collected at 16.5 ft (5 m) intervals on all sections. The soil samples were tested for gradation, Atterberg limits (unsuccessfully) and moisture-density relationships in the laboratory. Soil samples were also collected for in-situ moisture content determination by the gravimetric method in the laboratory. Typical results have been tabulated in Table 3.1. Figure 3.1 shows the moisture-density curves on the three test sections obtained from the standard Proctor tests. Both projects have sandy (SP or A-3) soils. Other relevant soil characteristics are shown in Table 3.1.

TABLE 3.1: Test Section Soil Characteristics

Project	US-56 Proof	US-56 Growth	I-70 Growth
% Passing # 200 Sieve (%)	4.2	6.8	8.4
Coefficient of Uniformity, C_u	2.1	4.7	4.2
Coefficient of Curvature, C_c	1.25	0.67	1.6
Soil Classification (AASHTO)	A-3	A-3	A-3
Plasticity	NP	NP	NP
Avg. In-situ Moisture content (%)	6.4	5.6	8.98
Optimum Moisture Content (OMC), (%)	10.4	10.2	11.7
Target moisture content (%)	5.4-15.4	5.2-15.2	6.7-11.7
Maximum Dry Density, MDD, (kg/m^3)	1916.0	2012.0	1838.8
Target dry density, (kg/m^3)	1820	1911	1747
Poisson’s ratio	0.35	0.35	0.35

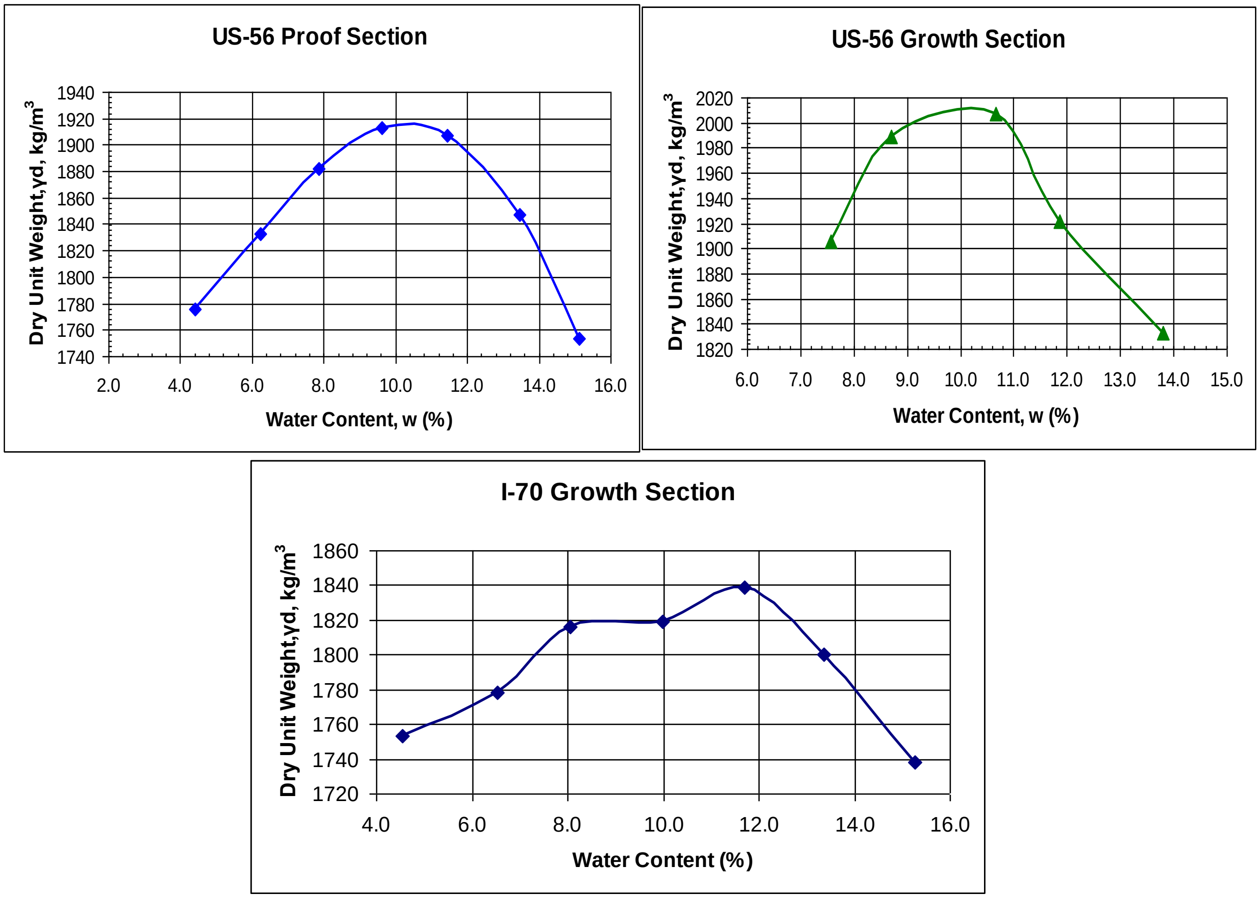

FIGURE 3.1: Moisture-Density curves from Standard Proctor Test

3.3 IC Roller Description

The IC roller used in this study was a Bomag VARIOCONTROL (BVC) single drum vibratory roller (Model BW 213 DH-4 BVC) as shown in Figure 3.2. The roller had a gross weight of 31,976 lbs (14,505 kg) and the weight on the single axle, steel drum was 20,283 lbs (9,200 kg). The working width was 83.9 inch (2130 mm). The speed of the roller was 0 to 8.1 mph (0-13 kmph). The vibration frequency was 1,680 vpm (28 Hz) and the amplitude was 0 to 0.094 inch (0-2.4 mm). The centrifugal force produced was 83,215 lbs (365 kN).

In this study, E_{VIB} data was continuously collected over the test sections. On the "proof' section on US-56, BVC stiffness data was collected after one pass of the roller. For the "growth" sections, E_{VIB} data was collected for each pass of the roller.

FIGURE 3.2: BVC roller compaction on a test section on US-56 near Hugoton, Kansas

3.4 In-situ Testing and Data Collection

In-situ testing was performed for the quality control of compaction. It involved some spot tests such as, Geogage for stiffness measurement, Falling Weight Deflectometer (FWD) and Light Falling Weight Deflectometer (LFWD) for modulus testing, the Nuclear Gage for density and in-situ moisture testing, and Dynamic Cone Penetrometer (DCP) for measuring the California Bearing Ratio (CBR). These methods are routinely used in compaction control and/or measuring soil stiffness characteristics.

3.4.1 Density and Moisture Measurements

The in-situ density measurements were done by a nuclear gage (Figure 3.3). Measurements were taken at 16.5 ft (5 m) intervals on all sections. In-situ moisture was also measured on those test sections locations using the nuclear gage. As mentioned earlier, soil samples were also collected for in-situ moisture content determination by the gravimetric method in the laboratory.

FIGURE 3.3: In-situ moisture and density measurement using nuclear gage on I-70

3.4.2 Stiffness, Deflection, and Cone Penetration Tests

The Geogage, Falling Weight Deflectometer (FWD), Light Falling Weight Deflectometer (LFWD) and Dynamic Cone Penetrometer (DCP) measurements were made at 16.5 ft (5 m) intervals. For the US-56 “proof” section, tests were done after one pass of the BVC roller. For the “growth” sections, tests were done after the final pass of the BVC roller.

3.4.2.1 Geogage

The soil stiffness gage or Geogage is a portable, nondestructive, and non-nuclear device that was used to measure the soil stiffness. It was 0.8 ft (250 mm) in height, resting on a 0.9 ft (280 mm) diameter base, and weighed about 22 lbs (10 kg). The base was a rigid ring-shaped foot on the soil surface. The applied force and the displacement-time history were measured by two velocity sensors. According to the manufacturer, the geogage vibrates and produces small changes in vertical force with displacement within the 6,000 to 12,000 vpm (100 to 200 Hz) frequencies. The in-situ soil stiffness was measured at each frequency and then finally, the average value was recorded. It measured stiffness up to 0.7 to 1 ft (220 to 310 mm) of depth from the contact surface. The geogage stiffness can also be used to determine the Young's modulus (*16)*. Figure 3.4 shows the in-situ stiffness measurement on US-56 "growth" section after the final pass of the IC roller.

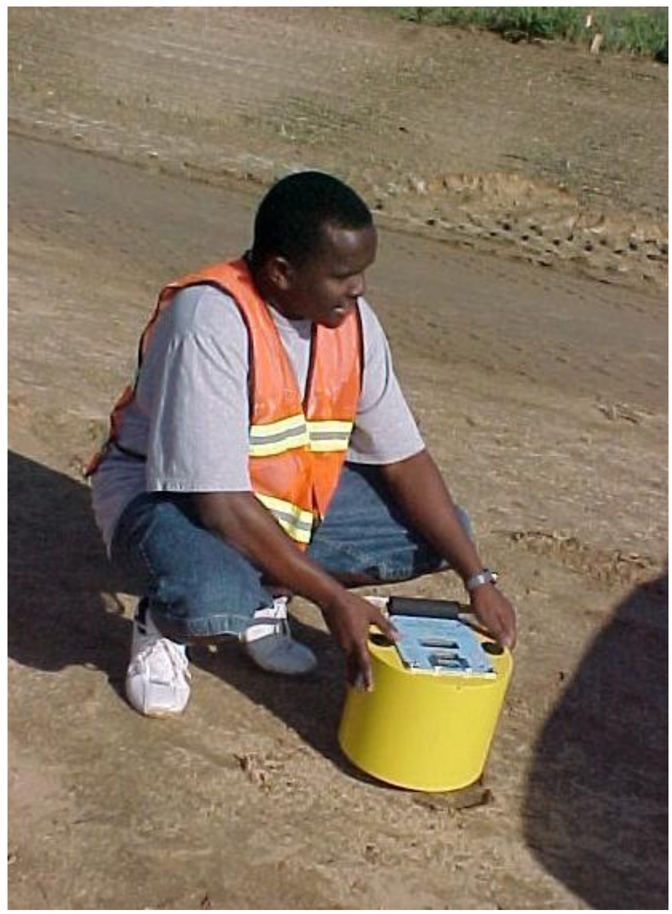

FIGURE 3.4: Stiffness measurements by Geogage, on US-56 section

3.4.2.2 Falling Weight Deflectometer (FWD)

The Dynatest model 8000 FWD system was used in this study to obtain the in-situ deflection data. The impulse force was created by dropping a target mass of 2500±200 lbs (1134±91 kg) from a certain height. This load level was recommended by George (*17*) for bare subgrade testing using an FWD. The load was transmitted to the subgrade through a load plate with a diameter of 18 inch (457 mm) to provide a load pulse in the form of a half sine wave with a duration of 25 to 30 ms. The load magnitude was measured by a load cell. Figure 3.5 shows the deflection measurements made by FWD device on the US-56 “proof “section.

FIGURE 3.5: Deflection measurements on US-56 section by FWD

Deflections were measured using seven sensors mounted on a bar that was lowered on to the pavement surface automatically with the loading plate. One of the sensors was located at the center of the plate while the other six were located at a radial distance of 12 inch (305 mm) center to center. The measured deflections at different stations were used to back-calculate the modulus of the subgrade soil. There are some general techniques that match the measured deflections with those calculated from theory. Example computer programs that make use of this technique include EVERCLAC 5.0, MODCOMP and MODULUS 6.0. In this study, EVERCALC 5.0 was used to backcalculate the subgrade modulus from the in-situ deflection data. In most cases, full deflection basin was used. In several instances, the seventh sensor data was ignored since the deflection recorded by this sensor was more than the sixth sensor. Figure 3.6 shows the normalized deflection basin plotted during backcalculation.

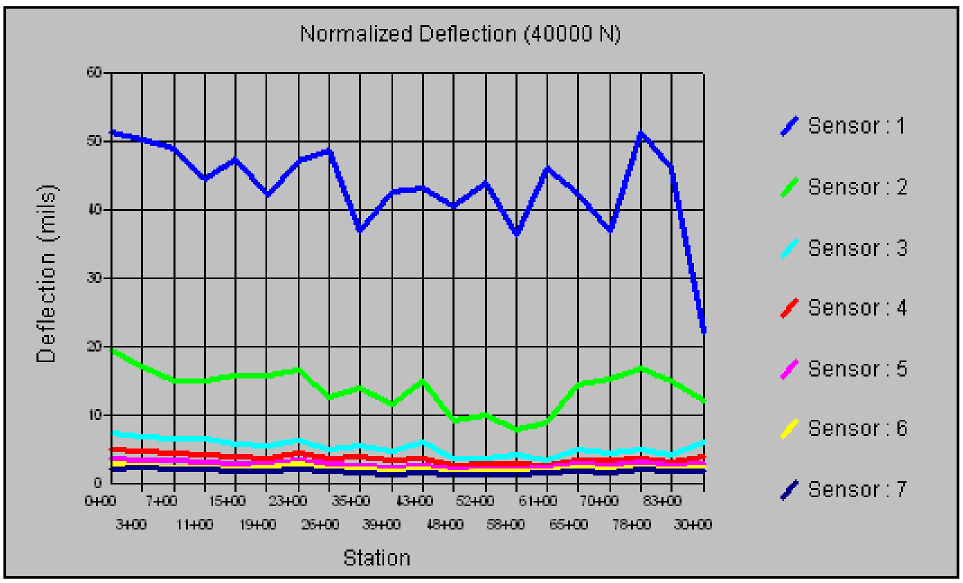

FIGURE 3.6: Normalized deflection basins on US-56 section (station 15+00) by EVERCALC 5.0

In a few cases, the whole basin was discarded when the root-mean square (RMS) error in backcalculation was deemed too high. The first sensor deflection was also used to backcalculate the subgrade soil elastic modulus from the Boussinesq equation shown later.

3.4.2.3 Light Falling Weight Deflectometer (LFWD)

Recently hand-held, falling weight deflectometer devices have become available for surface deflection measurements. The Prima 100 LFWD device was used to evaluate the in-situ soil modulus in this study. Figure 3.7 shows the LFWD testing on the I-70 test section to measure in-situ deflection.

The device consisted of four major parts: sensor body, loading plate, buffer system, and the sliding weight. The sensor body enclosed both the load cell and the geophone. The loading plate, buffer system and the sliding weight were attached to the sensor body. A 12 inch (300 mm) diameter steel loading plate, which also doubled as the sensor body, was used in this study. The LFWD device measured both force and deflection. The elastic modulus of the subgrade soil was calculated from the surface deflection using the following Boussinesq equation:

FIGURE 3.7: Deflection measurements by LFWD on I-70 section

$$E_{LFWD}(0) = \frac{k \cdot (1-\nu^2) \cdot \sigma_o \cdot a}{d_o} \qquad \text{Equation 3.1}$$

Where,

E_{LFWD} = LFWD modulus (MPa);

$k = \frac{\pi}{2}$ and 2 for rigid and flexible plate, respectively;

d_o = deflection at center (μm);

σ_o = Applied stress (kPa);

ν = Poisson's Ratio; and

a = plate diameter (mm).

In this study, a rigid plate was assumed during modulus calculation from the Boussinesq analysis.

3.4.2.4 Dynamic Cone Penetrometer (DCP)

Dynamic Cone Penetrometer was initially developed in South Africa as an in-situ pavement evaluation technique for continuous measurement with the depth of pavement layers and subgrade soil parameters (*18*). Since then this device has been used extensively in South Africa, United Kingdom, US, Australia and many other countries because it is simple, economical, and less time consuming than most other available methods. The DCP used in this study was provided by Managing Technology, Inc., Overland Park, Kansas to KDOT in the early nineties. The KDOT DCP consisted of a slender steel rod with a cone tip at the end (Figure 3.8). The cone tip was made of hardened steel and was angled at 30^0 with a diameter at its head of 0.8 inch (20 mm). The hammer which slided down the steel rod had a height of 23 inch (575 mm) and weighed 18 lbs (8 kg). The unit had two aluminum blocks and a reference beam that aided in measuring the penetration depth during testing. For subgrade evaluation in this study, the DCP was penetrated down from the top of the compacted subgrade. During testing, the number of blows vs. depth was recorded. The "DCP value" was defined as the slope of the blow vs. depth curve (in mm per blow) at a given linear depth segment.

FIGURE 3.8: DCP testing on I-70 test section in Kansas

Correlation between DCP and CBR: The California Bearing Ratio (CBR) test measures the static penetration resistance of a soil as a function of penetration of a cylinder prior to reaching the ultimate shearing value of the soil. The CBR is defined as a percentage determined by the ratio of the resistance in psi at 0.1 inch (2.5 mm) penetration of the soil under test to the resistance of a standard, well graded, crushed stone at the same penetration .1 inch (2.5 mm), and then multiplied by 100. This standard penetration stress is usually taken to be 1,000 psi (6,895 kPa).

In order to assess the structural properties of the pavement subgrade, the DCP values are usually correlated with the CBR of the pavement subgrade soil *(19):*

$$\log CBR = 220 - 0.71 \times \log DCP^{1.5} \qquad \text{Equation 3.2}$$

(R^2 = 0.95, N = 74)

where the DCP is in mm per blow.

This relationship was verified for a wide range of pavement and subgrade materials *(18)*. Additional laboratory and correlation work conducted at the University of Kansas *(19)* and by the U.S. Army Corps of Engineers (Waterways Experiment Station) *(20)* generally supported the relationship described in Equation (3.2), but indicated considerable data scatter. It was recommended the DCP limit of 1.0 inch/blow (25 mm/blow) be correlated to a CBR of 8 for the silty/clay soils although the actual DCP value of the soil was way above this limit *(14)*. After calculating the CRB values, the modulus of soil was calculated using CBR-modulus relationship proposed by M-EPDG *(21)*. The proposed relationship is as follows:

$$M_r = 2555 \times CBR^{0.64} \qquad \text{Equation 3.3}$$

Where,

M_r =Resilient modulus of soil in psi

CBR = California Bearing Ratio

CHAPTER 4 - RESULTS AND DISCUSSION

4.1 General

As mentioned before, the in-situ stiffness of embankment soil was measured by Bomag IC roller. IC roller reports continuous measurement of soil stiffness along the entire test section. Stations at 16.4 ft (5 m) interval were marked along the test sections. Thus each 328 ft (100-m) test section had 21 test locations for discrete measurements by Geogage, FWD, LFWD, DCP and the nuclear gage. The Geogage measured soil stiffness values. Soil density and moisture measurements were obtained with the nuclear gage and speedy moisture tester respectively. The modulus values from the in-situ deflections measured by FWD were backcalculated using EVERCALC 5.0 backcalculation software. The modulus values were also backcalculated from the Boussinesq equation using the first sensor deflection data. This equation was again used to backcalculate the modulus from the LFWD deflection data. DCP values were used to calculate CBR values from the DCP-CBR correlation developed by the Corps of Engineers. Then the modulus value was calculated using the CBR-Modulus relationship in M-EPDG.

The variation of soil stiffness measured by the IC roller was examined along the test section. Stiffness variation with in-situ moisture content and percent compaction was also investigated. A statistical analysis was performed to obtain the point statistics of the stiffness/modulus value obtained from different testing methods. A correlation matrix among these stiffness/modulus values was also developed using the statistical software SAS. The following sections present the analysis and discussion of the results obtained from different tests.

4.2 BVC Stiffness on US-56 "Proof", "Growth" and I-70 "Growth" Sections

BVC stiffness (E_{VIB}) measurements were made after a single pass on a 328 ft (100 m) "proof" section on US-56 that had been compacted by a conventional vibratory roller. Other BVC stiffness measurements were taken on 328-ft (100 m) "growth" section on both US-56 and I-70 that had been compacted by the multiple passes of an IC roller. The results are shown in Figure 4.1.

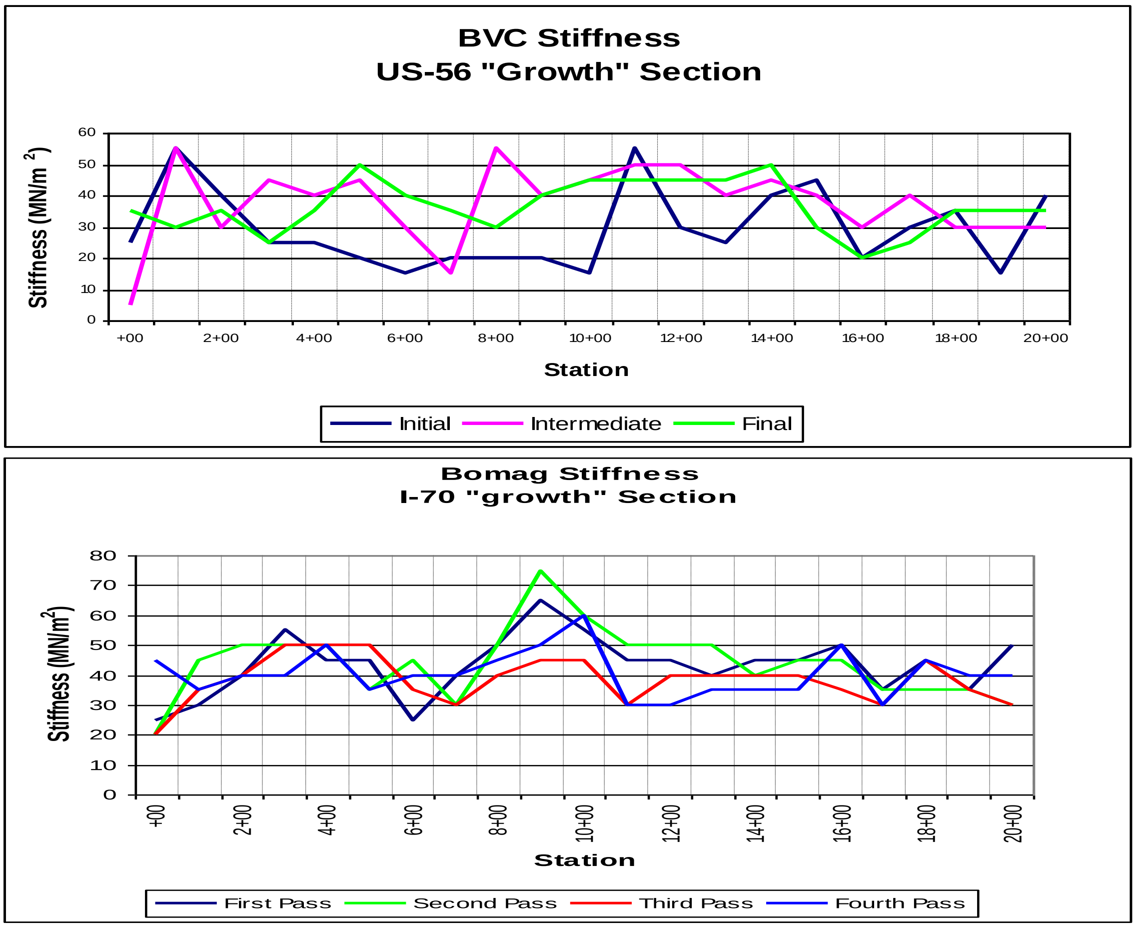

FIGURE 4.1: Stiffness developed and measured by IC roller on I-70 and US-56

The results in Figure 4.1 show that in general, density increases with multiple passes of the IC roller, but at a few locations density decreases. This phenomenon may happen due to presence of excess moisture at these locations.

On the US-56 “proof” section, mean IC stiffness (E_{VIB}) was 9 ksi (62 MPa) and it varied from 4 ksi (30 MPa) to 18 ksi (120 MPa). US-56 “growth” section showed a mean stiffness value of 5 ksi (36 MPa) with the range being from 2.9 ksi (20 MPa) to 7.25 ksi (50 MPa). On I-70, the mean E_{VIB} was 6 ksi (40 MPa), and it varied from 4 to 9 ksi (30 to 60 MPa). As shown in Figure 4.2 indicates, there were a number of soft spots along these small stretches of the embankment. Due to continuous measurement of the soil stiffness, it was possible for the IC roller to identify these locations.

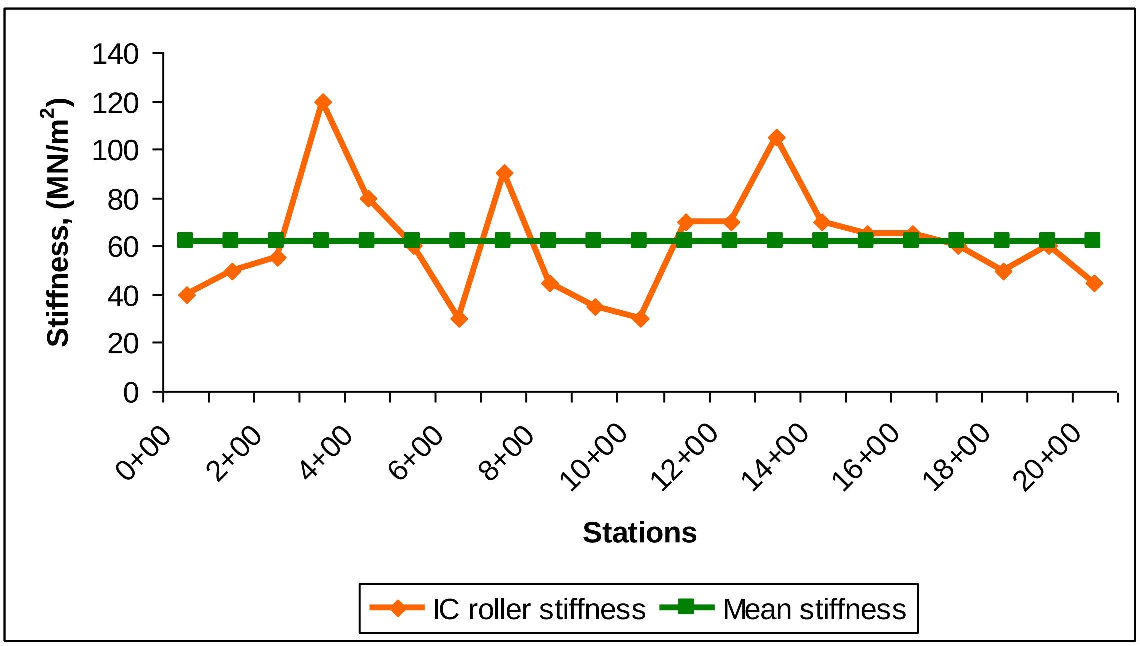

(a)

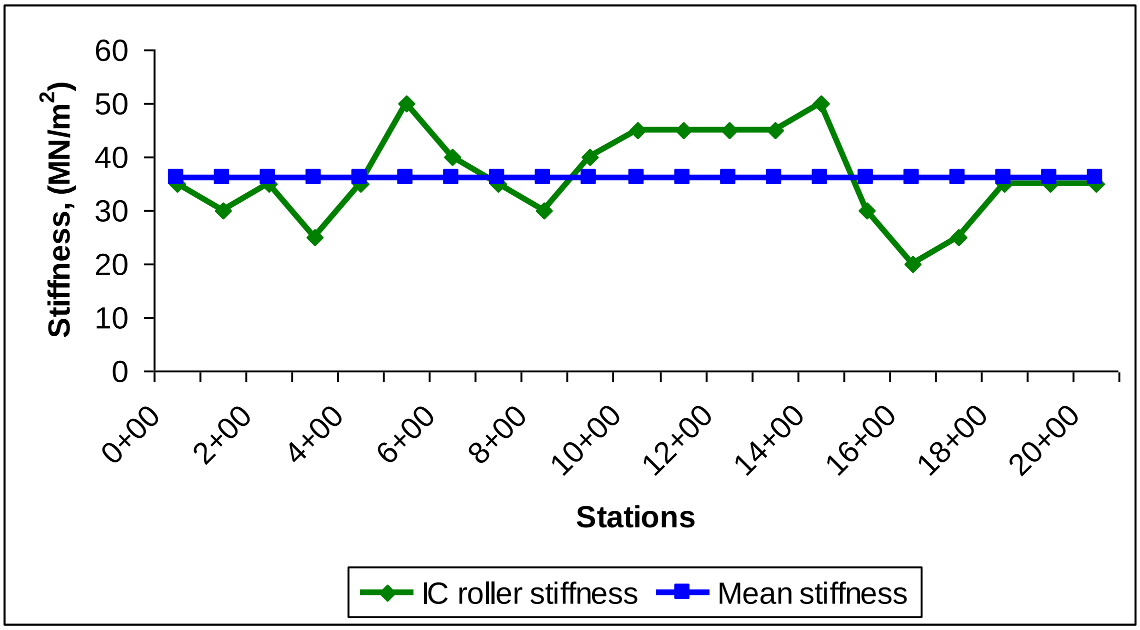

(b)

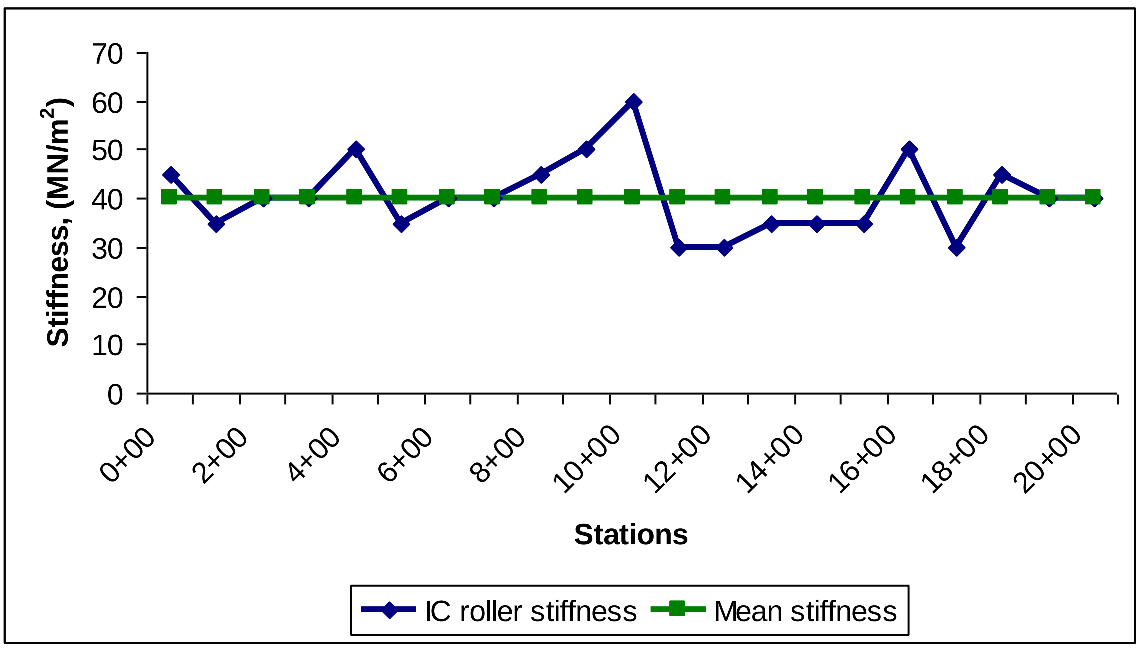

(c)

FIGURE 4.2: Spatial variation of IC roller stiffness on (a) US-56 "proof", (b) US-56 "growth" and (c) I-70 "growth"

4.3 Variation of IC Roller Stiffness with Moisture Content

Subgrade soil is susceptible to moisture variation after construction of the highway pavement. Briaud and Seo (*6*) have indicated that the soil at lower moisture content will have higher modulus values. This effect is more pronounced for the clay-type soil. On the other hand, density gives the compactness of the soil particles and determines how they are arranged in a given volume. But, unfortunately there is no correlation between the soil density and modulus, and the same density can be obtained for at least two different moisture contents (on either side of the standard Proctor compaction curve). That is why it is not possible to control soil compaction on the basis of the dry density alone. Figure 4.3 shows the relationship between the IC stiffness and the in-situ moisture content for the test sections on US-56 and I-70. The trends in these graphs clearly indicate that the IC roller stiffness was somewhat sensitive to the field moisture content. Higher moisture content resulted in lower vibration modulus.

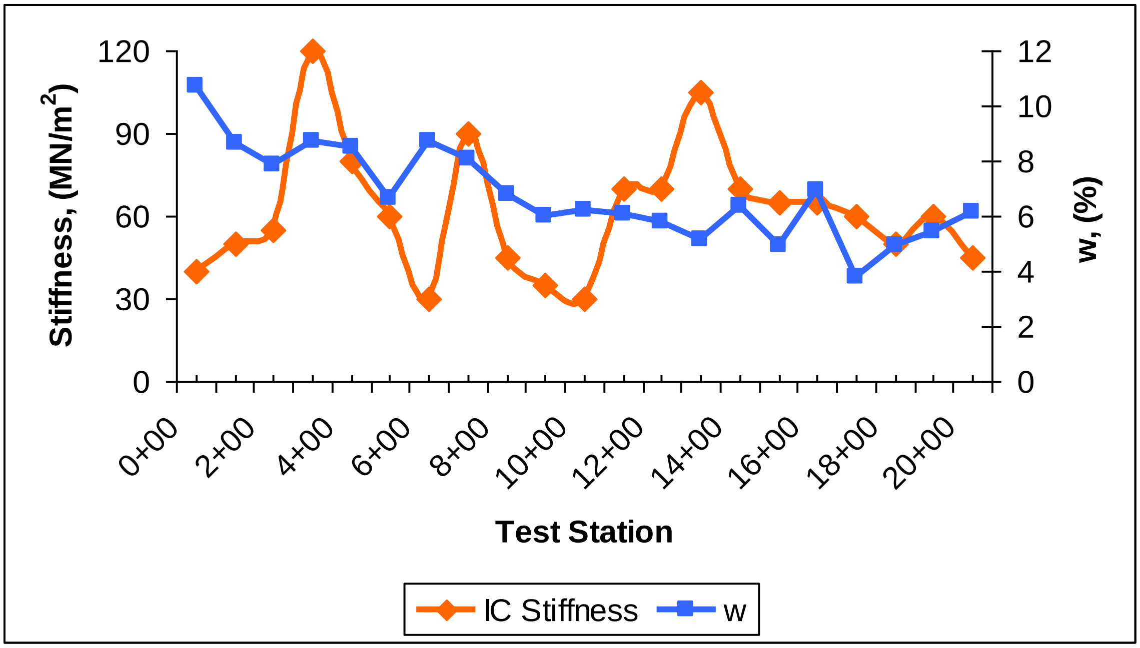
Stiffness, (MN/m^2)
w, (%)
Test Station
0+00
2+00
4+00
6+00
8+00
10+00
12+00
14+00
16+00
18+00
20+00
IC Stiffness
w

(a)

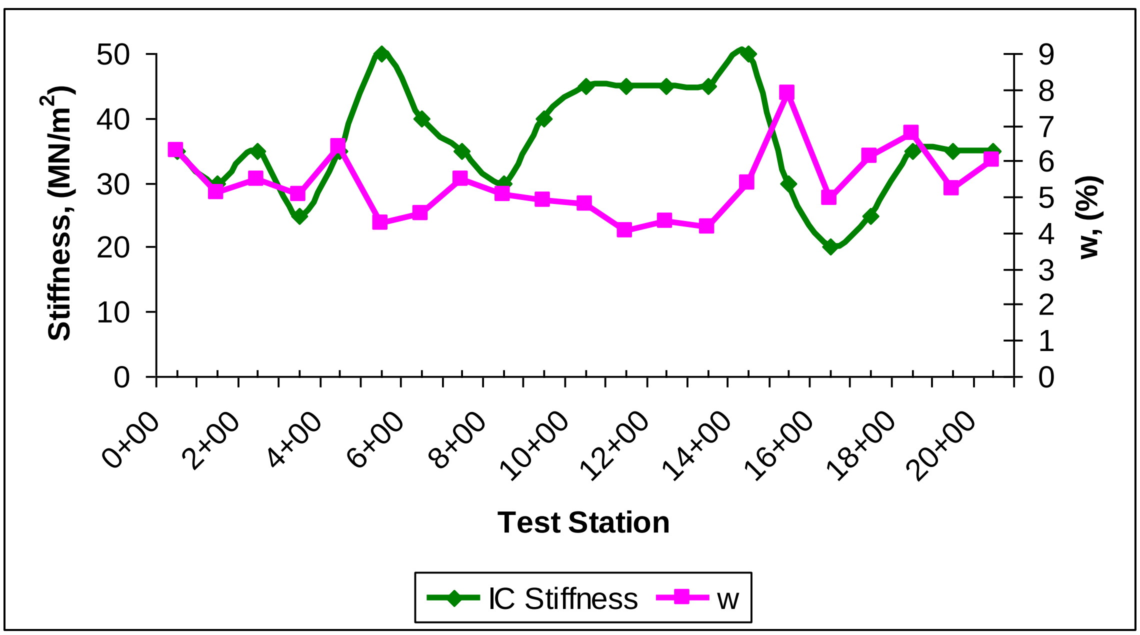
Stiffness, (MN/m^2)
w, (%)
Test Station
0+00
2+00
4+00
6+00
8+00
10+00
12+00
14+00
16+00
18+00
20+00
IC Stiffness
w

(b)

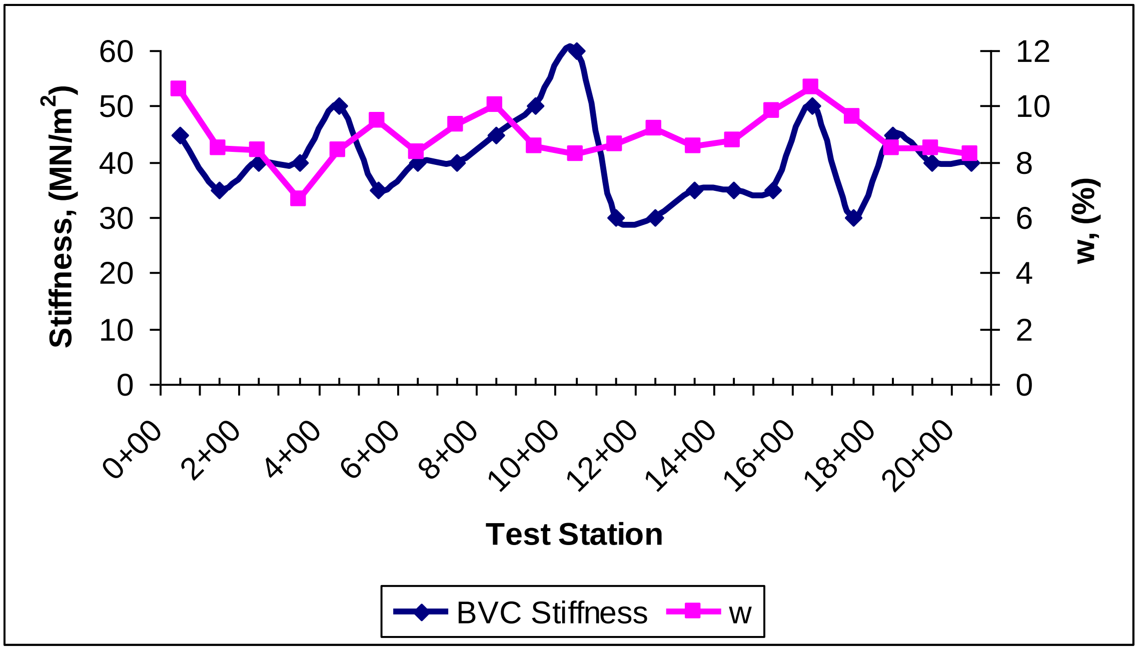

(c)

FIGURE 4.3: Variation of IC roller stiffness with in-situ moisture content on (a) US-56 "proof", (b) US-56 "growth" and (c) I-70 "growth" section.

In order to study the variation of in-situ stiffness developed by IC roller with field moisture content further, the moisture differential curve was also plotted. The moisture differential (Δw) was calculated by subtracting the field moisture content from the optimum moisture content (OMC) obtained in the laboratory from the standard Proctor test. Figure 4.4 shows the relationship between the IC roller stiffness and the deviation in in-situ moisture content (from OMC) for the test sections. The positive difference indicates the in-situ moisture content was below the optimum moisture content. The trends in these graphs clearly indicate that the IC roller stiffness, in general, is sensitive to the field moisture content. At moisture contents near the optimum, IC roller vibration modulus was generally higher.

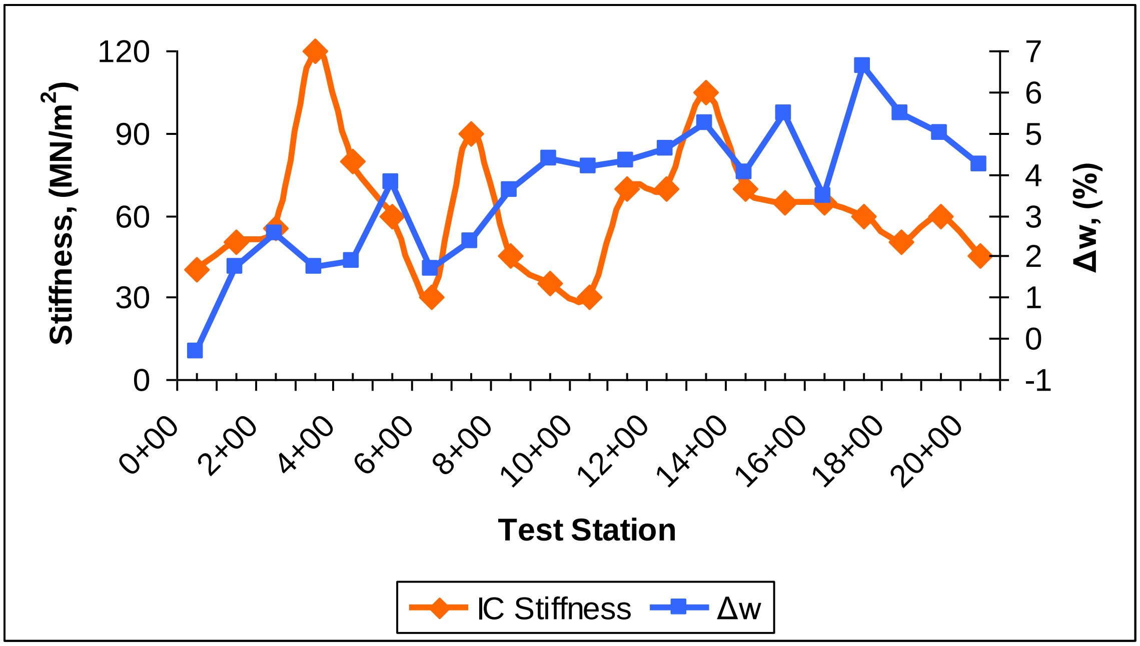

Stiffness, (MN/m²)
120
90
60
30
0
7
6
5
4
3
2
1
0
-1
Δw, (%)
0+00
2+00
4+00
6+00
8+00
10+00
12+00
14+00
16+00
18+00
20+00
Test Station
IC Stiffness
Δw

(a)

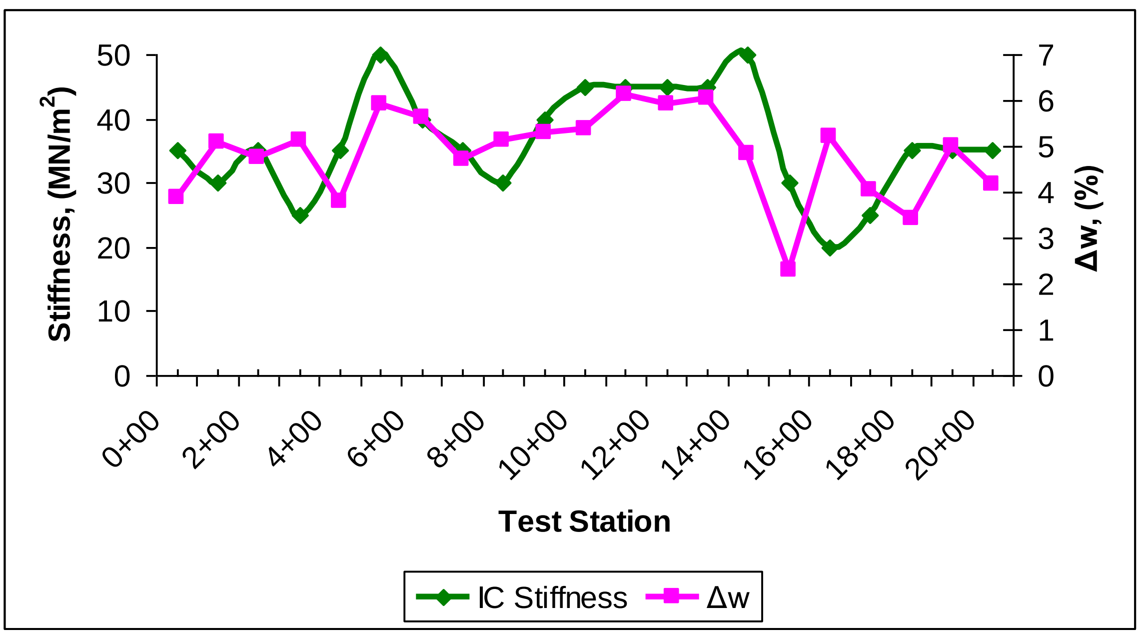

Stiffness, (MN/m²)
50
40
30
20
10
0
7
6
5
4
3
2
1
0
Δw, (%)
0+00
2+00
4+00
6+00
8+00
10+00
12+00
14+00
16+00
18+00
20+00
Test Station
IC Stiffness
Δw

(b)

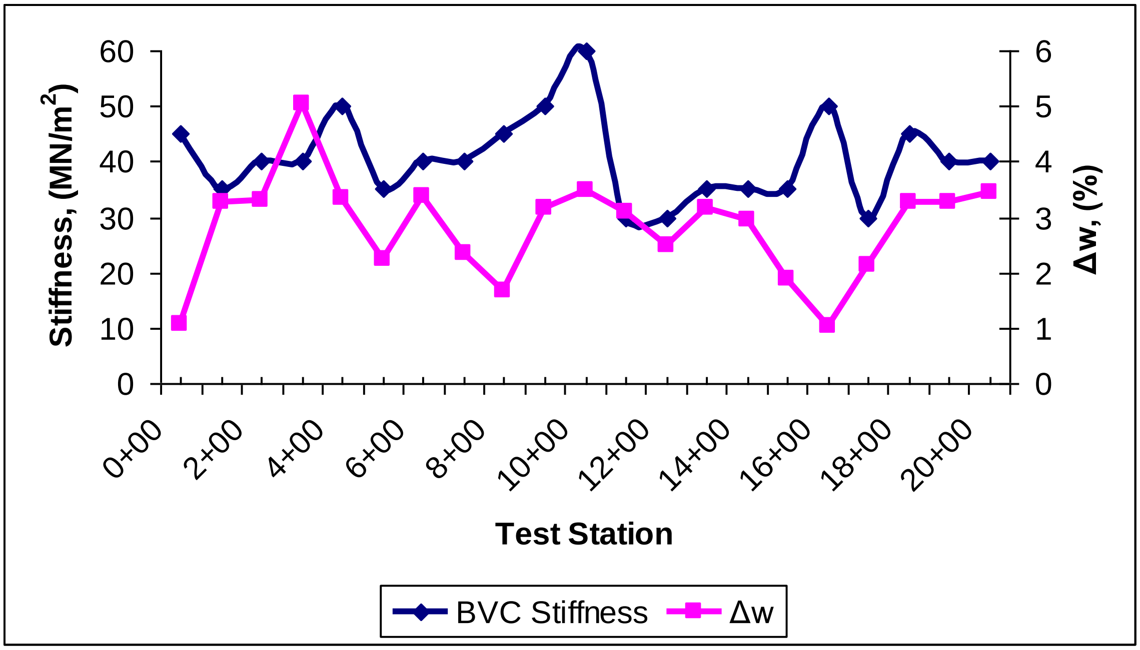

(c)

FIGURE 4.4: Variation of IC roller stiffness with moisture differential on (a) US-56 "proof", (b) US-56 "growth" and (c) I-70 "growth" section.

4.4 Variation of IC Stiffness with Compaction Level

The relationship between the in-situ dry density (obtained after compaction and expressed in terms of the maximum dry density from the standard Proctor test), and IC roller stiffness was also examined. This was done due to the fact that the current practice of embankment compaction control in Kansas is based on the percent compaction obtained from the maximum dry density (MDD) value in the standard Proctor test. The in-situ dry density is expressed in terms of percent compaction using the following relations:

$$\gamma_{d-in-situ} = \frac{\gamma_w}{1+w} \qquad \text{Equation 4.1}$$

Here,

$\gamma_{d-in-situ}$ =In-situ dry density

γ_w = In-situ wet density

w =In-situ moisture content (%)

Then, the % compaction is expressed as:

$$\%compaction = \frac{\gamma_{d-in-situ}}{\gamma_{d-SPT}} \qquad \text{Equation 4.2}$$

Where, γ_{d-SPT} = Laboratory dry density from Standard Proctor Test

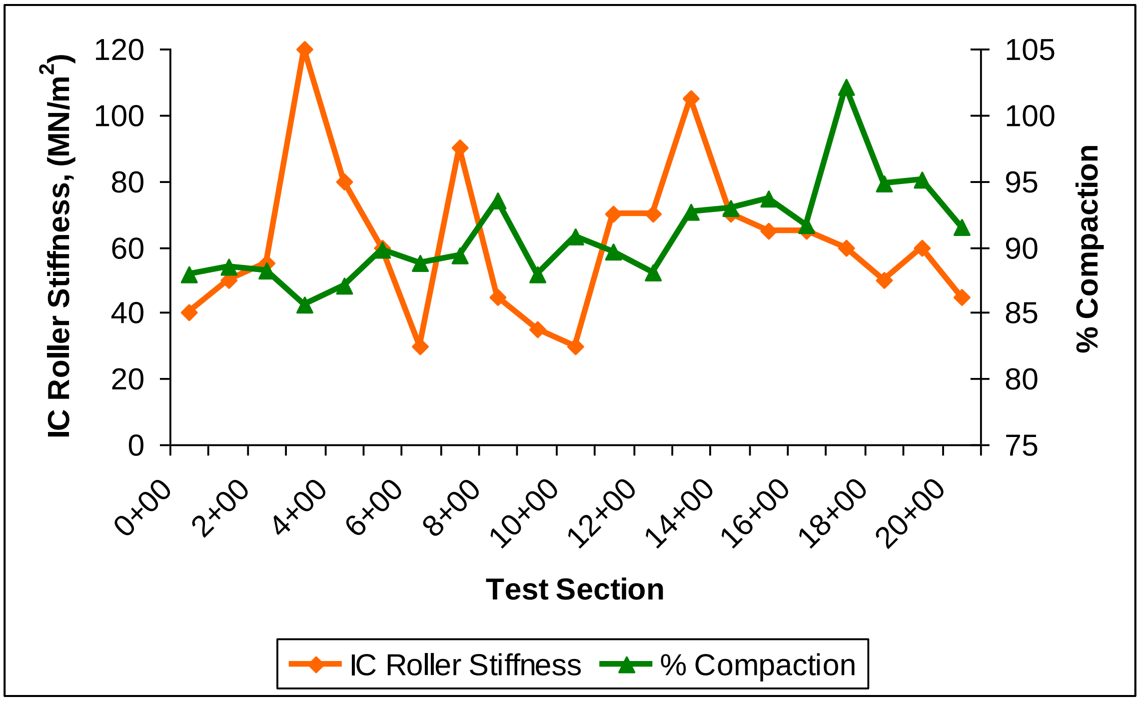

IC Roller Stiffness, (MN/m²)
120
100
80
60
40
20
0
105
100
95
90
85
80
75
% Compaction
0+00
2+00
4+00
6+00
8+00
10+00
12+00
14+00
16+00
18+00
20+00
Test Section
IC Roller Stiffness
% Compaction

(a)

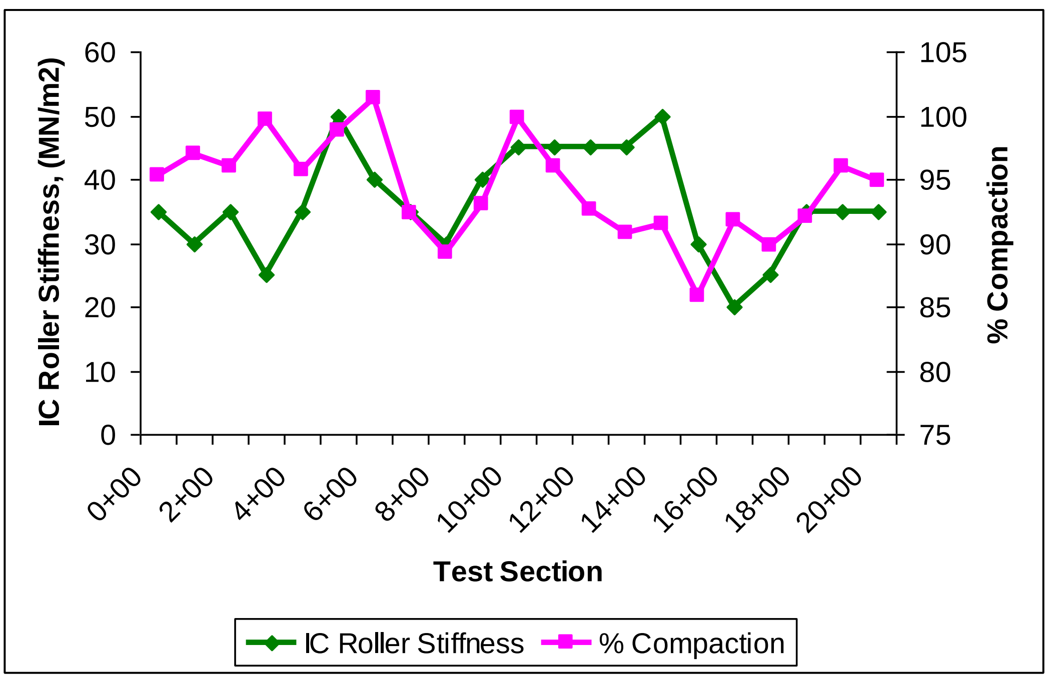

IC Roller Stiffness, (MN/m2)
60
50
40
30
20
10
0
105
100
95
90
85
80
75
% Compaction
0+00
2+00
4+00
6+00
8+00
10+00
12+00
14+00
16+00
18+00
20+00
Test Section
IC Roller Stiffness
% Compaction

(b)

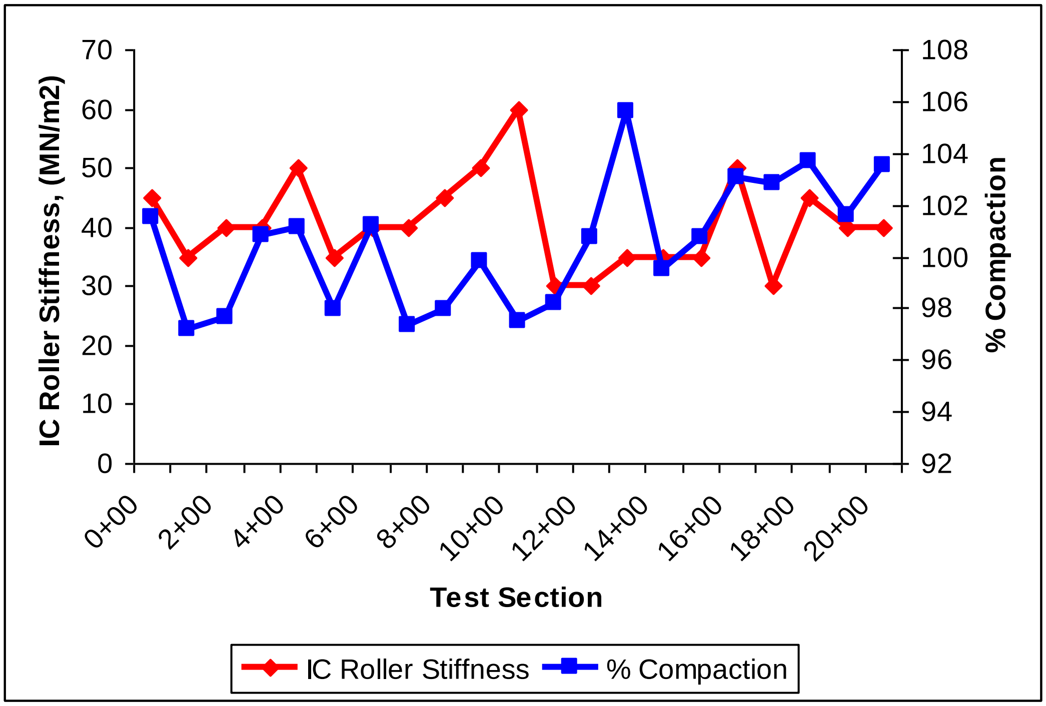

(c)

FIGURE 4.5: Relationship between IC roller stiffness and percent compaction for (a) US-56 "proof", (b) US-56 "growth" and (c) I-70 "growth" sections

Figure 4.5 shows the relationship between the IC roller stiffness and percent compaction obtained from the two sections on US-56 and I-70. The US-56 results show that lower IC roller stiffness was obtained for both very high and very low percent compaction. Although the I-70 test section showed higher levels of percent compaction, the trend was almost similar to that observed on the US-56 test section. This finding is very significant since it indicates the need for developing the "target" stiffness for the IC rollers for a specific type of soil. When the preselected stiffness value is entered prior to the compaction, the IC roller automatically controls the compaction process until the target stiffness value is obtained. At that point, the roller reduces or eliminates the compactive effort on subsequent passes. If these target values are low, the resulting density will be too low where as high target values will result in overcompaction. The results of this study tend to prove this point.

4.5 Variation of IC Roller, Geogage, LFWD, and FWD Stiffness

FHWA (*4*) reported that some European and Asian countries now use compaction specifications that contain modulus-based compaction control. In those specifications, minimum target modulus must be obtained in addition to the target moisture content and percentage of the Proctor density. The countries that have switched to modulus-based compaction control have typically compared their roller modulus with the field plate loading test modulus. The specifications vary from one country to another but they only vary in their minimum target modulus values depending on traffic, material type, and subgrade soil classification. For example, typical values of roller stiffness in one European specification have been reported to be 6.5 ksi (45 MPa) and 18 ksi (120 MPa) for low traffic roads and freeways, respectively (6). In the United States, the plate modulus test (or plate loading test) is not used by all states as a standard acceptance tool. However, Geogage, Dynamic Cone Penetrometer (DCP), light falling weight deflectometer (LFWD) and falling weight deflectometer (FWD) have become popular tools for subgrade evaluation. Table 2 shows the test conditions for various tests done on the projects in this study. The table also shows the mean stiffness and moduli obtained from the IC roller and other tests. It is to be noted that all tests were done at different vertical pressure. It is well known that the subgrade soil is stress dependent –the soil modulus varies with the deviator stress and to some extent, confining pressure. For sandy soils, the modulus increases with increasing deviator stress. Thus the layer modulus changes with depth. This is potentially a source of problem when comparing stiffness and modulus results from different tests. In this study, efforts were made to keep the applied vertical stresses of FWD and LFWD similar.

TABLE 4.1: Applied Vertical Stresses and Moisture Content During IC Compaction and Testing

Test Section	Test	Applied Vertical stress, σ_d (kPa)	Field Moisture Content *w* (%)	OMC *w* (%)	Average Stiffness/Modulus (MPa)
US-56 "proof"	IC Roller	92.6-277.8	6.2 – 9.9	10.4	61.7
	Geogage	25.0			7.96
	LFWD	130.9 – 162.5			64.1*
	FWD	67.6 – 116.5			73.3*
US-56 "growth"	IC Roller	92.6-277.8	4.05 – 7.9	10.19	36.4
	Geogage	25.0			11.4
	FWD	130.9 – 162.5			72.4*
I-70 "growth"	IC Roller	92.6-277.8	6.2 – 9.9	11.7	40.5
	Geogage	25.0			4.9
	LFWD	118.3 – 136.4			26.4*
	FWD	52.4 – 102.73			29.8*

* from Boussinesq equation

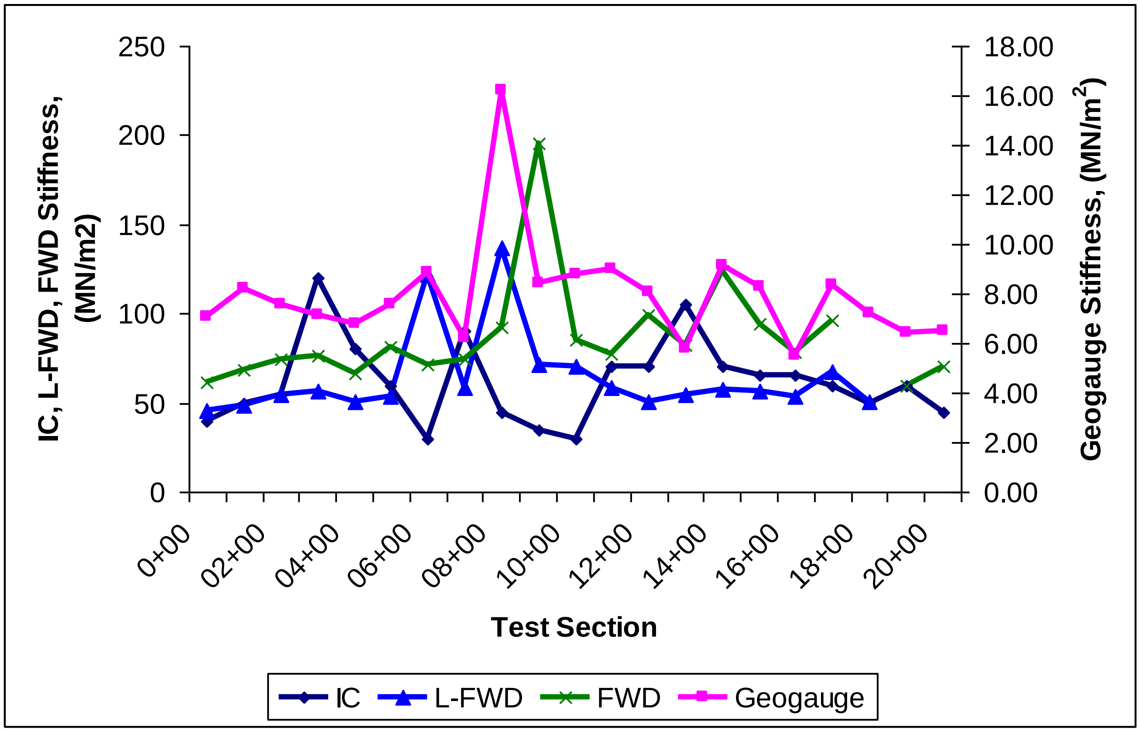
IC, L-FWD, FWD Stiffness, (MN/m2)
Geogauge Stiffness, (MN/m2)
Test Section
IC
L-FWD
FWD
Geogauge

(a)

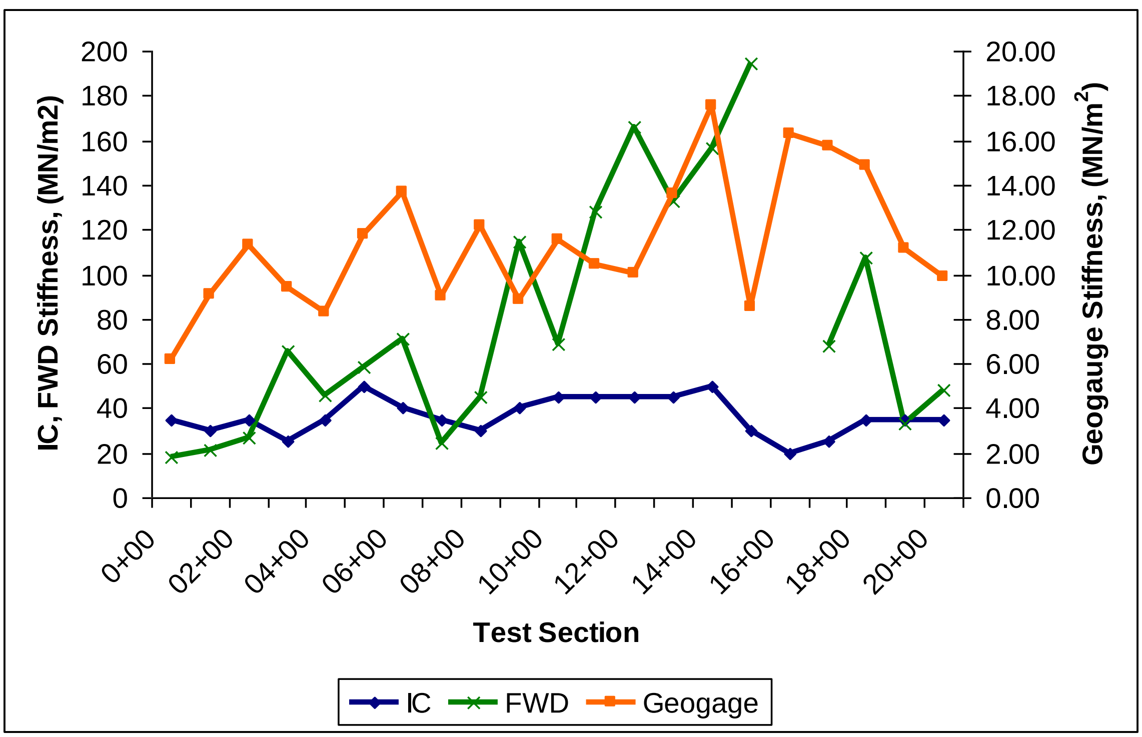
IC, FWD Stiffness, (MN/m2)
Geogauge Stiffness, (MN/m2)
Test Section
IC
FWD
Geogage

(b)

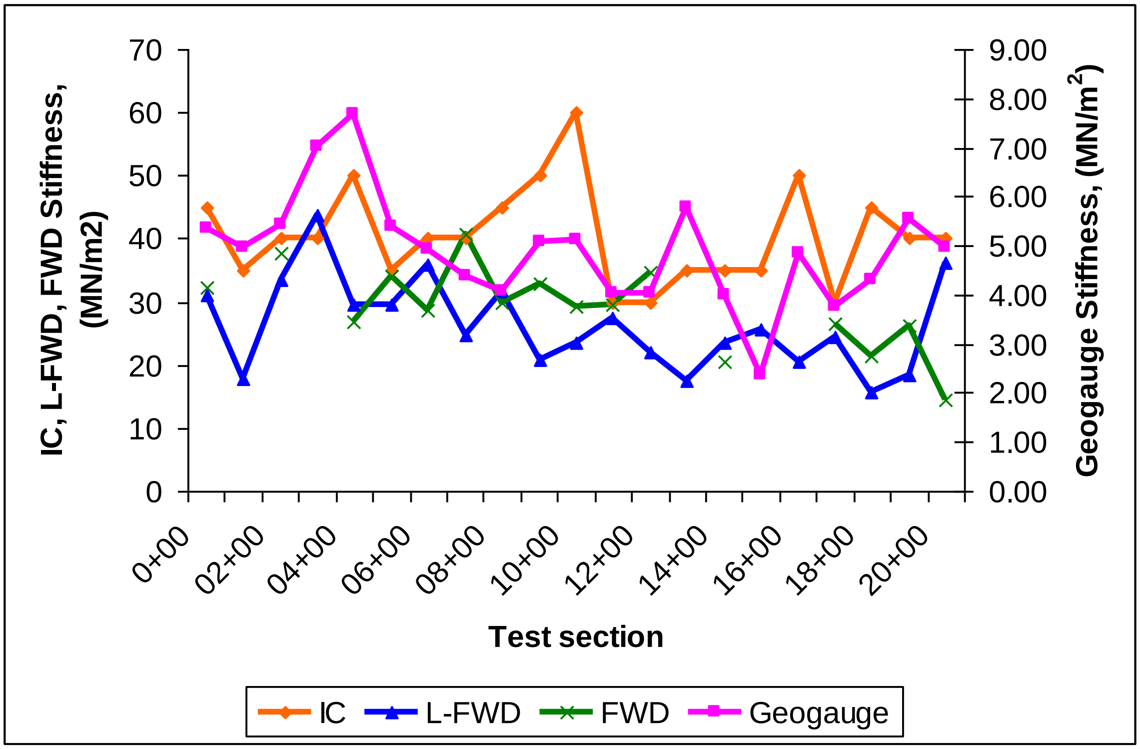

(c)

FIGURE 4.6: Variation of IC roller, FWD, LFWD and Geogage stiffness on (a) US-56 "proof", (b) US-56 "growth" and (c) I-70 "growth" sections

Figure 4.6 illustrates the variation of various stiffness and moduli obtained at different test locations on the US-56 "proof" and "growth" and I-70 "growth" sections. The US-56 "growth" section did not have any LFWD data. The highest variation was obtained for the IC roller stiffness and the LFWD-derived modulus. The trend of data in Figure 4.6(a) shows a good correlation between the Geogage stiffness and the LFWD backcalculated modulus on the US-56 "proof" section. On this section, the mean stiffness and moduli values obtained from the IC roller, LFWD and FWD (Boussinesq's equation) were also somewhat close.

However, the above trend is not evident on the US-56 and I-70 'growth" sections. As expected, the mean modulus values from LFWD and FWD were similar. However, as illustrated in Figure 4.6(b) and 4.6(c), no definite correlation is evident among the IC stiffness, Geogage stiffness, and LFWD and FWD backcalculated moduli. Further statistical analysis was performed with the stiffness and modulus values calculated from different test methods to check correlation among the different measures.

4.6 Statistical Analysis of Test Results

A correlation matrix was developed to investigate the correlation among the stiffness values. Table 4.2 tabulates the statistical summary of the IC roller stiffness and other stiffness and moduli results obtained in this study. IC roller stiffness and Geogage stiffness were the outputs of these pieces of equipment. Boussinesq's equation was used to backcalculate the soil elastic modulus from both LFWD and FWD in-situ deflection data. FWD modulus was further calculated using the EVERCALC 5.0 backcalculation software using the full deflection basin from all seven or six sensors. The CBR/DCP modulus was calculated from the correlation between CBR and the resilient modulus.

Statistical summary shows that the stiffness values are highly variable on US-56 “proof” and “growth” sections. The highest coefficient of variation (COV) of around 38% was obtained for the IC roller and LFWD device on the US-56 proof section. The highest COV value (67%) was observed for the FWD modulus on the US-56 “growth” section. However, the above trend was not evident on the I-70 “growth” section as shown in Table 4.2. The stiffness and modulus values were much less scattered on this section. As expected, the mean modulus values from LFWD and FWD were similar. The maximum stiffness value was obtained from the DCP test on both US-56 “proof” and I-70 “growth” section. The minimum stiffness value was measured by Geogage.

TABLE 4.2: Statistical Summary of Stiffness and Moduli Results

Test Section	Parameter	Mean (MPa)	Std. Dev. (MPa)	Coeff. Of Var. (%)	Range (MPa)	n
US-56 "Proof"	BVC Stiffness	61.7	23.2	37.5	90.0	21
	Geogage Stiffness	7.96	2.2	27.4	10.96	21
	LFWD Modulus*	64.1	24.1	37.6	91.3	19
	FWD Modulus**	86.5	29.7	34.4	135.9	20
	FWD Modulus *	73.3	19.2	26.2	87.8	21
	CBR/DCP Modulus***	129.6	28.3	21.8	98.8	21
US-56 "growth"	BVC Stiffness	36.43	8.24	22.61	30	21
	Geogage Stiffness	11.40	2.96	25.97	11.36	21
	FWD Modulus**	79.73	53.03	66.51	176.85	20
	FWD Modulus *	72.41	40.17	55.48	130.05	21
	CBR/DCP Modulus***	125.69	17.88	14.22	61.65	21
I-70 "Growth"	BVC Stiffness	40.5	7.7	19.1	30.0	21
	Geogage Stiffness	4.91	1.1	23.1	5.3	21
	LFWD Modulus*	26.4	7.2	27.4	28.1	21
	FWD Modulus**	29.1	6.6	22.7	26.2	16
	FWD Modulus *	29.8	6.4	21.3	23.8	21
	CBR/DCP Modulus***	97.3	8.2	8.4	34.2	21

* from Boussinesq equation; **from backcalculation; *** from correlation

4.6.1 Correlation Matrix

A Correlation matrix describes correlation among M numbers of variables. It is a square symmetrical (M x M) matrix with the (ij)th element equal to the correlation coefficient ij between the (i)th and the (j)th variable. The diagonal elements (correlations of variables with themselves) are always equal to 1.00. Correlation coefficients can range from -1.00 to +1.00. The value of -1.00 represents a perfect negative correlation while a value of +1.00 represents a perfect positive correlation. A value of 0.00 represents a lack of correlation. A correlation matrix is always a symmetric matrix

The correlation among the soil stiffness obtained from the IC roller and Geogage, and the subgrade soil moduli obtained from the LFWD, FWD, and DCP (with CBR correlation) data was also examined statistically. Correlation tables were developed using the SAS statistical software *(22)*

TABLE 4.3: Correlations among IC and Geogage Stiffness, LFWD and FWD Moduli, and CBR on US-56 "Proof" Section

	IC	Geogage	LFWD	FWD (Backcalculated)	FWD (Boussinesq equation)	CBR/DCP
IC	**1.0**	**-0.35 0.12***	**-0.39 0.096***	**-0.19 0.43***	**-0.21 0.36***	**-0.44 0.04***
Geogage		**1.0**	**0.78 <0.0001***	**0.24 0.31***	**0.83 <0.0001***	**0.72 0.0002***
LFWD			**1.0**	**0.11 0.68***	**0.63 0.004***	**0.86 <0.0001***
FWD (Backcalculated)				**1.0**	**0.36 0.12***	**0.18 0.45***
FWD (Boussinesq equation)					**1.0**	**0.47 0.033***
CBR/DCP						**1.0**

*** p-value**

TABLE 4.4: Correlations among BVC, Geogage, FWD Moduli, and CBR on US-56 "Growth" Section

	IC	Geogage	FWD (Backcalculated)	FWD (Boussinesq equation)	CBR/DCP
IC	1.0	0.04	0.30	0.47	-0.13
Geogage		1.0	0.36	0.12	0.34
FWD (Backcalculated)			1.0	0.90	0.58
FWD (Boussinesq equation)				1.0	0.42
CBR/DCP					1.0

TABLE 4.5: Correlations among BVC, Geogage, LFWD and FWD Moduli, and CBR on I-70 "Growth" Section

	IC	Geogage	LFWD	FWD (Backcalculated)	FWD (Boussinesq equation)	CBR/DCP
IC	1.0	0.39 0.085*	-0.001 0.99*	-0.03 0.93*	-0.05 0.82*	0.05 0.83*
Geogage		1.0	0.32 0.16*	0.037 0.89*	-0.04 0.86*	0.27 0.24*
LFWD			1.0	0.008 0.98*	-0.08 0.75*	-0.08 0.73*
FWD (Backcalculated)				1.0	0.97 <0.0001*	-0.44 0.087*
FWD (Boussinesq equation)					1.0	-0.26 0.26*
CBR/DCP						1.0

* p-value

Results in Table 4.3 for the US-56 “proof” section tend to confirm the observation in Figure 4.6(a). The table shows about 78% dependency of Geogage in-situ stiffness on the LFWD stiffness at 95% confidence level with a p-value less than 0.0001. The Geogage stiffness also has a good correlation with the modulus obtained from CBR in the DCP test. However, results in Table 4.5 for the I-70 section show about 32% dependency of the Geogage stiffness on the LFWD modulus at 95% confidence level with a p-value equal to 0.1607. None of the test results seems to have a strong correlation with the IC stiffness on this section. Further testing may be necessary to develop such a correlation. It may be mentioned that the IC roller stiffness has been successfully correlated with the plate loading test results in Europe. It appears that larger plated helps to test a large soil sample that could be considered somewhat representative of the soil subgrade.

4.6.2 Reasons for Poor Correlation among Different Measures of Stiffness and Moduli

The poor correlations among the IC roller-generated soil stiffness and stiffness and moduli measured or derived from the soil stiffness gage, LFWD, and FWD was further investigated by the volume of influence space of each measurement technique in the subgrade. It is to be noted that the differences in stress states of these measures are shown in Table 4.1 and had been discussed earlier. In this section, based on the area of the foot print of the soil stiffness gage, LFWD, and FWD, and the approximate sensing depth for each piece of equipment *(23),* the volume of influence space in the subgrade was calculated. Figure 4.7 illustrates the volume of influence space schematically for each measure.

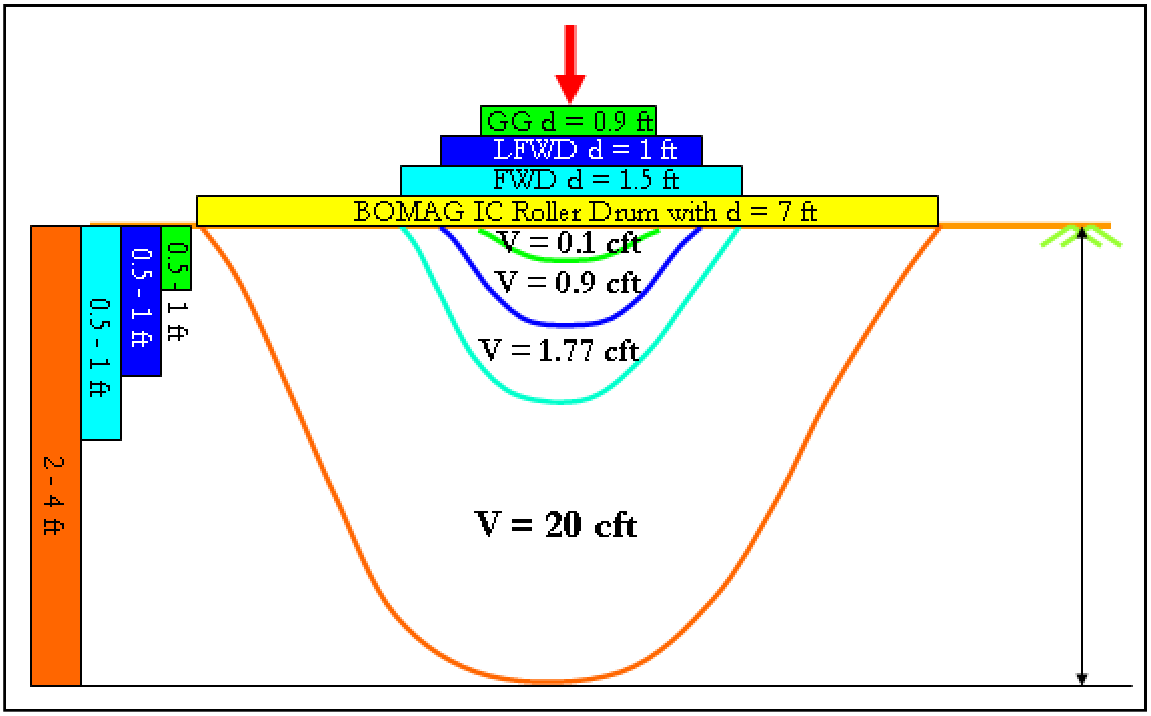

FIGURE 4.7: Volume of influence space in subgrade soil

It shows that the soil stiffness gage had the lowest influence space of 0.1 cft (0.0003 cubic meter) whereas the IC roller influence space volume was 200 times of that. It is obvious that each measure was "sensing" a separate volume of soil, and the IC roller was clearly by large had the highest sample size among all measurement methods. This partly explains why a universal correlation among the outputs of all these pieces of equipment was not found. However, it is possible that if the influence space volume of any of the measurement method can be increased, a better correlation with the IC roller stiffness may be found. FWD seems to be the logical choice since it can accommodate a larger diameter plate (about 30 inches or 762 mm). In that case, the volume of influence space of FWD would increase by almost three times.

CHAPTER 5 - MECHANISTIC-EMPIRICAL PAVEMENT DESIGN (M-E PDG) ANALYSIS

5.1 General

Mechanistic Empirical Pavement Design Guide (M-E PDG) is an advanced pavement design and analysis methodology that has been developed by NCHRP and is being implemented nationwide. M-E PDG analysis method requires an input of either estimated or measured moduli for each of the pavement materials in the roadway cross-section. This design procedure is integrated into a software program. In this study, version 1.0 of this software was used.

5.2 M-E PDG Design Approach

The M-E PDG is a mechanistic empirical design procedure based on elastic layer theory of the pavement analysis. It is a complex pavement analysis tool with many input factors to characterize the pavement materials, climate, traffic and the construction. The design approach followed in M-EPDG is briefly illustrated in Figure 5.1. This is an iterative process and includes the following basic steps:

1. The trial design is developed by the designer using several input values such as traffic, foundation properties, climate, and material properties.
2. The software estimates the damage and key distresses over the design life.
3. The design is verified against the performance criteria at a preselected level of reliability. The design may be modified to meet performance and reliability requirements of a particular project.

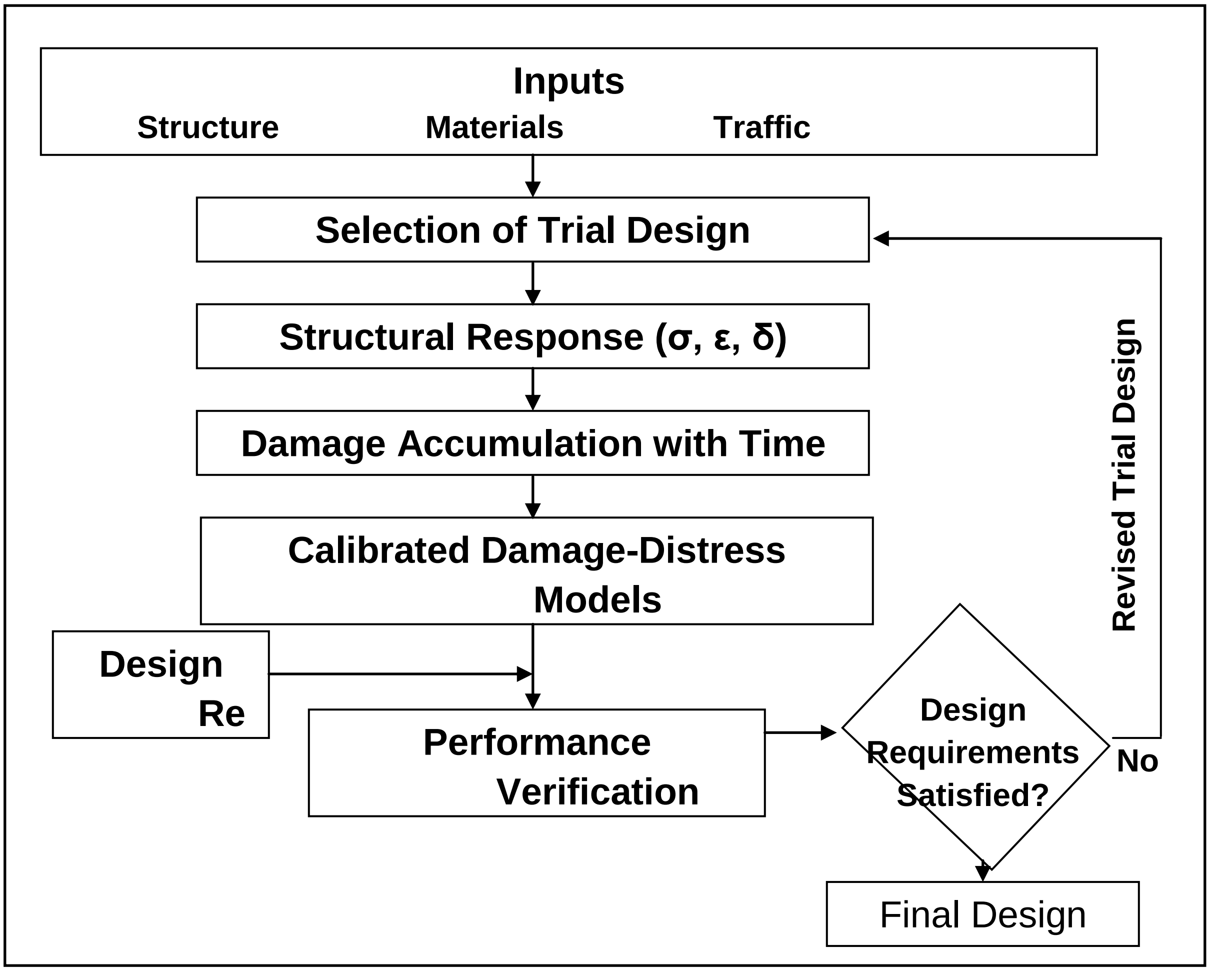

FIGURE 5.1: Design framework of M-EPDG 2000, (1)

5.3 Overview of the Design Process of M-EPDG

M-EPDG uses an innovative trial approach for selecting design inputs. Figures 5.2 and 5.3 illustrate the overall design process for flexible and rigid (JPCP) pavement section. In M-EPDG design process, traffic spectra, materials, and climatic factors are combined with structural elements to develop a trial design. Structural foundation includes different layer arrangement. Properties, design and construction features of HMA (flexible pavement)/ PCC (rigid pavement) and other paving materials are also needed in trial input section. Pavement responses to the combined effects of dynamic traffic load and climate are computed using finite element and elastic layer computer models. Cumulative damage in the pavement over the design life of the structure is calculated using incremental damage approach. The design life is divided into two-week time periods for flexible pavements and one-month for rigid pavements. In each time increment, the daily, seasonal, and long-term changes in material properties, traffic, and climate are considered. The accumulated damage is then evaluated based on the failure criteria which were established based on acceptable pavement performance at the end of the design life. The distress types considered in M-EPDG are rutting, fatigue cracking, and thermal cracking in asphalt-surfaced pavements. The joint faulting and transverse cracking in jointed plain concrete pavements, and punchouts in continuously reinforced concrete pavements are considered as distresses in design guide. In addition, pavement smoothness is considered through the commonly used International Roughness Index, or IRI. Expected performance is also evaluated at the given reliability level. Iteration continues if the design does not meet the established criteria.

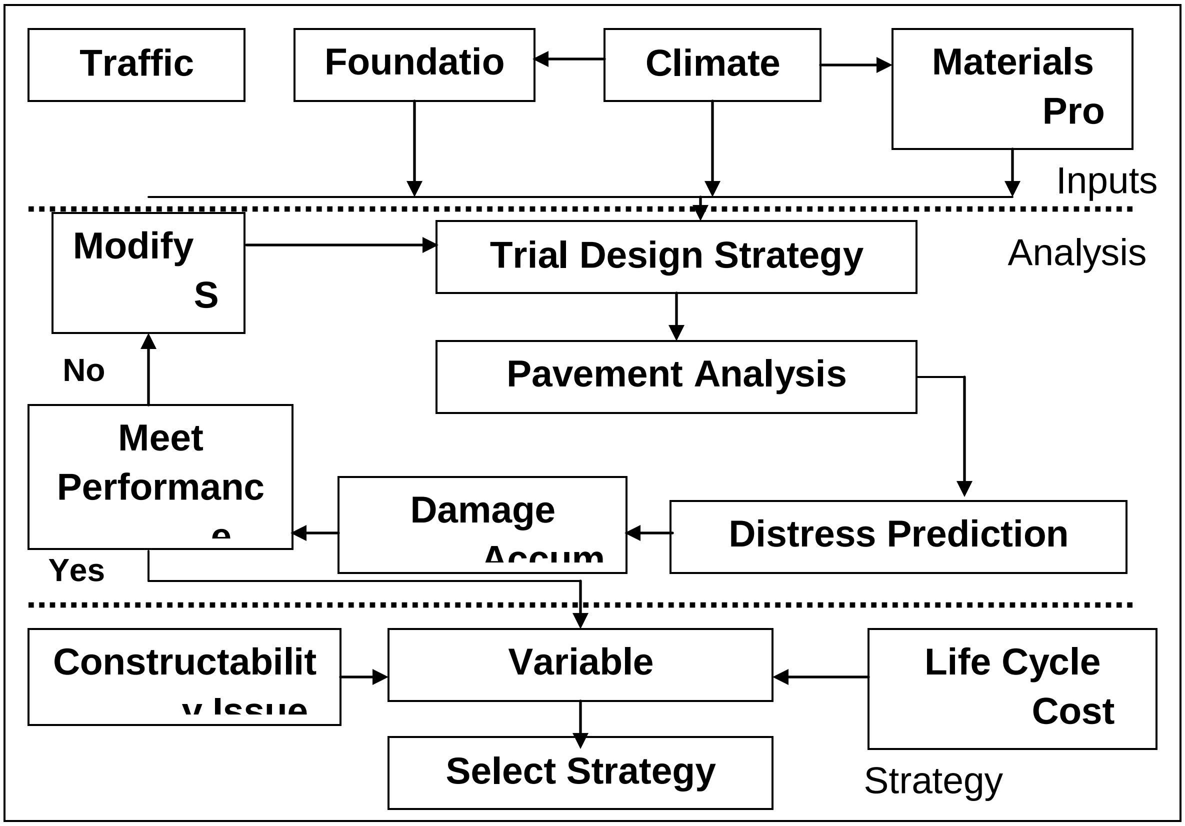

FIGURE 5.2: M-EPDG design process for flexible pavement, (1)

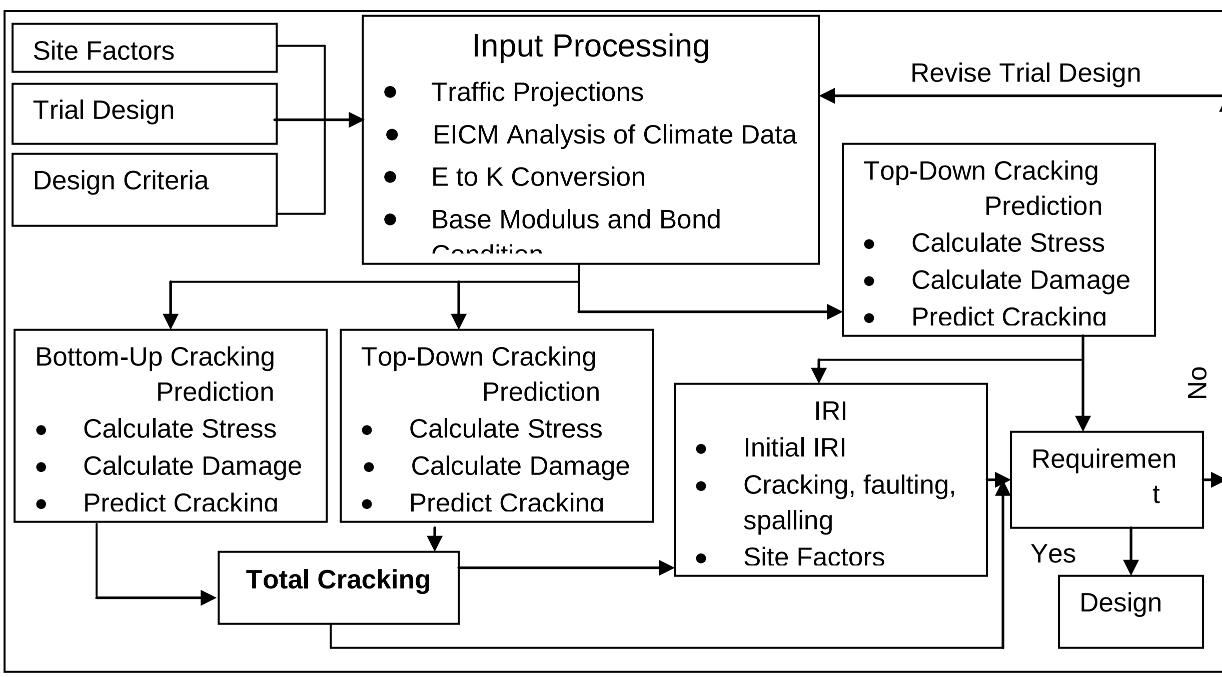

FIGURE 5.3: M-EPDG design process for JPCP, (1)

5.4 Test Sections

As mentioned before, two pavement reconstruction projects, one on US-56 and one on I-70, were selected for this study. The project on US-56 began at the Morton-Stevens County Line and extended to the east of the west city limit of Hugoton. The project had two 328 ft (100 m) test sections. The other project, located on Interstate route 70, began at the Salina-Dickinson County Line and extended to 2.7 km east of RS 187. A test section of 328 ft (100 m) length was selected at this project location.

The proposed design alternate for the reconstruction of US-56 test section is a full depth asphalt concrete pavement. For the I-70 section, both full depth asphalt concrete pavement and Portland cement concrete pavement (PCCP) are planned as two design alternates. The design analysis to get the cross sections was performed by the 1993 *AASHTO Guide for Design of Pavement Structures*. The design subgrade resilient moduli were obtained from the laboratory testing. Figure 5.4 and Table 5.1 show the design cross sections and details of the test sections respectively.

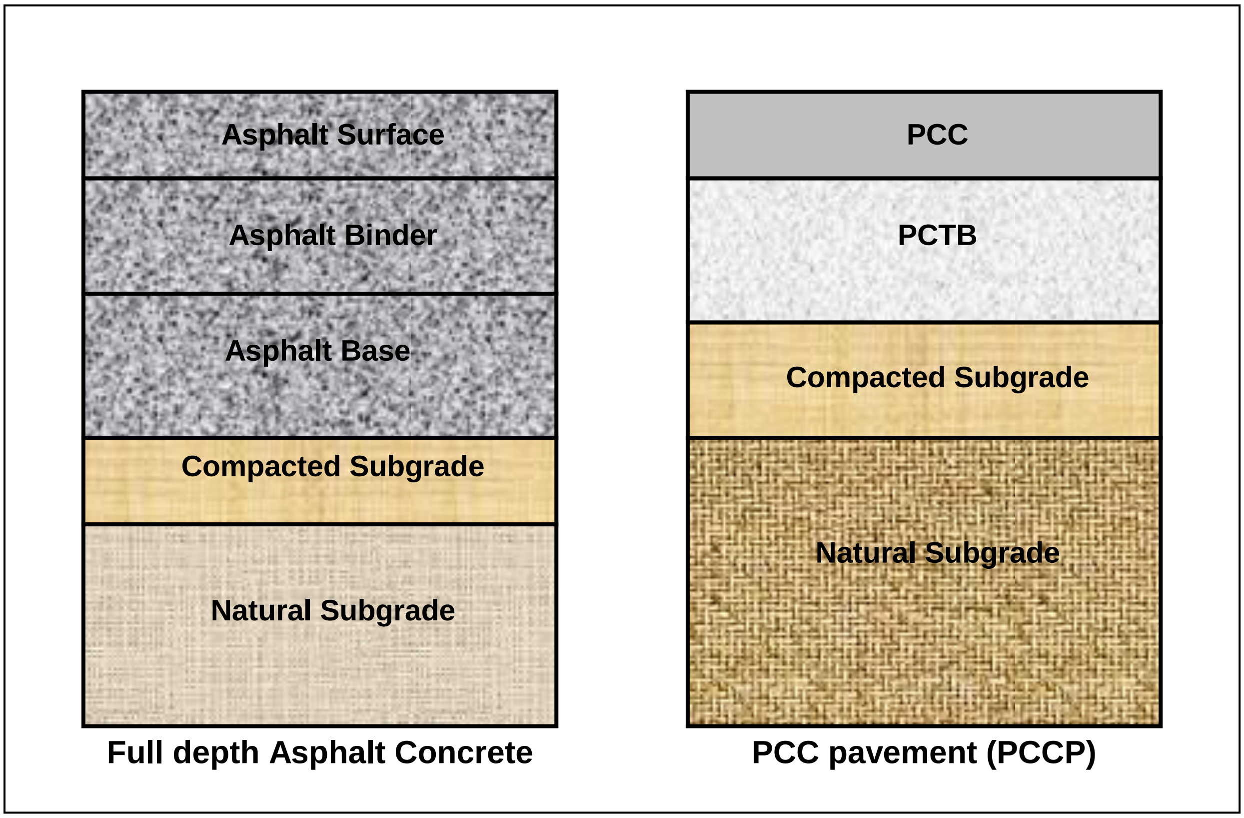

FIGURE 5.4: Full Depth Flexible Pavement (US-56, I-70 Section) and PCCP (I-70) layered system

TABLE 5.1: Project Details of the Test Sections

Project ID	Route	Traffic Direction	Pavement type	Thickness (inch)	Mix Design	Binder Grade
56-095 K-6400-01	US-56	EB	Full Depth AC	13.4	SM-9.5A	70-28*
					SM-19A	70-28*
					SM-19A	64-22**
70-21 K-6794-01	I-70	EB	Full Depth AC	18.1	SM-9.5A	70-28*
					SM-19A	70-28*
					SM-19A	64-22**
70-21 K-6794-01	I-70	EB	JPCP	12.6	-	-

*Binder Grade of Wearing course and Asphalt binder ; ** Binder Grade of Asphalt base

The JPCP on I-70 has a 15 ft (4.6 m) joint spacing with dowel bars of 1.575 inches (40 mm) diameter. The PCC slab will be constructed on Portland cement stabilized base and lime treated subgrade. The AASHTO soil classification of the natural subgrade soil type is primarily Non-Plastic A-3. The top 6 inch (150 mm) of the natural soil is to be treated with lime for subgrade modification. The compaction of the subgrade soil is specified to be to be 95% or greater of the standard Proctor density with the moisture content equal to or not lower than 5% below the optimum moisture content. The PCC slab thickness is 12.6 inch (320 mm). The 28-day design modulus of rupture of concrete is 595 psi (4.1 MPa) and the 28-day elastic modulus is 4,003,042 psi (27,600 MPa).

The full depth bituminous concrete pavement sections on both US-56 and I-70 have thickness of 13.4 inch (360 mm) and 18.1 inch (460 mm), respectively and are to be constructed on a compacted subgrade (Figure 5.4). The detailed mixture properties and binder specifications are listed in Table 5.1. The AASHTO soil classification of the natural subgrade soil type is Non-Plastic A-3. The 6.0 inch (150 mm) of the natural soil is to be treated with lime. The compaction specifications are the same as those for JPCP.

The base year annual average daily traffic (AADT) on these sections is 18,200 on I-70 and 3,660 on US-56. The percent truck is 20% on I-70 and 5% on US-56.

5.5 Design Inputs of M-EPDG (Version 1.0) Analysis

Design inputs are the most significant aspects in the mechanistic-empirical pavement design. The basic design inputs required for the M-EPDG analysis are: (1) inputs for the pavement structures, such as, layer thickness, material type, etc.; (2)

inputs under which the pavement is designed to perform (traffic, climate, etc.); and finally (3) inputs for the material and mix design properties of the layers.

The ME-Design Guide recommends that the designer use the subgrade resilient modulus (M_R) obtained from laboratory testing following AASHTO T 307 or NCHRP Project 1-28. The following $k_1 - k_2 - k_3$ consecutive model is used to predict the M_R value at the optimum moisture content (OMC);

$$M_{Ropt} = k_1 \times p_a \times \left(\frac{\theta}{p_a}\right)^{k_2} \times \left(\frac{\tau_{oct}}{p_a} + 1\right)^{k_3} \qquad \text{Equation 5.1}$$

Where,

$M_{Ropt} =$ Resilient modulus at OMC;

$k_1, k_2, k_3 =$ Regression parameters;

$p_a =$ Atmospheric pressure;

$\theta = J_1 = \sigma_1 + \sigma_2 + \sigma_3 =$ Stress invariant; and

$\tau_{oct} = \frac{1}{3}\sqrt{(\sigma_1 - \sigma_2)^2 + (\sigma_1 - \sigma_3)^2 + (\sigma_2 - \sigma_3)^2} =$ Octahedral shear stress.

In the M-EPDG analysis, three levels of inputs can be provided to analyze and design the pavement. “Level 1” is an advanced design procedure at the highest level of reliability under heavy traffic condition. The generalized $k_1 - k_2 - k_3$ model is directly applied to ME-design if “Level 1” subgrade design input is selected. The design inputs require site specific data collection and lab testing.

“Level 2” computes the subgrade resilient modulus using its relationship with other subgrade properties, such as, the California Bearing Ratio (CBR) or R-value, Dynamic Cone Penetration (DCP), water content and plasticity index (PI) (21). This data is user specified and is used to routine design when lab data is not available.

For input "Level 3", the resilient modulus at optimum moisture content is selected on the basis of soil classification and sieve analysis. M-EPDG analysis also adjusts the subgrade modulus for each design period (month) by accounting for the seasonal variation in unbound material properties. The designer is allowed to provide modulus value either for each design period or at optimum moisture content.

In this study, "Level 3" input with direct input of subgrade modulus was selected to evaluate the subgrade modulus. The following section will briefly describe and summarize all the inputs used in the M-EPDG analysis for the full depth asphalt concrete (AC) and JPCP test sections.

5.5.1 General Inputs

In general inputs, "*General Information"* allows the designer to specify the pavement type (flexible and rigid pavement), design life, pavement construction month, traffic opening month etc. "*Site Identification"* provides information of a particular project location, project ID, begin and end of mile posts and traffic direction (NB, SB, EB, and WB). *Analysis Parameters* describes the analysis type and performance criteria to predict the pavement performance over design life. The simulation of uncertainties and variability occur during pavement design establish the reliability level by considering certain potential errors of selected design inputs. Design reliability can be expressed as:

$$R = P\,[\text{Distress over Design Period} < \text{Critical Distress Level}] \qquad \text{Equation 5.2}$$

The parameters required in this design input section are IRI and the performance criteria to verify the trial design. The designs that meet the applicable performance criteria are then considered feasible from both structural and functional viewpoints. The M-EPDG recommended reliability level of each distress type is based on the roadway functional classification *(1)*. In this study, the test sections were functionally classified as Rural Interstate and Principal Arterials (rural). A design reliability of 90% was used for all test sections based on the M-EPDG recommendations *(24)*. Table 5.2 shows the failure criteria for JPCP and AC pavement at 90% reliability level considered during analysis.

TABLE 5.2: Performance Criteria for JPC Pavement and Full Depth Asphalt Concrete Pavement

Pavement Type	Performance Criteria	Limit	Reliability (%)
JPCP	Terminal IRI, (in/mile)	172	90
	Transverse Crack (% slab crack)	15	90
	Mean Joint Faulting, (inch)	0.12	90
Full Depth Asphalt Concrete	Initial IRI, (in/mile)	63	90
	Terminal IRI, (in/mile)	172	90
	AC surface down cracking, (ft/500)	2,000	90
	AC bottom up cracking, (%)	25	90
	AC thermal fracture, (ft/mile)	1,000	90
	Chemically stabilized layer, (Fatigue Fracture)	25	90
	Permanent Deformation, AC layer, (in)	0.25	90
	Permanent Deformation, Total pavement, (in)	0.75	90

5.5.2 Design Traffic Inputs

Traffic data is a key data element for the design and analysis of pavement structures in M-EPDG. The axle load distribution obtained from traffic module accurately determines the axle loads that will be applied on the pavement during each time increment of the damage accumulation process. To create this axle load distribution, the software requires input data regarding the traffic volumes and loads, and hourly distribution for the base year, and estimated growth over the design life.

The initial 2-way Annual Average Daily Traffic (AADT) are 18,200 and 3,660 for I-70 and US-56, respectively. The percent heavy trucks are 20% and 5% for I-70 and US-56, respectively. Both are divided roads with two lanes in each direction. The initial two way AADTT value was calculated using the percent heavy trucks of ADT and AADT value obtained from the project traffic survey report. The percentages of truck in the design lane and in the design direction are 100% and 60%, respectively on all test locations. The posted speed limit on all test sections is 70 mph which was used as the operational traffic speed for the base year in M-EPDG analysis.

Default values were used for other traffic volume adjustment factors, and monthly adjustment factors in the M-EPDG analysis. A monthly adjustment factor of 1.0 was used for all vehicle classes (4-13 by FHWA). The default values of vehicle class distribution and hourly truck distributions were also used. A compound traffic growth rate of 2% was used on both US-56 and I-70 project traffic survey report. For all test sections, the default values recommended by M-EPDG level 3 traffic inputs for axle load distribution factors, number of axle per truck and axle configurations were taken into account during analysis.

5.5.3 Climate Inputs

The Enhanced Integrated Climatic Model (EICM) software is used to model temperatures and moisture profiles in the pavement and subgrade. M-EPDG recommends the user to accumulate the weather data from the weather stations in the vicinity. It also suggests collecting the weather data for at least 24 months *(25)*. In this analysis, the project-specific virtual climatic data was generated by interpolating the weather database from selected weather stations near the project area. The information about the depth of ground water table was not available at the project locations. Hence, M-EPDG recommended value of 10 feet was used for the depth of the ground water table in the analysis.

5.5.4 Structural Inputs

This is the fourth set of inputs required by the M-E PDG software for evaluation of the trial design. The inputs specify the structural, design, and material aspects of the trial design chosen for the performance evaluation.

5.5.4.1 US-56 Full Depth Asphalt Concrete Pavement Section

According to the project investigation report, the top surface or wearing course of US-56 pavement section has a 1.575-inch (40-mm) bituminous layer (SM-9.5T) with PG 70-28. The upper part of the base course or asphalt binder has a 2.36-inch (60-mm) bituminous layer (SM-19A) with PG 70-28 and the lower asphalt base has a 9.45-inch (240-mm) bituminous layer (SM-19A) with PG 64-22. Table 5.3 shows the input values for the asphalt concrete layers in this project. Six inch (150 mm) “Natural Subgrade” was considered in the M-EPDG run to investigate the sensitivity of the design towards the compacted subgrade modulus.

5.5.4.2 I-70 Full Depth Asphalt Concrete and PCC Pavement Sections

Project reconstruction report on I-70 anticipates that the alternate 1 on pavement section is a full depth asphalt concrete pavement (Figure 5.4). The top surface or wearing course has a 1.575-inch (40 mm) bituminous layer (SM-9.5T) with PG 70-28. The upper layer or the binder course has a 2.36-inch (60 mm) bituminous layer (SM-19A) with PG 70-28 and the lower asphalt base has a 14.2-inch (360 mm) bituminous layer (SM-19A) with PG 64-22. Table 5.3 shows the input parameters for the asphalt concrete layers in the M-EPDG analysis. Six inch (150 mm) “Natural Subgrade” was considered in the M-EPDG run.

Alternate 2 on I-70 section is a JPCP structure with stabilized base and compacted subgrade. In this study, the project was assumed to have liquid sealant. Dowel diameter was calculated from the PCC slab thickness as one-eighth of the slab thickness in inches as shown in Table 5.4. No shoulder edge support was considered during analysis. The selected width of the slab was the same of the lane width 12 ft (3.66 m). The PCC mixture material and strength properties of the PCC slab are shown in Table 5.4. The base is 4.0 inch (100 mm) thick and is chemically stabilized with Portland cement. The base material properties, and layer strength used in the analysis are also listed Table 5.4.

TABLE 5.3: Layer and Material Inputs for Flexible Pavement Analysis on I-70 and US-56

Input Parameters	Input Values	
	I-70	US-56
Layer 1:(SM-9.5T)		
Material Type	Asphalt Concrete	Asphalt Concrete
Layer Thickness, (inch)	1.575	1.575
Asphalt General:		
Reference Temperature (^{0}F)	68	68
Poisson's Ratio	0.25	0.25
Effective Binder Content (%)	11.2	11.2
% Air Voids	4	4
Total Unit Weight (pcf)	145.64	145.64
Binder Grade (PG)	70-28	70-28
Layer 2:(SM-19A)		
Material Type	Asphalt Concrete	Asphalt Concrete
Layer Thickness, (inch)	2.36	2.36
Asphalt General:		
Reference Temperature (^{0}F)	68	68
Poisson's Ratio	0.25	0.25
Effective Binder Content (%)	10.5	10.5
% Air Voids	4	4
Total Unit Weight (pcf)	146.52	146.52
Binder Grade (PG)	70-28	70-28
Layer 3:(SM-19A)		
Material Type	Asphalt Concrete	Asphalt Concrete
Layer Thickness, (inch)	14.2	9.45
Asphalt General:		
Reference Temperature (^{0}F)	68	68
Poisson's Ratio	0.25	0.25
Effective Binder Content (%)	10.5	10.5
% Air Voids	4	4
Total Unit Weight (pcf)	146.52	146.52
Binder Grade (PG)	64-22	64-22

TABLE 5.4: Input Parameters for M-EPDG Rigid Pavement (JPCP) Analysis on I-70 Test Section

Input Parameters	Input Values
Design Features:	
Joint Spacing, (ft)	15
Dowel Bar Diameter, (t*/8), (inch)	1.575
Dowel Bar Spacing, (inch)	12
Layer 1:PCC Slab	
Slab Thickness, (inch)	12.6
Unit Weight, (pcf)	140
Poisson's Ratio	0.2
Mix Properties:	
Cement Type	II
Cementitious Material Content, (lb/yd^3)	653.4
Water/Cement Ratio	0.44
Aggregate Type	Limestone
Strength Properties:	
28 Days Modulus of Rupture (psi)	595
28 Days Modulus of Elasticity (psi)	4006,042
Layer 2: Cement Stabilized Base	
Layer Thickness, (inch)	3.94
Unit Weight, (pcf)	135
Poisson's Ratio	0.15
Elastic/Resilient Modulus, (psi)	500,000

*t = PCC slab thickness

"Natural Subgrade" of 6.0 inch (150 mm) was used in this analysis. The subgrade moduli used were obtained from three different sources: (1) average stiffness obtained by the IC roller on the test sections; (2) average backcalculated moduli obtained from the Falling Weight Deflectometer tests at 10 different locations on each test section. The backcalculation was done using an elastic layer backcalculation program and Boussinesq's equation; and (3) from the laboratory resilient modulus testing of the subgrade soil samples. Table 5.5 shows the input details for the subgrade layer. It is interesting to note that the laboratory resilient modulus of the A-3 soil on US-56 is 3,481 psi (24 MPa) as compared to the 16,500 psi (113.8 MPa) recommended by M-EPDG for A-3 soils. The FWD backcalculated and IC roller moduli are also lower than the recommended value. Although the backcalculated moduli from the FWD data are somewhat closer, the discrepancy is more evident for the I-70 project. Here again for the A-3 soil for the JPCP project, the M-EPDG recommended subgrade modulus value is 16,000 psi (110.3 MPa). The subgrade modulus from the laboratory test is almost one third of the M-EPDG value, and the moduli obtained from the FWD and IC roller are also about one-third to about one-fourth of the recommended value. Although the in-situ moisture contents on the I-70 test section during IC roller and FWD measurements varied from +1% to +5% of the optimum moisture content, the difference is staggering.

TABLE 5.5: Subgrade Properties for Flexible/Rigid Pavement Analysis of I-70 and US-56 Test Sections

Input Parameters	Input Values		
	I-70	US-56 "proof"	US-56 "growth"
Soil Type Layer Thickness, (inch) Poisson's Ratio	A-3 6.0 0.35	A-3 6.0 0.35	A-3 6.0 0.35
Input Subgrade Modulus FWD (Backcalculated), (psi) FWD (Boussinesq equation), (psi) IC Roller, (psi) Lab Data, ((psi)	4,321 4,221 5,874 3,626	12,546 10,631 8,992 3,481	11,560 10,501 5,279 3,481
M-EPDG Recommended (A-3soil), (psi)	14,000 – 35,500		
Plasticity Index (PI) Maximum Dry Density (MDD), (pcf) Optimum Moisture Content (OMC), (%)	NP 114.7 11.7	NP 119.6 10.4	NP 125.6 10.2

5.6 Prediction on Distresses from M-EPDG Analysis

5.6.1 International Roughness Index (IRI)

The predicted IRI by the design analysis on both flexible and JPCP sections passed the performance criteria assigned during the trial analysis. Table 5.6 summarizes the M-EPDG smoothness prediction after 20 years. In general, the table shows that the IRI values increase with decreasing subgrade strength. The JPCP is less sensitive to the subgrade modulus compared to the flexible pavements. On the I-70 section, the IRI value on the AC alternate section increases 4.3% with 38% decrease in subgrade modulus while the increase in IRI for the JPCP alternate is only 0.9%. Similar trend is evident on both the US-56 “proof” (IRI increases 9.9% with 72% decrease in subgrade modulus) and the “growth” (IRI increases 9.2% with 69.8% decrease in subgrade modulus) sections. However, the 20-year predicted IRI values indicate that the effect of the subgrade modulus on this parameter is insignificant. This indicates that the pavement designs obtained from the 1993 AASHTO Design Guide are sufficient from a functional view point.

TABLE 5.6: IRI Evaluations by M-EPDG Analysis

Project Location	Pavement Type	Subgrade M_R (psi)	Predicted Distress, IRI (inch/mile)	Predicted Reliability (%)	Target Reliability (%)	Comment
US-56 "proof"	Flexible	12,546*	95.9	99.74	90	Pass
		10,631**	96.7	99.7	90	Pass
		8,992***	97.6	99.65	90	Pass
		3,481†	105.4	98.83	90	Pass
US-56 "growth"	Flexible	11,560*	97	99.69	90	Pass
		10,501**	97.5	99.65	90	Pass
		5,279***	102.6	99.21	90	Pass
		3,481†	105.9	98.75	90	Pass
I-70	Flexible	5,874***	109.9	97.93	90	Pass
		4,321*	112.7	97.19	90	Pass
		4,221**	113	97.13	90	Pass
		3,626†	114.6	96.62	90	Pass
	JPCP	5,874***	74.5	99.99	90	Pass
		4,321*	74.9	99.99	90	Pass
		4,221**	74.9	99.99	90	Pass
		3,626†	75.2	99.99	90	Pass

*****FWD backcalculated modulus
** FWD Boussinesq equation
***IC Roller
†Lab Data

5.6.2 Total Deformation

It is accepted that the total surface deformation is highly influenced by the subgrade modulus. In fact, the currently used Shell and Asphalt Institute mechanistic-empirical pavement design procedures use vertical compressive strain on the top of the subgrade layer as one of the critical responses in design. The predicted distress of total deformation by the M-EPDG analysis is also a significant output for the flexible pavements. Figure 5.5 shows the total deformation on US-56 and I-70 sections.

The predicted total deformation decreases with increasing subgrade modulus for all test sections. The total deformation on the US-56 sections varies from 0.22 inch (5.6 mm) to 0.47 inch (11.9 mm) while the I-70 flexible alternate section experiences deformation of 0.51 inch (12.95 mm) to 0.63 inch (16 mm). Figure 5.5 (c) shows that the I-70 flexible section failed at 90% reliability level due to decrease in subgrade modulus (38%). The section also failed in the "deformation of the AC layer only" distress. However, on US-56 sections, no failure was observed despite a 72% decrease in the subgrade modulus though these sections are about 6 inches thinner than the I-70 asphalt section.

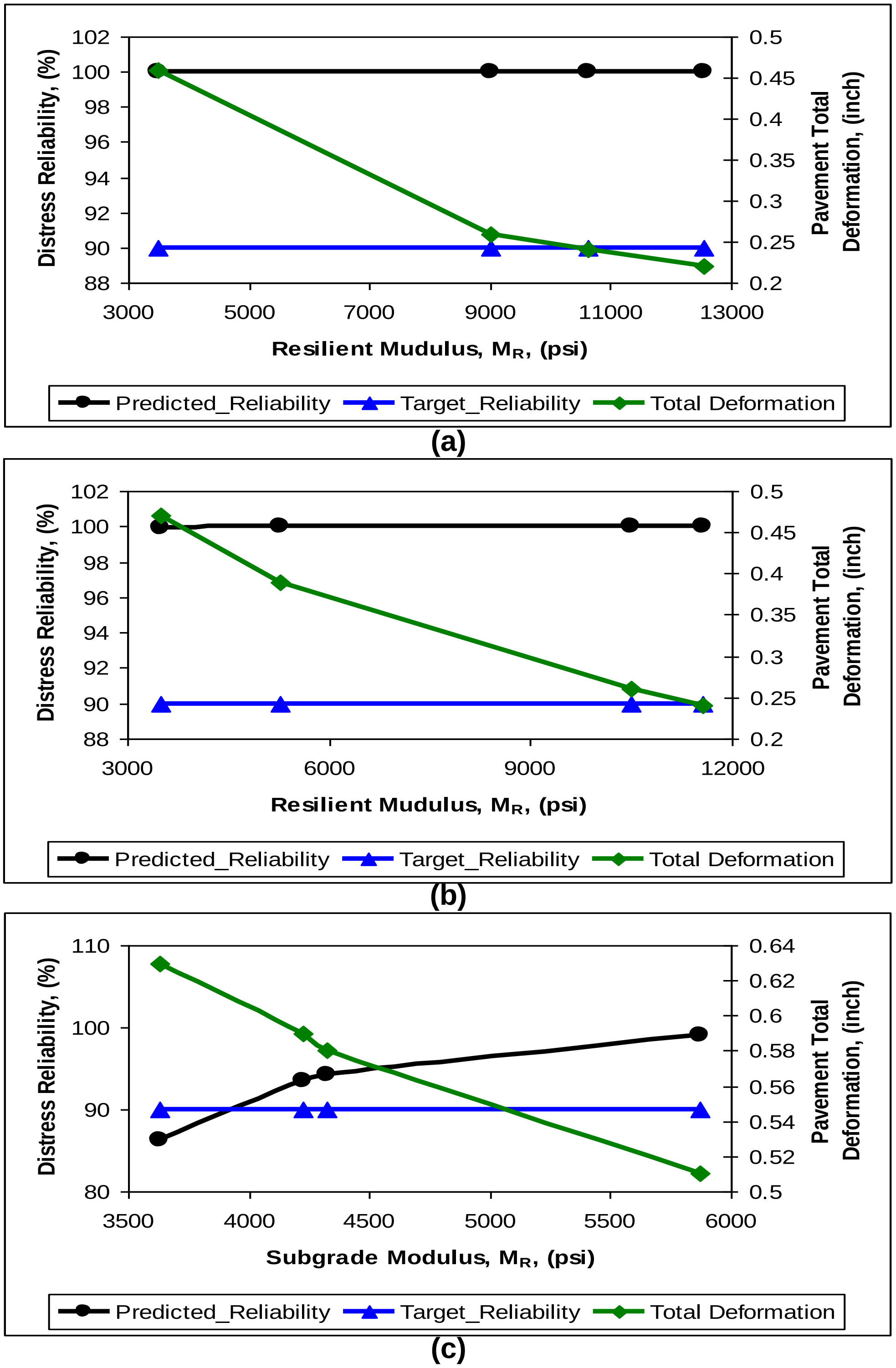

FIGURE 5.5: Predicted total deformation on (a) US-56 “proof” and (b) US-56 “growth” and (c) I-70 section

The possible reason could be the difference in AADTT values during the design period on these project locations. The base year AADT on I-70 section is 18,200 with 20% truck traffic while US-56 has a base year AADT of 3,660 with 5% truck traffic. It appears that the truck traffic repetitions at least early in the life of the pavement have a very large influence on the permanent deformation of the flexible pavements. This also raises the issue of the influence of the base thickness. A previous M-EPDG global sensitivity analysis showed that the annual average daily truck traffic, asphalt concrete (AC) thickness and subgrade strength have potential influence on flexible pavement performance while effect of binder grade is insignificant *(26)*. The effect of AC base was studied here to understand the interaction between the AC base thickness and the subgrade modulus.

The flexible pavements in this study were analyzed with respect to two different AC base thicknesses. Figure 5.6 shows the variation in total pavement deformation and the corresponding distress reliability for different subgrade moduli and AC base thickness.

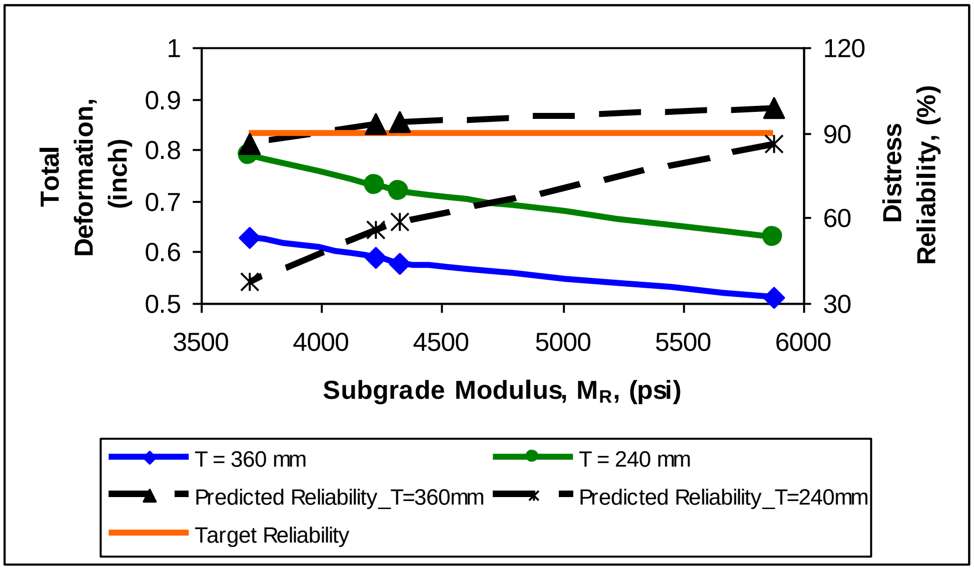

FIGURE 5.6: Effect of subgrade strength on total deformation at different base thickness

The figure illustrates that the total deformation increases rapidly with decreasing AC base thickness. The difference in predicted deformation for two different thicknesses remains the same irrespective of subgrade modulus. The difference is about 26% when the subgrade modulus is equal to 3,626 psi (25 MPa). At a subgrade modulus of 5,874 psi (62 MPa), the difference is approximately 23%. Figure 5.6 also shows that for about 14.2 inch (360 mm) base thickness and subgrade modulus of 5,874 psi (62 MPa) the total deformation performance criterion is satisfied with a predicted distress reliability of 94.3%. At base thickness of 9.45 inch (240 mm), the same subgrade modulus failed to satisfy the same total deformation criterion (predicted distress reliability 60.4%). This indicates that the AC base thickness has more influence on the total pavement deformation than the foundation layer.

5.6.3 Effect of Subgrade Modulus on Design PCC Slab Thickness

The effect of subgrade modulus on the PCC slab thickness of JPCP pavements was also investigated for different subgrade moduli. The slab thickness was varied from 9.5 inch (240 mm) to 13.5 inch (340 mm). The subgrade modulus was varied from 3,000 psi to 7,000 psi (48.3 MPa). Two key distresses on JPCP, IRI and percent slabs cracked, were analyzed based on the preselected performance criteria. Figure 5.7 illustrates the results obtained from the design analysis.

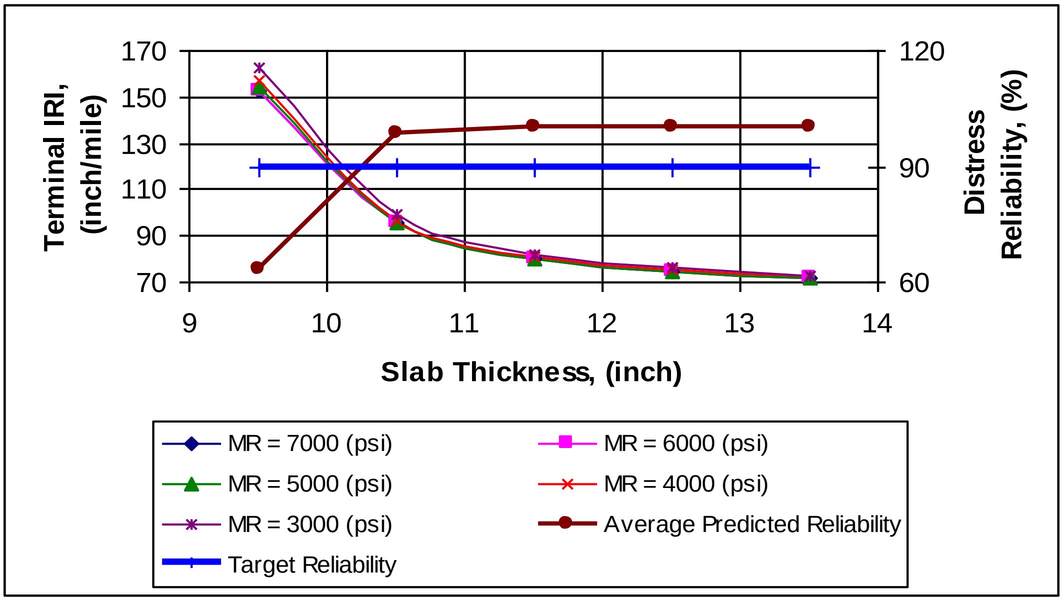

(a)

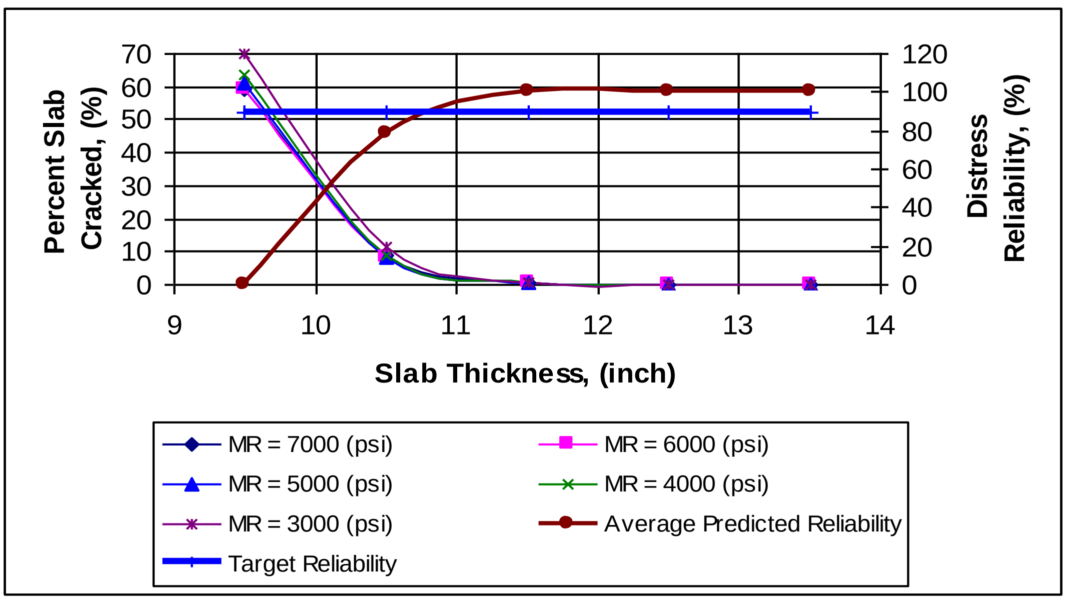

(b)

FIGURE 5.7: Evaluation of (a) IRI and (b) % slabs cracked at different slab thickness based on subgrade modulus

The results in Figure 5.7 show that IRI and percent slabs cracked are not sensitive to the subgrade modulus. However, both IRI and percent slabs cracked are significantly influenced by the PCC slab thickness. The predicted distresses are satisfactory at 90% target reliability up to the PCC slab thickness of 11 inch (279.4 mm). This may indicate that the influence of subgrade modulus on slab thickness in the JPCP pavement design is insignificant.

5.7 Determination of Target Modulus by M-EPDG Analysis

A study on intelligent compaction on Kansas highway embankments attempted to develop "target" soil stiffness for pavement subgrade (*27*). Most European specifications have developed target stiffness for soil subgrade depending upon soil type. The success of the intelligent compaction control concept also fully depends on the preassigened "target" modulus value of the compacted soil material. In this study, the "target" modulus was taken as the minimum subgrade soil modulus that would be required for a given base thickness and truck traffic while satisfying all performance criteria at pre-selected design reliability (Figure 5.8).

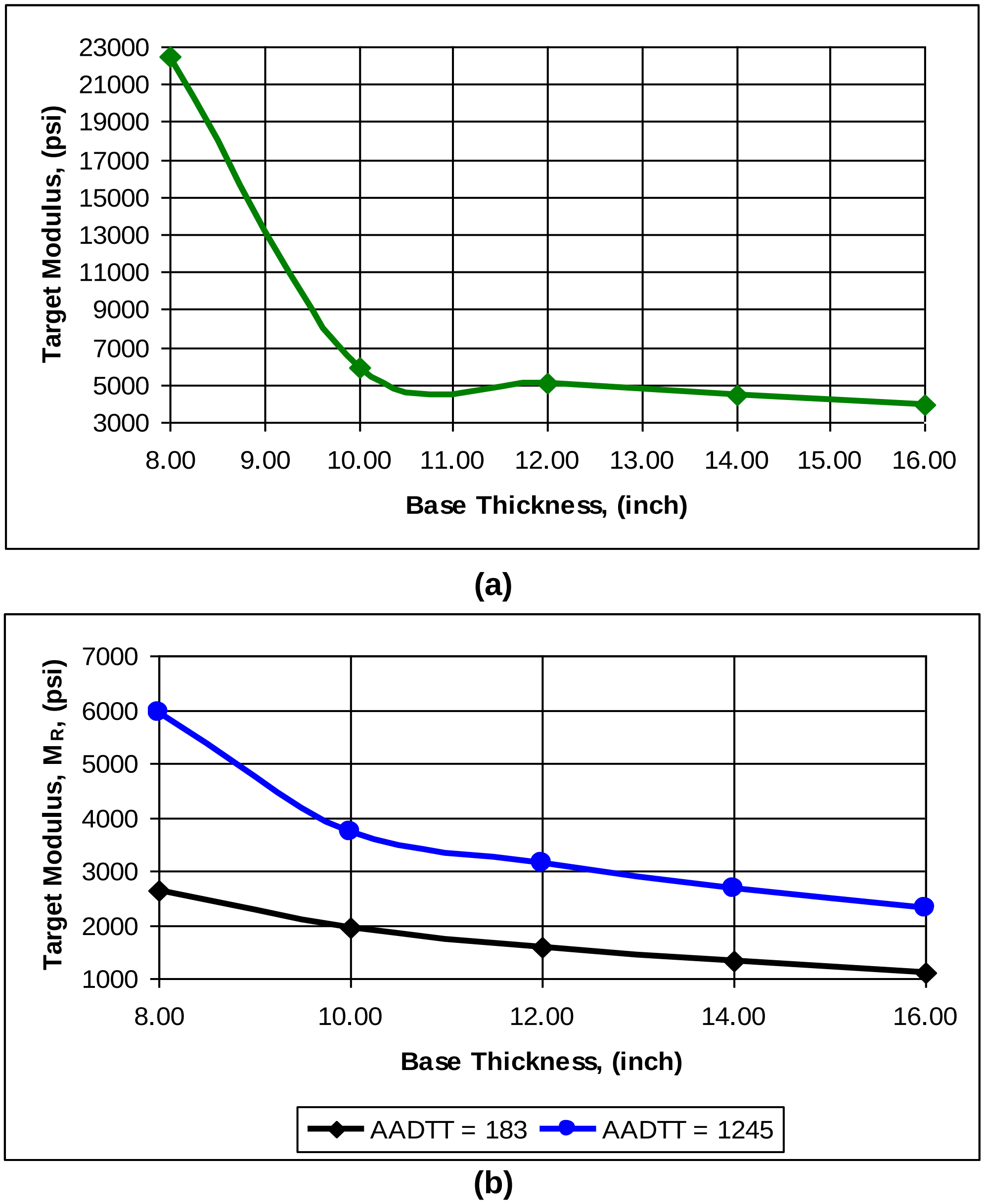

FIGURE 5.8: "Target" subgrade modulus @ 90% reliability on (a) I-70 and (b) US-56

Figure 5.8 shows the "target" subgrade stiffness values required on both project locations at 90% reliability. It is evident that the "target" modulus decreases with increasing base thickness on both test locations. On the US-56 section with a base thickness of 9.45 inch (240 mm), the "target" subgrade stiffness value is about 2,290 psi (15.8 MPa) and 4,737 psi (32.7 MPa), respectively, at different truck traffic volumes. On the I-70 section, the “target” subgrade modulus value of 4,500 psi (31.0 MPa) is obtained for the 14.2-inch (360 mm) base.

TABLE 5.7: “Target” Modulus and Measured/Calculated Modulus on US-56 and I-70 Sections

Test Section	Method	Subgrade Resilient Modulus, M_R, (psi)	
		Measured/Calculated	Target (M-EPDG)
US-56 “proof”	FWD (Boussinesq)	10,524	2,290* 4,737**
	FWD (Backcalc)	12,438	
	IC Roller	**8,449**	
	Lab data	3,481	
US-56 “growth”	FWD (Boussinesq)	10,395	2,290* 4,737**
	FWD (Backcalc)	11,454	
	IC Roller	**5,727**	
	Lab data	3,481	
I-70	FWD (Boussinesq)	4,278	4,500***
	FWD (Backcalc)	4,179	
	IC Roller	**5,674**	
	Lab data	3,626	

* AADTT = 183
** AADTT = 1,245
*** AADTT = 3640

Table 5.7 shows that the average moduli measured by the IC roller on US-56 “proof” section (8,449 psi), I-70 (5,874 psi) and on US-56 “growth” (5,727 psi) sections are higher than the “target” values under different traffic conditions. The lab moduli that were used in 1993 AASHTO Design Guide design for the US-56 sections are satisfactory for low truck traffic condition (AADTT = 183) but not for higher AADTT

(1,245). Also on I-70, the “target” subgrade modulus is higher than the laboratory design value. These results show that the “target” subgrade modulus for intelligent compaction control can be derived based on the soil type and asphalt base thickness from the M-EPDG analysis well in advance of construction.

5.8 Estimation of the Regression Constants for M-E Pavement Design

In M-E pavement design, the resilient modulus is estimated using a generalized constitutive model *(1).* A linear or nonlinear regression analysis is used to fit the model using laboratory generated resilient modulus test data. The nonlinear elastic coefficients and exponents of the constitutive model are estimated using this nonlinear regression analysis. The simplified general model (NCHRP 1-28A), derived from eq. 5.1 and used in this analysis is as follows:

$$M_r = k_1 p_a \left(\frac{\sigma_d + 3\sigma_3}{p_a}\right)^{k_2} \left(\frac{\sqrt{2}}{3}\frac{\sigma_d}{p_a} + 1\right)^{k_3} \qquad \text{Equation 5.3}$$

Where,

M_r = Resilient modulus, (psi);

σ_1 = Major principal stress (= $\sigma_d + \sigma_3$);

σ_2 = Intermediate principal stress = σ_3 (for M_r test on cylindrical specimen);

σ_3 = Minor principal stress/confining pressure;

σ_d = Deviator stress;

p_a = Normalizing stress (atmospheric pressure or 14.7 psi); and

k_1, k_2, k_3 = Regression constants (obtained by fitting the laboratory M_r data to the equation).

The simplified constitutive model was solved in this study using the SAS nonlinear regression. From above relation, the coefficient k_1 is proportional to the Young's modulus and hence its values should be positive as M_r can not negative. A higher value of bulk stress will result in higher M_r and the soil will behave as stiff materials. Therefore, the regression exponent, k_2, should be positive to support the model output. Again, the exponent k_3 is related to the octahedral shear stress and should be negative since the increasing shear stress will result in softening of the unbound material.

Estimation of nonlinear regression coefficients k_1, k_2 and k_3 is extremely important since they are used as level 1 input in M-E PDG design analysis to estimate the actual M_r. As mentioned earlier, level 1 design procedure is highly recommended by M-EPDG, when data is available, and is applicable to new pavement, reconstruction, and rehabilitation design.

In this study, the resilient modulus testing was performed in the KDOT laboratory using samples collected from three different test sections. The chamber confining pressure ranged from 2 psi to 6 psi (13.8 kPa to 41.4 kPa) and the deviator stress varied from 2 to 10 psi (13.8 to 68.9 kPa) for a particular confining pressure. The length and diameter of the specimen were 5.52 inches (140 mm) and 2.85 inch (72 mm), respectively. Moisture content ranged from OMC±2% at 90%, 95%, and 100% compaction level. Table 5.8 shows the summary of test results on soil samples from three different test sections.

TABLE 5.8: Laboratory Resilient Modulus Test Results on US-56 and I-70 Sections

Test Section	% Compaction	Moisture Content	Confining pressure, σ_3, (psi)	Deviator Stress, σ_d, (psi)	Resilient Modulus, M_r, (psi)	Comments
I-70	90	9.7	6	2 to 8	1,945 – 9,295	Failed, partial M_r
		11.7	-	-	-	Failed
		13.7	-	-	-	Failed
	95	9.7	6	2 to 6	4,942-5,480	Failed, partial M_r
		11.7	6	2 to 4	2,647-3,437	Failed, partial M_r
		13.7	-	-	-	Failed
	100	9.7	6	2 to 8	4,847-5,958	Failed, partial M_r
		11.7	6	2 to 6	4,367-5,141	Failed, partial M_r
		13.7	-	-	-	Failed
US-56 "growth"	90	8.2	-	-	-	Failed
		10.2	6	2-10	5,200	Pass
		12.2	6	2-6	3,260-4,334	Failed, partial M_r
	95	8.2	-	-	-	Failed
		10.2	6	2-10	3,589-4,151	Failed, partial M_r
		12.2	6	2-10	2,901-3,379	Failed, partial M_r
	100	8.2	-	-	-	Failed
		10.2	-	-	-	Failed
		12.2	6	2-6	2,851-3,231	Failed, partial M_r
US-56 "proof"	90	8.3	-	-	-	Failed
	95	10.3	-	-	-	Failed
	100	12.3	-	-	-	Failed

The estimated regression coefficients using the nonlinear SAS regression model (Appendix A) are presented in Tables 5.9 and 5.10. No coefficients were obtained for the US-56 “proof” section as the resilient modulus testing was unsuccessful on the samples from that section.

TABLE 5.9: Estimated Regression Coefficient k_1, k_2 and k_3 on US-56 Section

% Compaction	Moisture Content	k_1	k_2	k_3	No. of	Comments
90	8.2	Fails			0	
	10.2	344	0.06	-0.097	15	Reasonable
	12.2	648	-5.89	11.95	3	Unrealistic (k_2<0 & k_3>0)
95	8.2	Fails			0	
	10.2	340	-1.55	2.82	6	Unrealistic (k_2<0 & k_3>0)
	12.2	220	0.32	-0.98	10	Reasonable
100	8.2	Fails			0	
	10.2	Fails			0	
	12.2	0.0142	45.38	-71.55	4	Unrealistic (k_2 & k_3 significantly high and k_1 very small)

TABLE 5.10: Estimated Regression Coefficient k_1, k_2 and k_3 on I-70 Section

% Compaction	Moisture Content	k_1	k_2	k_3	No. of	Comments
90	9.7	2.66	25.42	-45.51	4	Unrealistic (k_2 & k_3 significantly high and k_1 very small)
	11.7	Fails			0	
	13.7	Fails			0	
95	9.7	0.034	44.15	-71.46	3	Unrealistic (k_2 & k_3 significantly high and k_1 very small)
	11.7	Fails			0	
	13.7	Fails			0	
100	9.7	198.7	2.07	-2.07	4	Relatively Reasonable
	11.7	1.78	26.10	-45.85	3	Unrealistic (k_2 & k_3 significantly high and k_1 very small)
	13.7	Fails			0	

The success of nonlinear regression analysis is completely dependent on the amount of available data. From these tables, it is clear that the coefficient values with higher number of observations are realistic and reasonable. Figure 5.9 shows the comparison of data between the $M_{r\text{-measured}}$ (MR) and the $M_{r\text{-calculated}}$ (MRHAT) from the nonlinear regression analysis on the US-56 test section for two different sets of observations.

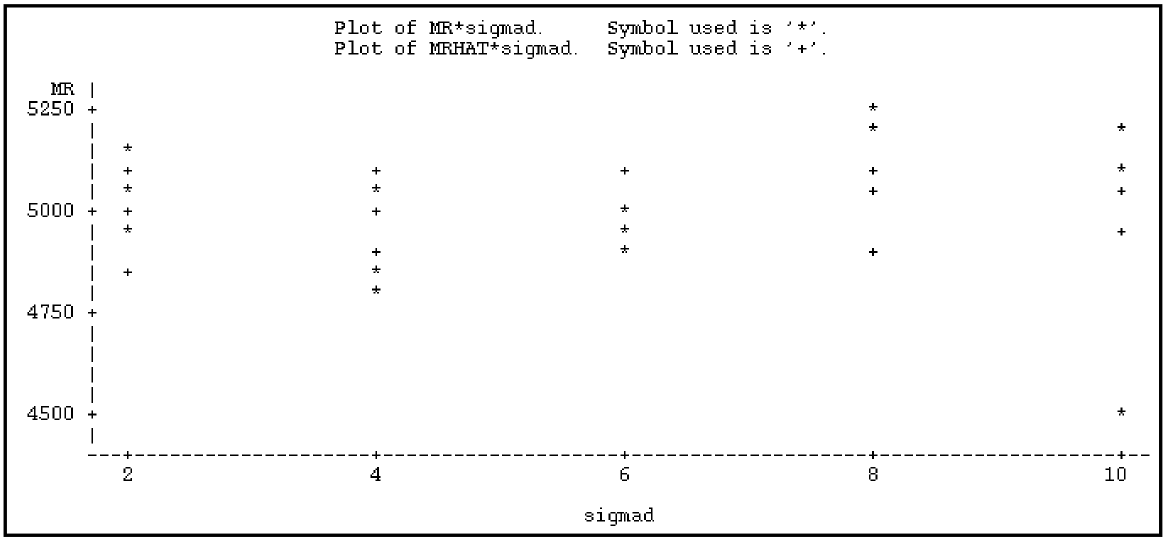

(a)

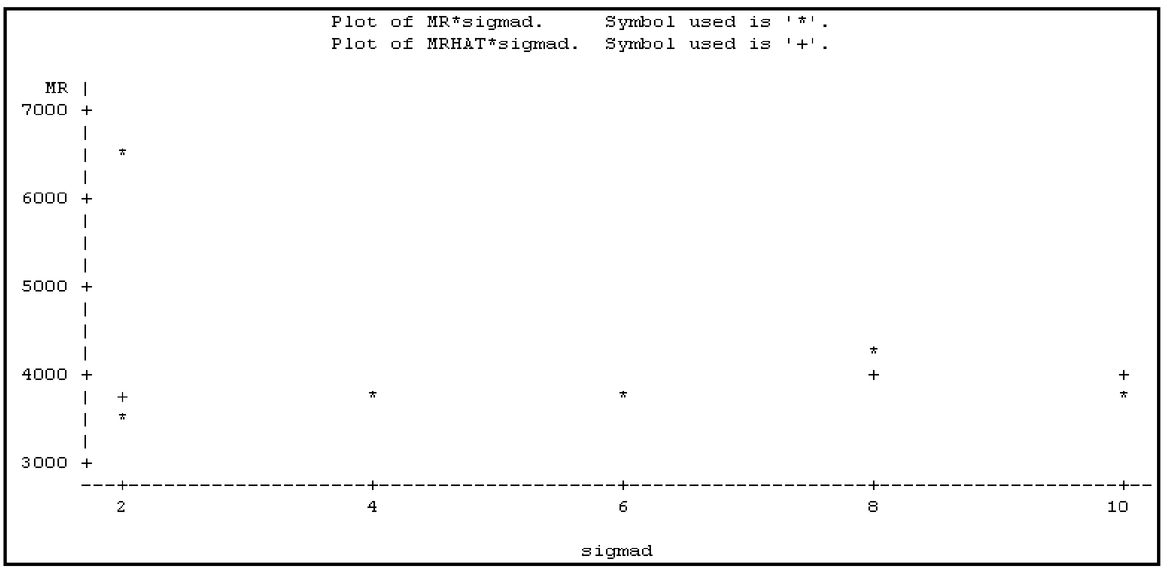

(b)

FIGURE 5.9: Fitness of M_r data in SAS Nonlinear regression (a) (No. of Obs.=15), (b) (No. of Obs.=6)

These figures show that the laboratory measured M_r and estimated M_r from regression analysis are close to each other when the number of observations was 15. However, when the number of observations was 6, no such correspondence was observed.

CHAPTER 6 - CONCLUSIONS AND RECOMMENDATIONS

6.1 Conclusions

This study was conducted to investigate the compaction quality control of highway embankment soil in Kansas using a new technology called Intelligent Compaction Control. Subgrade soil of three different test sections from two reconstruction projects on US-56 and I-70 were compacted using IC roller. Other spot tests such as stiffness measurements by soil gage, in-situ deflection measurements by FWD and LFWD and DCP test were also performed on the test locations. Some laboratory testing was also performed to characterize the test section subgrade soil. Finally, M-EPDG (Mechanistic Empirical Pavement Design) analysis was performed to investigate the effect of subgrade soil strength on the pavement distress level and also to fix a “target” modulus for the field compaction quality control.

Based on this present study, the following conclusions can be made:

- Due to continuous measurements of the in-situ stiffness of the subgrade soil under compaction, the intelligent compaction (IC) roller is able to identify the soft spots with lower stiffness in the spatial direction.
- The IC roller stiffness is somewhat sensitive to the field moisture content. In-situ moisture content close to the optimum moisture content will result in higher roller stiffness.
- “Target” stiffness values need to be selected in intelligent compaction control because both very high and very low maximum densities achieved during compaction may yield lower IC roller stiffness.

- No good correlation was observed among IC roller stiffness and other stiffness/modulus values obtained from the soil stiffness gage, LFWD, FWD and DCP test data.
- Correlation between the soil stiffness gage stiffness and the LFWD moduli was found to be significant for the US-56 section. However, no such correlation was found on I-70.
- The reason for poor correlation is the discrepancy arises from different testing devices. The discrepancy seems to occur due to the fact that different equipments were capturing response from different volumes of soil on the same test section. The lowest space volume was measured by soil stiffness gage while the maximum volumetric depth was obtained by IC roller. FWD and LFWD covered the intermediate volumetric depth of influence.
- M-EPDG analysis shows that the predicted total pavement deformation and roughness are sensitive to the subgrade modulus for flexible pavements. In Jointed Plain Concrete Pavements, the key distresses are insensitive to the subgrade modulus.
- AC base thickness has more influence on the total pavement deformation than the foundation layer. However, truck traffic plays an even more significant role in controlling this distress.
- The influence of subgrade modulus on the slab thickness in the JPCP pavement design is insignificant.

- The “target” subgrade modulus for intelligent compaction control roller can be derived based on the soil type and asphalt base thickness well before construction by doing M-EPDG analysis.
- Nonlinear Regression Coefficients of constitutive model in M-E design are estimated from laboratory resilient modulus test data. The coefficient values are inconsistent since the resilient modulus test was not successful most of the time and hence resulted less number of observations.

6.2 Recommendations

Based on this study, the following recommendations are made:

- The subgrade soil stiffness is very sensitive to in-situ moisture content and IC roller has been proven to be a very effective tool to identify those soft spots. Thus the IC roller can be used for “proof rolling”.
- Plate loading test is known to have a very good correlation with the IC roller stiffness. FWD tests can be performed on subgrade using a larger diameter plate (about 30 inches or 762 mm) to develop a better correlation between the IC roller stiffness and the soil moduli backcalculated from the FWD data.

REFERENCES

1. Part 1: Introduction. *Guide for Mechanistic-Empirical Design of New and Rehabilitated Pavement Structures.* Final Report, NCHRP Project 1-37A. Transportation Research Board, National Research Council, Washington, D.C., July 2007.

2. BOMAG. *Heavy Equipment, Compaction Control and Documentation System BTM.* Brochure, BOMAG Schriftenreihe, Boppard, Germany.

3. NCHRP, *Intelligent Soil Compaction System*. Request for Proposal for NCHRP Project 21-09, National Cooperative Highway Research Program, Transportation Research Board, Washington, D.C., September 2005.

4. Horan, B., and T. Ferragut, *Intelligent Compaction Strategic Plan*. FHWA, U. S. Department of Transportation, April 2005.

5. Petersen, J. S., S. A. Romanoschi, M. A. Onyango, and M., Hossain. *Evaluation of Prima Light Falling-Weight Deflectometer as Quality Control Tool for Compaction of Fine Grained Soils.* Paper No. 07-1326, Preperint CD-ROM of the 86th Transportation Research Board Annual Meeting, Transportation Research Board, Washington, D.C., January, 2007.

6. Briaud, J. L. and J. Seo, *Intelligent Compaction: Overview and Research Needs*. Draft Report by the Texas A &M University, 2003. *Available at* *http://www.webs1.uidaho.edu/bayomy/trb/afh60/Intcompaction_Briaud_Septemeber2004.pdf*

7. Kloubert, H., Intelligent VARIOCONTROL rollers with integrated quality control system for soil compaction – principles, measurement, applications. Presentation made at the 83rd Annual Meeting of the Transportation Research Board, Washington, D.C., 2004.

8. Briaud, J.L. and J. Seo. *Intelligent Compaction: Overview and Research Needs*. Draft Report by the Texas A &M University, December 2003.

9. Sandstrom, A. and C. Pettersson. *Intelligent systems for QA/QC in soil compaction*, Presentation made at the 83rd Annual Meeting of the Transportation Research Board, Washington, D.C., 2004.

10. Anderegg, R. and K. Kaufman. *Intelligent Compaction with Vibratory Rollers; Feedback Control Systems in Automatic Compaction and Compaction Control*. Transportation Research Record; Journal of the Transportation Research Board No. 1868, Transportation Research Board, Washington, D.C., 2004, 124-134.

11. BOMAG Variocontrol, *Automatic optimization of compaction on single drum rollers for soils and granular base compaction*, Technical Literature, 2004.

12. Kim, D., T. Nantung, N. Z. Siddiki, and J. R. Kim. *Implementation of the New Mechanistic-Empirical Design for Subgrade Materials-Indiana Experience.* TRB Preprint CD-ROM Paper #07-0463, 86th Annual Meeting of the Transportation Research Board, Washington, D.C., 2007.

13. Petersen, D.L., J. Siekmeier, C. Nelson, and R. L. Peterson. *Intelligent Soil Compaction Technology: Results and a Roadmap Toward Widespread Use*. Transportation Research Record: Journal of the Transportation Research Board, No. 1975, Transportation Research Board, Washington, D.C., 2006, pp. 81-88.

14. Krober, W., R. Floss, and W. Wallrah. *Dynamic Soil Stiffness as Quality Criterion for Soil Compaction.* Technical Paper, BOMAG Schriftenreihe, Boppard, Germany.

15. Anderegg, R. *ACE AMMANN Compaction Expart.* Technical Paper, Ammann Verdichtung AG, Langenthal, Swiss.

16. Sawangsuriya, A., J. P. Bosscher, and B. T. Edil, Laboratory Evaluation of the Soil Stiffness Gauge. In *Transportation Research Record: Journal of the Transportation Research Board, No 1808*, TRB, National Research Council, Washington, D. C., 2002, pp. 30-37.

17. George, K.P. Falling Weight Deflectometer for Estimating Subgrade Resilient Moduli. Final Report No. FHWA/MS-DOT-RD-03-153, Mississippi Department of Transportation, Jackson, December 2003.

18. Livneh, M., and I. Ishai. Pavement and Material Evaluation by a Dynamic Cone Penetrometer. *Proc., Sixth International Conference on the Structural Design of Asphalt Pavement*, Vol. 1, Ann Arbor, Michigan, 1987, pp. 665-674.

19. Mau, R. R. *Correlation of the Automated Cone Penetrometer, Dynamic Cone Penetrometer, and California Bearing Ratio*. M.S. Thesis. Department of Civil Engineering, University of Kansas, Lawrence, January 1989.

20. Webster, S. L., R. H. Grau, and T. P. Williams. *Description and Application of Dual Mass Dynamic Cone Penetrometer*. USACE Waterways Experiment Station, Vicksburg, Mississippi, May 1992.

21. Part 2: Design Inputs. *Guide for Mechanistic-Empirical Design of New and Rehabilitated Pavement Structures.* Final Report, NCHRP Project 1-37A. Transportation Research Board, National Research Council, Washington, D.C., July 2007.

22. SAS. *Statistical Analysis System*, The SAS Institute, Carey, North Carolina., 1999

23. Petersen, D. L., M. L. Erickson, R. Roberson, and J. Siekmeier. *Intelligent Soil Compaction: Geostatistical Data Analysis and Construction Specifications*. Paper No.07-2858, Preperint CD-ROM of the 86th Transportation Research Board Annual Meeting, Transportation Research Board, Washington, D.C., January, 2007.

24. Khazanovich, L., C. Celauro, B. Chadbourn, J. Zollars, and S. Dai. *Evaluation of Subgrade Resilient Modulus Predictive Model for Use in Mechanistic-Empirical Pavement Design Guide.* Transportation Research Record: Journal of the Transportation Research Board, n 1947, Transportation Research Board of the National Academics, Washington, D.C., 2006, p 155-166.

25. Barry, C. R. and C. Schwartz. *Geotechnical Aspects of Pavements.* Report no. FHWA NHI-05-037. National Highway Institute, Federal Highway Administration, Washington, D.C., January 2005.

26. Graves, R. C., and K. C. Mahboub. *Pilot Study in Sampling-Based Sensitivity Analysis of NCHRP Design Guide for Flexible Pavements.* Transportation Research Record: Journal of the Transportation Research Board, n 1947, Transportation Research Board of the National Academics, Washington, D.C., 2006, p 123-135.

27. Rahman, F., M. Hossain, M. M. Hunt, and S. A. Romanoschi. *Intelligent Compaction Control of Highway Embankment Soil.* TRB Preprint CD-ROM Paper #07-2962, 86th Annual Meeting of the Transportation Research Board, Washington, D.C., 2007.

APPENDIX A

SAS NONLINEAR REGRESSION ANALYSIS

INPUT AND OUTPUT FILES

SAS Input File:

US-56 Test section (90% Compaction @ OMC)

```
data Resilient;
  input sigma3 sigmad MR;
datalines;
6  2  5131.3
6  4  5052.8
6  6  5004.1
6  8  5193.4
6 10  5185.5
4  2  5038.0
4  4  4837.6
4  6  4954.0
4  8  5235.7
4 10  5124.3
2  2  4968.9
2  4  4784.6
2  6  4924.6
2  8  5210.8
2 10  4490.5
;
proc nlin data=Resilient method=GAUSS noitprint hougaard;
parms k1=0
      k2=0
                        k3=-6;
model MR=k1*14.7*(((sigmad+3*sigma3)/14.7)**k2)*(((0.4714*sigmad/14.7)+1)**k3);
der.k1= 14.7*(((sigmad+3*sigma3)/14.7)**k2)*(((0.4714*sigmad/14.7)+1)**k3);
der.k2=
        (k1*14.7*(((sigmad+3*sigma3)/14.7)**k2)*(((0.4714*sigmad/14.7)+1)**k3))*log((
        sigmad+3*sigma3)/14.7);
der.k3=
        (k1*14.7*(((sigmad+3*sigma3)/14.7)**k2)*(((0.4714*sigmad/14.7)+1)**k3))*log((
        0.4714*sigmad/14.7)+1);
output out=new p=MRhat r=MRresid
run;

proc plot data=new;
   plot MR*sigmad='*' MRhat*sigmad='+' / overlay;
run;
```

SAS Output File:

US-56 Test section (90% Compaction @ OMC)

Estimation Summary

Method	Gauss-Newton
Iterations	6
Subiterations	1
Average Subiterations	0.166667
R	1.415E-6
PPC(k3)	7.185E-6
RPC(k3)	0.000677
Object	1.873E-8
Objective	426059.9
Observations Read	15
Observations Used	15
Observations Missing	0

The NLIN Procedure

Source	DF	Sum of Squares	Mean Square	F Value	Approx Pr >F
Regression	3	3.7648E8	1.2549E8	3534.57	<.0001
Residual	12	426060	35505.0		
Uncorrected Total	15	3.7691E8			
Corrected Total	14	548638			

Parameter	Estimate	Approx Std Error	Approximate 95% Confidence Limits		Skewness
k1	343.5	8.6757	324.6	362.4	0.0421
k2	0.0600	0.0327	-0.0113	0.1313	0.00893
k3	-0.0976	0.1468	-0.4174	0.2221	0.00643

Approximate Correlation Matrix

	k1	k2	k3
k1	1.0000000	0.2966818	-0.9057739
k2	0.2966818	1.0000000	-0.4981702
k3	-0.9057739	-0.4981702	1.0000000

K - TRAN

KANSAS TRANSPORTATION RESEARCH
AND
NEW - DEVELOPMENTS PROGRAM

A COOPERATIVE TRANSPORTATION RESEARCH PROGRAM BETWEEN:

KANSAS DEPARTMENT OF TRANSPORTATION

THE UNIVERSITY OF KANSAS

KANSAS STATE UNIVERSITY